1986

# Sediment deposition modeling of channel-sound systems /

Craig L. Young
*Lehigh University*

# Sediment Deposition Modeling of Channel-Sound Systems

by

Craig L. Young

A Thesis

Presented to the Graduate Committee

of Lehigh University

in Candidacy for the Degree of

Master of Science

in

Civil Engineering

Lehigh University
1986

Certificate of Approval

This thesis is accepted and approved in partial fulfillment of the requirements for the degree of Master of Science.

12-18-85
(date)

Professor in Charge

Chairman of Department

# Acknowledgements

The author would like to express his great appreciation to Dr. Richard N. Weisman for his continuous advice and encouragement throughout this study and to Dr. Gerard P. Lennon for his timely insight and support. Their combined efforts helped to make this study a success.

This work is the result of research sponsored by NOAA, Office of Sea Grant, Department of Commerce, under Grant No. NA85AA-D-SG084 (Project No. R/S-6). The Civil Engineering Department Chairman is Dr. Irwin J. Kugelman.

The author also wishes to acknowledge Catherine Miller for her assistance in typing the figures and tables.

Finally, the author wishes to express thanks for the tremendous support from his parents and friends, and for the opportunities and abilities given him by God.

# Table of Contents

# List of Figures

# List of Tables

# Abstract

A sediment deposition model is developed for application to Great Sound, New Jersey. A determination of the average annual accumulation rate is of primary interest. The settling tank concept is used for the model, employing a plug flow approach to the tidal hydrodynamics. Assumptions inherent in this modeling technique include no mixing between plugs, a uniform vertical velocity profile, and simplified geometry.

Model inputs were based on hydrodynamic and sediment data obtained for Great Sound by other investigators, including initial flow volume in the Sound at mean low water, the inflow hydrograph and tidal range, the sediment sizes, concentrations and settling velocities, and a frequency versus concentration relationship.

The model simulates a single tidal cycle in Great Sound for spring, neap and mean tidal conditions at various sediment concentrations. Three tests were run to define the sediment deposition characteristics of the Sound. The first test defined the relative impact of spring, neap and mean tidal events on the deposition. Deposition during mean tide equals the average of the spring and neap tide deposition. Concentration hydrographs for ebb flow were determined. The second test determined the average annual sediment accumulation rate in Great Sound to be 8.9 mm/yr. Model predictions compare favorably with predictions of other researchers. Finally, the distribution of the average annual accumulation across Great Sound is defined. In the third test, the relative influence of storm conditions versus predominant fair weather conditions was established. Only 8 storm days are required to match a year of fair weather deposition.

# Chapter 1
# Introduction

## 1.1 Background

The southern New Jersey coast is an area thriving in recreational and commercial activity. The wetlands area, landward of coastal barrier islands, provides the ingredients necessary to support a variety of wildlife. Specifically, finfish, shellfish, and bird life thrive here. Boaters, fishermen and naturalists all find the wetland-sound areas to be exciting, yet relaxing places of recreation. The wetlands region includes Great Sound, which is located landward of Seven Mile Beach where the resort cities, Avalon and Stone Harbor, are located (Figure 1-1). Great Sound has been the subject of extensive research by a variety of scientists and engineers, including geologists, biologists, environmentalists and hydrologists.

The Intracoastal Waterway, which supports seasonally heavy volumes of recreational boat traffic, traverses the Sound near its eastern edge. The Intracoastal Waterway must be maintained against excess sediment build-up by periodic dredging. Coastal sediment originating in ocean waters is transported through inlets and channels during flood tide. It eventually arrives in the Sound where low flow velocities create a depositional environment. The effects of sediment deposition in the region are significant in several ways. Deposition in the channel as it traverses the Sound is costly to dredge and can be hazardous to navigation. Excessive sediment deposition in the Sound may alter the state of shellfish life and therefore influence the ecosystem of the wetlands. Finally, the relative effects of sea level rise versus accumulating sediment may

also affect the long term stability of the landforms.

Previous field research provides an invaluable databank from which pertinent hydrodynamic and sediment data can be obtained for the analysis of sediment deposition. Schuepfer (1985) supplemented hydrodynamic field data taken in the Sound with a numerical model called HYDTID developed by Masch et al. (1977). The two-dimensional hydrodynamic model was used to predict flows and tidal heights for various tidal conditions in Great Sound. The model was calibrated against the field data for spring and neap tide events, and verified by simulating a mean tide event. Schuepfer's results include flow rate and water surface elevation hydrographs and tidal prisms.

Carney (1982) analyzed fine-grained sediment aggregation processes in Great Channel by collecting near-bottom and surface suspended samples. Settling velocity fractionation and an electronic size analysis were performed to better investigate sediment aggregation. The results of Carney's work includes particle size fractions, settling velocities, volumetric distribution of the size fractions, fraction densities and a concentration hydrograph. Griffiths (1986), in a study concurrent to this one, has also taken data to generate concentration hydrographs for fair weather and post storm conditions in the Sound. Griffiths' study is an attempt to show the dominant paths of sediment influx into Great Sound.

Kelley (1975) took stable lead, Pb, profiles of the bottom sediment in Great Sound. Based on these profiles, annual accumulation rates were estimated at between 5 and 10 mm/yr. Thorbjarnarson et al. (1984) used a lead isotope, Pb-210, geochronology to evaluate sediment accumulation rates in the western half of the Sound. Fifteen cores were taken, and a steady-state equation was

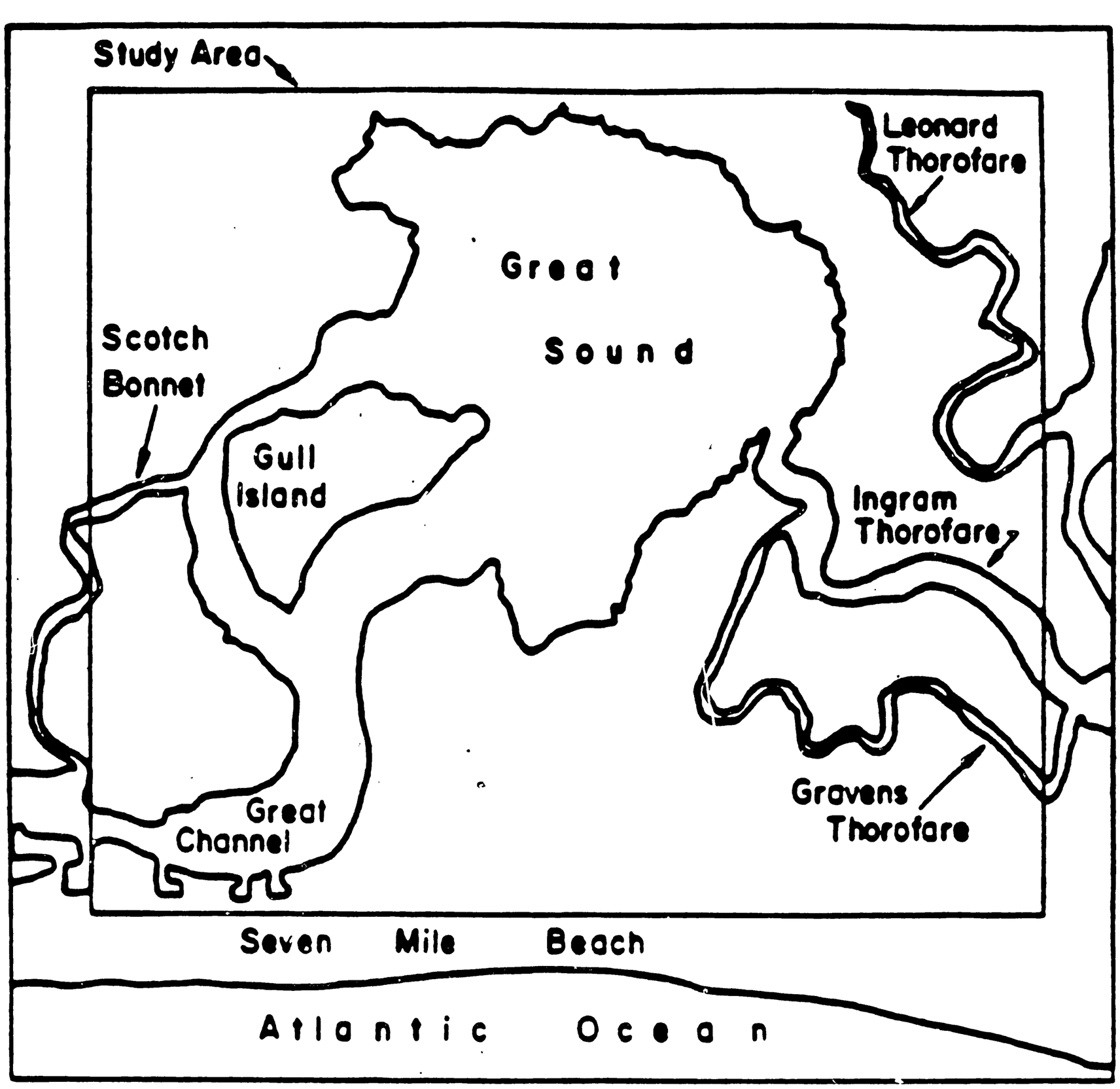


**Figure 1-1:** Map of the Study Area Landward of Seven Mile Beach Including Great Sound and its Main Feeder Channels Great Channel and Ingram Thorofare, after Schuepfer, 1985

used to evaluate the profiles. Sediment grain size data were determined from the cores, and maximum annual sediment accumulation rates predicted for the Sound. The study concluded that between 1 and 5 mm of sediment accumulates in the western half of Great Sound annually.

Another researcher, Faas (1984), has studied accumulation in sediment trap structures in Great Sound and other nearby tidal basins.

## 1.2 Objectives

Considering the impact of sediment deposition on Great Sound and the surrounding region (high dredge costs, navigation hazards and potential altering of the ecosystem and landforms), the need for a sediment deposition analysis of the Sound is evident. The abundance of hydrodynamic and sediment data available presents the opportunity to construct a sediment deposition model of the Sound. The purpose of this model is to define the sediment deposition in the Sound over space and time, while also determining which factors, such as spring tides, storm conditions, and average day conditions have the most influence on annual deposition.

Specific objectives for a sediment deposition model of the Sound are:

1. Adapt and test the utility of a settling tank model when applied to a tidal basin which considers basic hydrodynamic, sediment and meteorological characteristics, but does not include such factors as dispersion and resuspension.

2. Utilize available field data, including fluid and sediment inflows, tidal range, sediment particle characteristics and frequency of occurrence of varying meteorological conditions, as input data to the model.

3. Predict the annual sediment accumulation rate in the Sound and compare the model results with accumulation rate assessments determined by Pb profile testing of bottom sediments.

4. Analyze the distribution of sediment as a function of time in the

tidal cycle and position across the Sound.

5. Determine the relative affect of fair weather versus storm weather conditions.

6. Determine ebb flow concentration hydrographs.

7. Compare the rate of sediment deposition with current sea level rise predictions.

## 1.3 Overview of Sediment Deposition Modeling in the Coastal Environment

The result of this study is a model which analyzes sediment deposition in Great Sound. The model is purposely generalized to enhance its capabilities in other regions and perhaps for other problems. Previous researchers have both monitored and modeled sediment deposition in coastal regions and some are reviewed here.

Evans and Collins (1974) monitored the transportation and deposition of suspended sediment in a large embayment on England's east coast known as the Wash. One of the results of the study revealed that by determining the sediment flux over a single tidal cycle, useful data on sediment transport over much larger periods of time could be accurately calculated. These calculations were based on the average suspended sediment concentration as recorded at various times throughout the tidal cycle.

Wang (1985) applied the theory of turbulent jets in predicting the development of the Atchafalaya River Delta on the Gulf Coast. The primary factor influencing the pattern of sediment deposition was the inertial force of river effluent and associated turbulent diffusion. In the analysis, assumptions similar to those made for sediment deposition basins were evident. These

assumptions included: shallow receiving waters, a uniform velocity profile, and well-mixed conditions at the mouth. Also, the river-bay system was approximated by simple geometry. A numerical integration technique was used for obtaining analytical solutions.

Similar studies were also conducted by McAnally et al. (1984) on the Columbia River mouth, and Cole and Miles (1983) on the motion of cohesive sediment in the Thames in England.

Maa et al. (1985) modeled shoaling of fine, cohesive sediment in a Florida marina using a lumped parameter model solving the one-dimensional convective-dispersion equation assuming uniform concentration and a simple harmonic tidal variation. For a basin in which the water level variation due to the astronomical tide is the principle driving mechanism for circulation, the rate of shoaling was found to depend on the following factors:

1. Range and period of the tide
2. Basin depth
3. Suspended sediment concentration outside the basin which defines the input sediment concentration
4. Sediment settling velocity
5. Density of basin deposit

Concerning suspended sediment concentration, the study by Maa et al. (1985) showed that during storm conditions sediment loads tend to increase by up to two orders of magnitude over fair weather conditions. A concentration histogram was also developed by Maa et al. (1985) which describes the concentration-frequency relationship derived from measurements over a 265 day period.

## 1.4 Scope of This Study

The studies by Wang (1985), McAnally et al. (1985) and Cole and Miles (1983) use comprehensive finite difference schemes to describe the motion of sediment entering an estuary, while Evans and Collins (1974) and Maa et al. (1985) present extensive field data but use simple mass balance equations to describe sediment flux. Unlike the previous analyses, the present study applies the settling tank concept in modeling sediment deposition within Great Sound. Although future research will attempt to incorporate sediment deposition modeling within a two-dimensional hydrodynamic model for the Sound, the lumped settling tank modeling technique using one-dimensional hydrodynamics is appropriate in this initial phase of analysis for two basic reasons. First, based on limited input data and a very small depth, a three-dimensional approach is not presently justified. Second, the settling tank concept aptly describes a basin like Great Sound, which is of small areal extent with uniform bathymetry and low flow velocities. As previously stated, a basin like Great Sound presents an opportunity to evaluate a settling tank model's performance in the coastal environment. A plug flow approach to the hydrodynamics of the Sound is incorporated into the settling tank representation. Available field data from previous researchers are utilized by the resulting model as input data.

The physical characteristics of the Sound are described completely in the following section, including geographic, bathymetric, hydrodynamic and sediment characteristics. As a background to the model, the basic settling tank concept is developed. The adaptation of the settling tank concept to the Sound is then presented, with consideration given to tidal basins, tidal hydrodynamics and diffusion and dispersion processes. An analysis of fluid and sediment motion

occurring within each plug of flow concludes the development of the sediment deposition model. Finally, the model testing and results are presented and discussed in light of the results of previous researchers. Applicable conclusions and future considerations are also examined to complete the study.

This study does not consider the effects of resuspension, dispersion and circulating flow.

# Chapter 2
# Physical Characteristics of the Channel-Sound System

## 2.1 Geography and Topography

Great Sound is pictured in Figure 2-1. The Sound is of small areal extent, covering approximately 4.65 $km^2$. Two channels feed Great Sound, Ingram Thorofare from the northeast and Great Channel from the southeast. The Intracoastal Waterway, which traverses the Sound to the east, connects the two channels at an average depth of 3 meters. The bottom of the Sound is generally uniform, and the Sound has an average depth of 0.5 meters at mean low water (MLW). Dredge spoils located near the edge of the Intracoastal Waterway are the only exception to the otherwise uniform bottom. The Sound is surrounded by marshland which is innundated during spring tides. There is virtually no fresh water surface drainage from the mainland into the Sound.

## 2.2 Hydrodynamic Characteristics

Fluid motion in the Sound is dominated by the astronomical tide which floods the Sound through Ingram Thorofare and Great Channel. Tidal ranges at Reuben's Wharf (see Figure 2-1 for location) are shown for spring and neap tides in Figures 2-2 and 2-3. For all spring tide data 0.00 hours corresponds to 0.00 hours May 24, 1983, and for all neap tide data 0.00 hours corresponds to 0.00 hours June 1, 1983, as recorded by Schuepfer (1985). Typically, the spring tidal range is 1.5 meters and the neap range 1.0 meters. The mean tidal range, averaging 1.25 meters, is shown in Figure 2-4. Tidal prisms for Great Channel and Ingram Thorofare have been calculated using the HYDTID model by

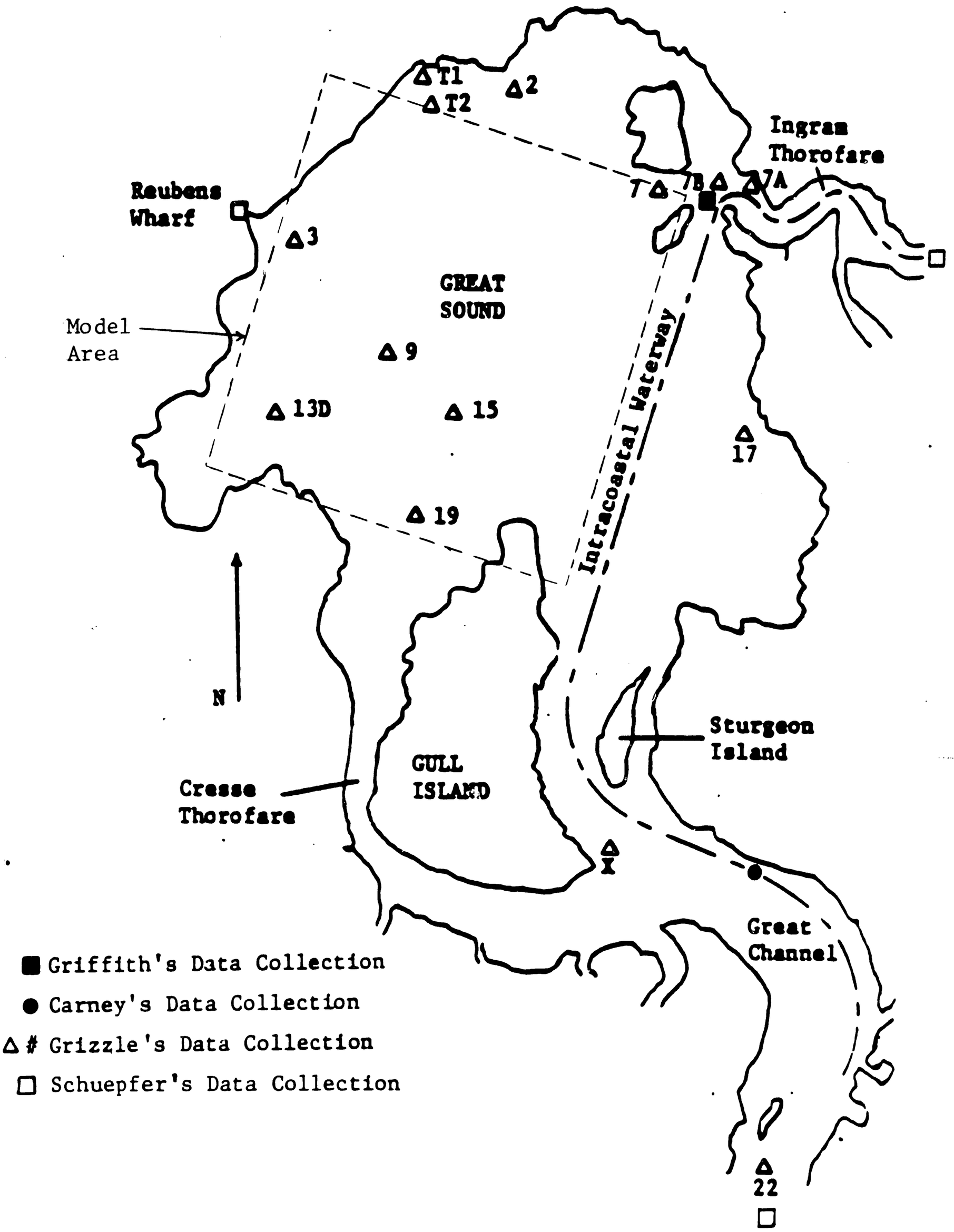


**Figure 2-1:** Map of Great Sound, New Jersey, Including the Intracoastal Waterway and Data Collection Sites

Schuepfer (1985). Field data used for model calibration was collected at Ingram Thorofare Bridge and Great Channel Bridge. Summing the tidal inflows through the contributing channels yields the total tidal prism entering the Sound and wetlands region during flood tide. The total mean tidal prism is $2.06 \times 10^7$ $m^3$. As previously stated in Section 2.1, the total area occupied by Great Sound is approximately 4.65 $km^2$. Incorporating Schuepfer's (1985) tidal data, it has been determined that 30% of the total mean tidal prism occupies Great Sound at slack high water. For the mean tidal condition then, the tidal prism for the Sound is $5.77 \times 10^6$ $m^3$. At MLW, a volume of $2.3 \times 10^6$ $m^3$ remains in the Sound. Therefore, for a mean tide, the total volume in the Sound at slack high water is $8.07 \times 10^6$ $m^3$.

Figures 2-5, 2-6 and 2-7 show the flow rate versus time for Ingram Thorofare and Great Channel for spring, neap and mean tidal conditions taken from Schuepfer (1985). Field data are shown along with the HYDTID output as verification of the spring and neap tide flow conditions. An average lag time of one hour can be observed between the two channels. Ingram Thorofare floods first, and Great Channel follows subsequently. The flood which enters through Great Channel has a one hour delay because of the weaker driving head in the channel (Schuepfer, 1985). These two channels dominate the incoming flood to the Sound. Cresse Thorofare, also pictured in Figure 2-1, provides negligible flow into the Sound relative to Ingram Thorofare and Great Channel.

Since the two channels flow in opposite directions within the Intracostal Waterway throughout the flood, a nodal point (where net flow is zero) exists between them. Based on hourly flow maps from the HYDTID model

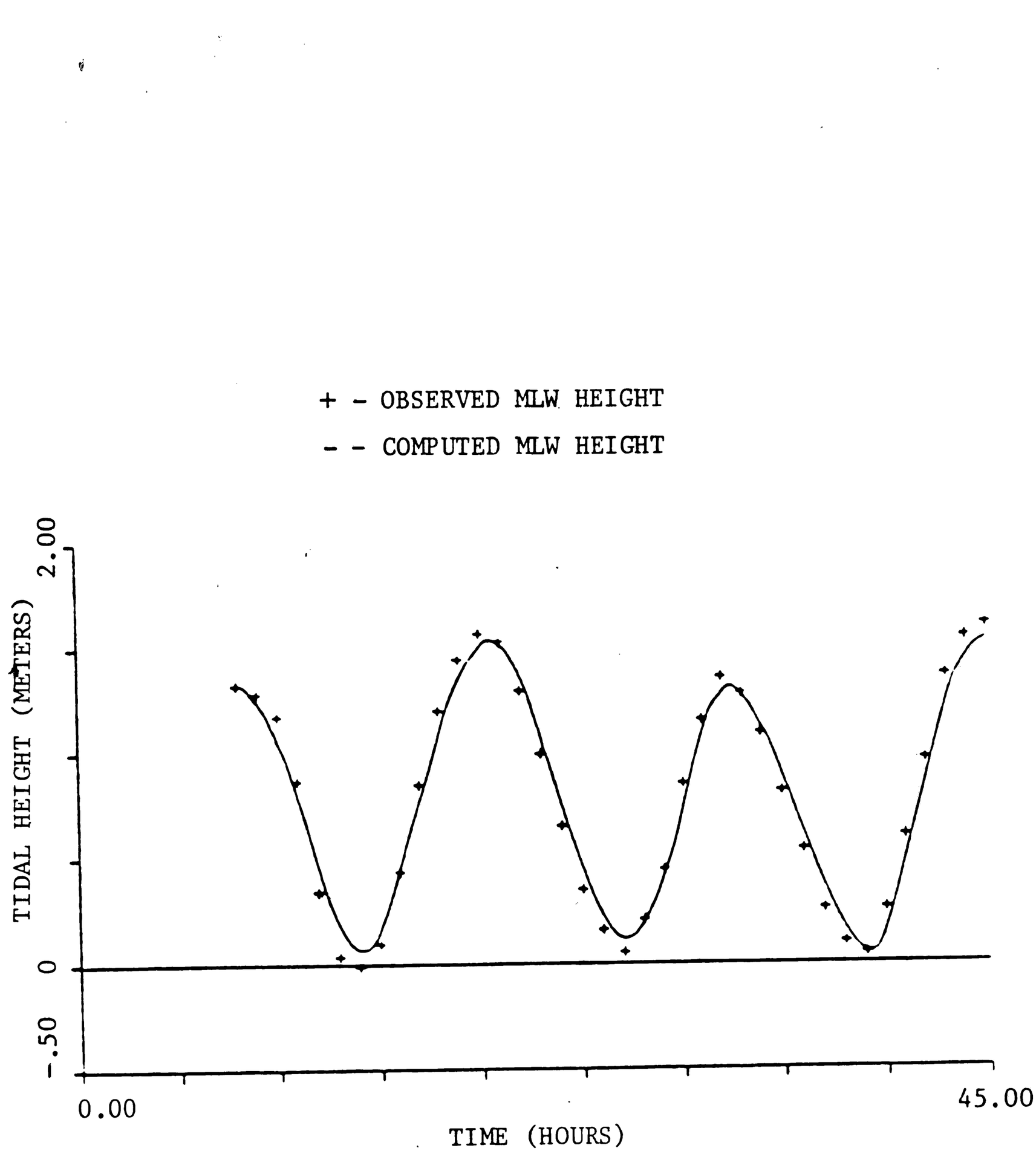


**Figure 2-2:** Water Surface Elevations for Spring Tide at Reuben's Wharf, after Schuepfer 1985

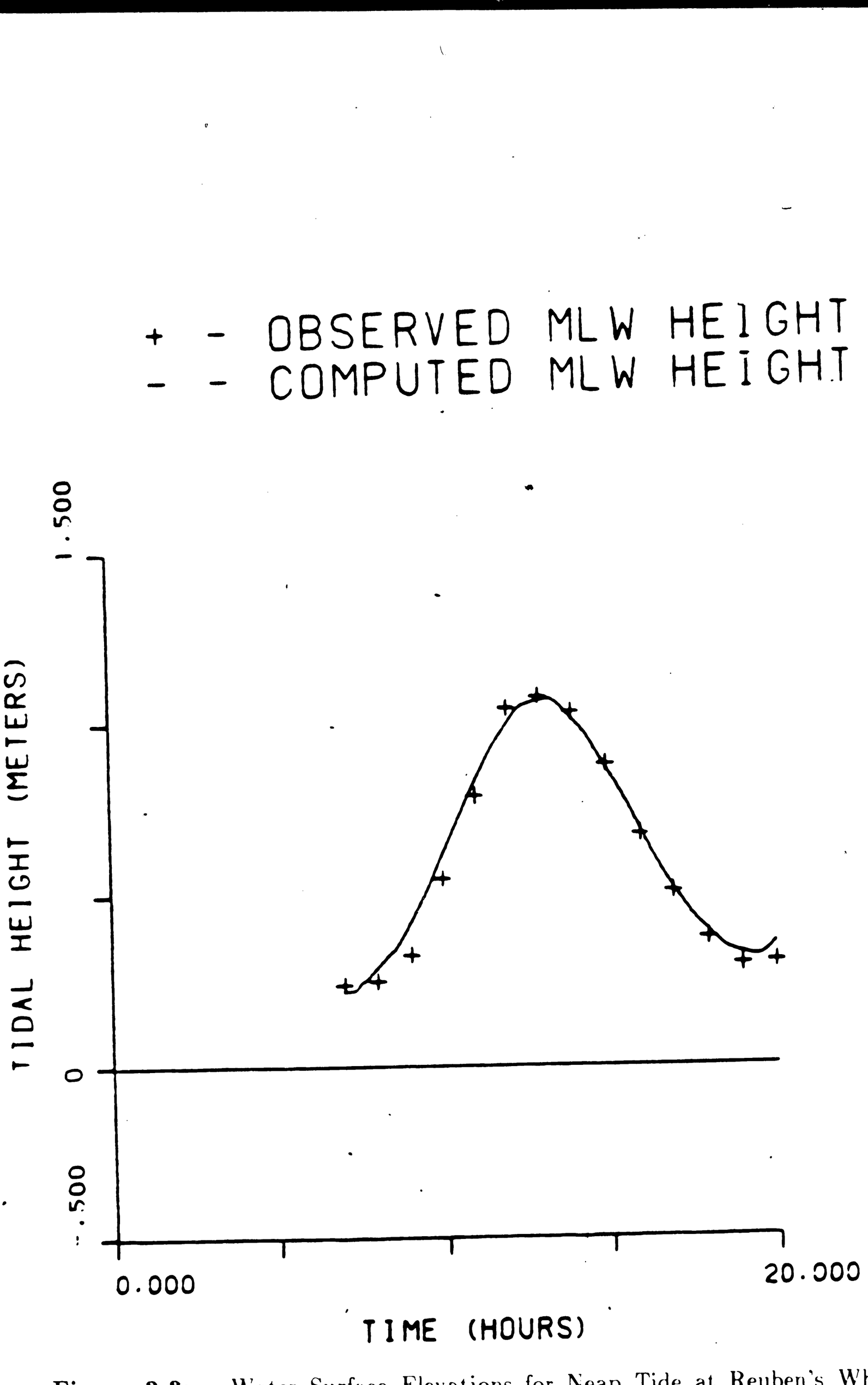


**Figure 2-3:** Water Surface Elevations for Neap Tide at Reuben's Wharf, after Schuepfer 1985

+ - OBSERVED MLW HEIGHT

- - COMPUTED MLW HEIGHT

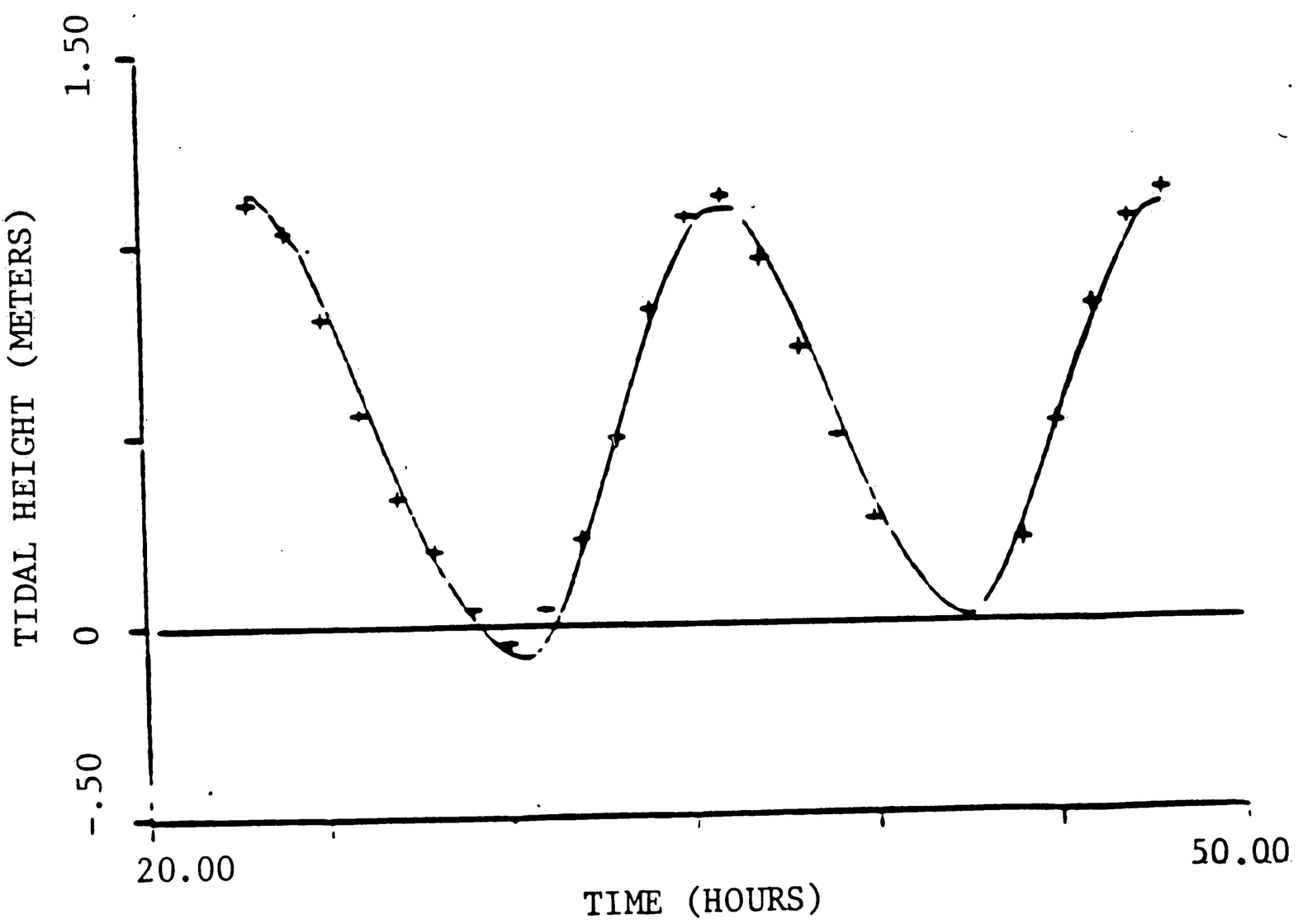


**Figure 2-4:** Water Surface Elevations for Mean Tide at Reuben's Wharf, after Schuepfer 1985

(Schuepfer, 1985), the nodal point begins between Gull and Sturgeon Islands (Figure 2-1) and gradually moves north along the Intracoastal Waterway as flow through Great Channel increases. Thus, initially, Ingram Thorofare dominates the flow through the Intracoastal Waterway in the nodal point region, but Great Channel contributes approximately equal flow discharge a few hours into the flood. Thus, on the flood, the Intracoastal Waterway is comparable to a line source of flow which spills over into Great Sound.

Flow velocities in the Sound have been recorded by Grizzle (1985) at the sites shown in Figure 2-1, and calculated throughout the Sound from the HYDTID model by Schuepfer (1985). Both researchers found maximum velocities to occur at peak flood, and typically reach 0.35 m/s independent of the tidal condition. At slack high and low tide the velocity is zero. This relatively low velocity range in the Sound contrasts with recorded velocities in the contributing channels of over 1 m/s. An example of a velocity profile from Great Sound, recorded by Grizzle (1985) at site #3 in Figure 2-1, is shown in Figure 2-8. This profile demonstrates the uniformity of the velocity over much of the depth under fair weather conditions.

Grizzle (1985) also determined shear velocities, $U_*$, in the Sound at all of his data collection sites. Table 2-1 shows the shear velocities with corresponding flow velocities for the various locations in the Sound given in Figure 2-1 at various times in the tidal cycle. The flow velocity range corresponds to various times in the tidal cycle, with near zero velocities occurring at slack low and slack high tide, and peak velocities in the range of 0.35 m/s occurring at peak flood.

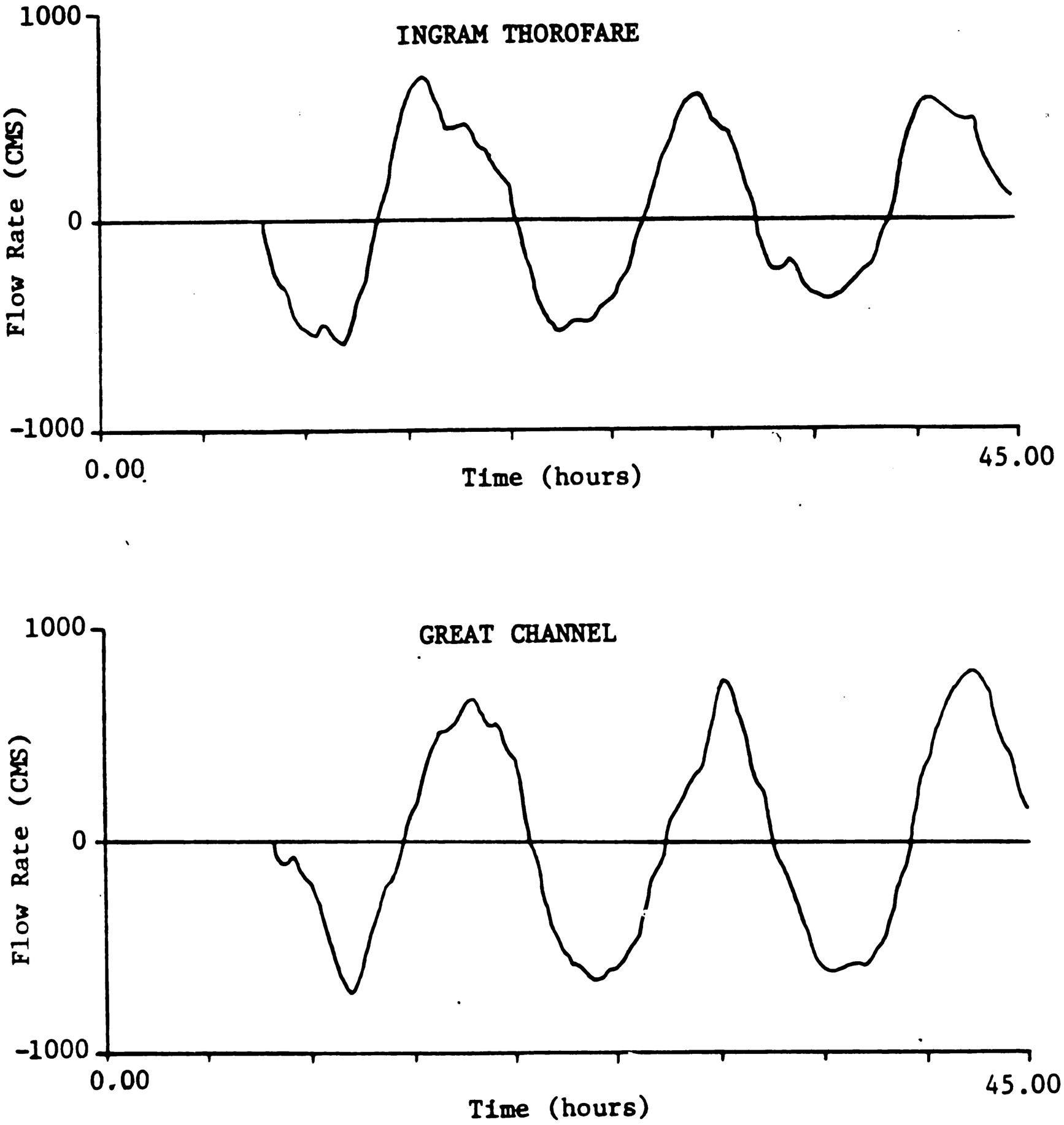


**Figure 2-5:** Flow Rate vs. Time in Ingram Thorofare and Great Channel, Spring Tide, after Schuepfer 1985

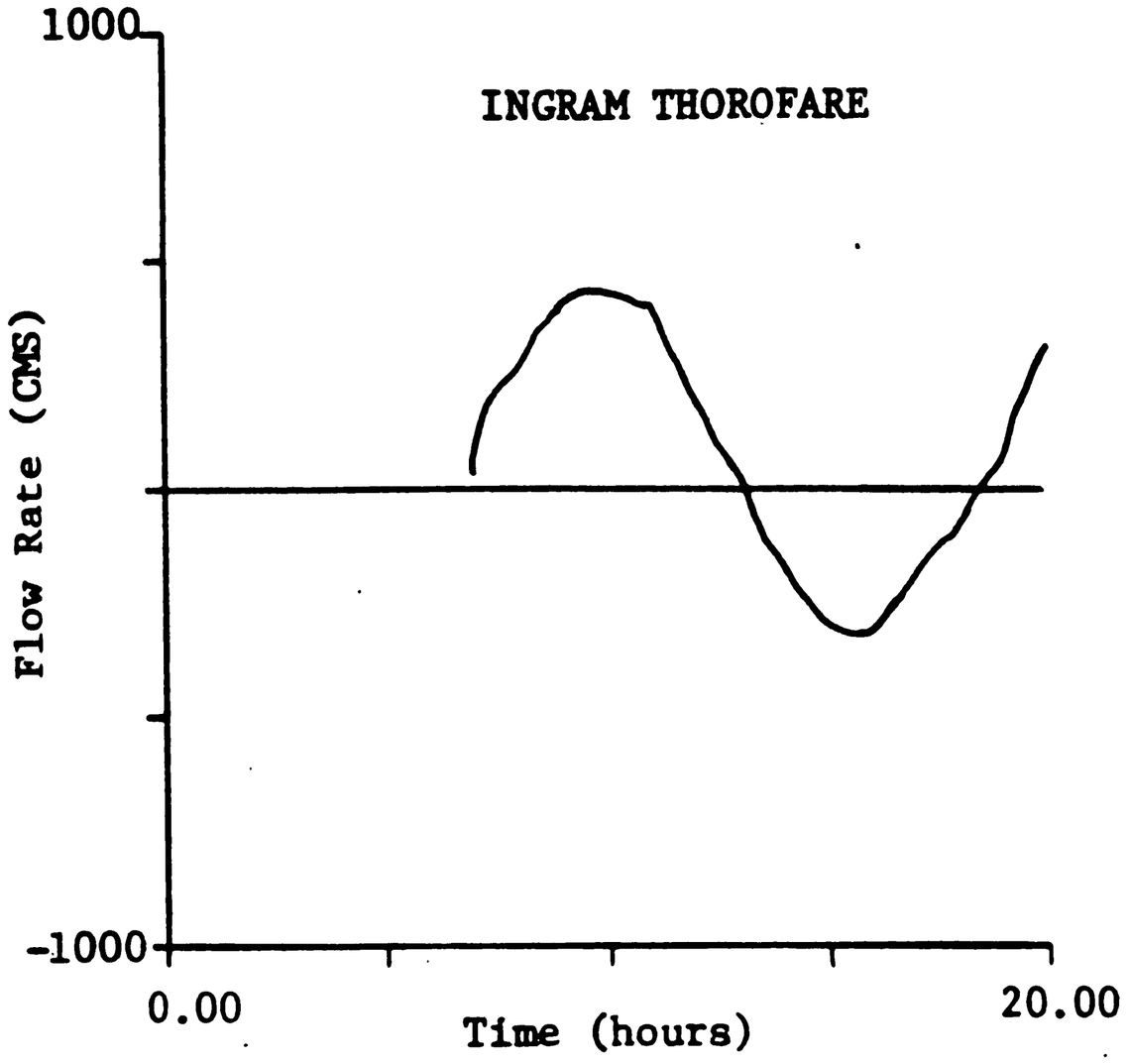


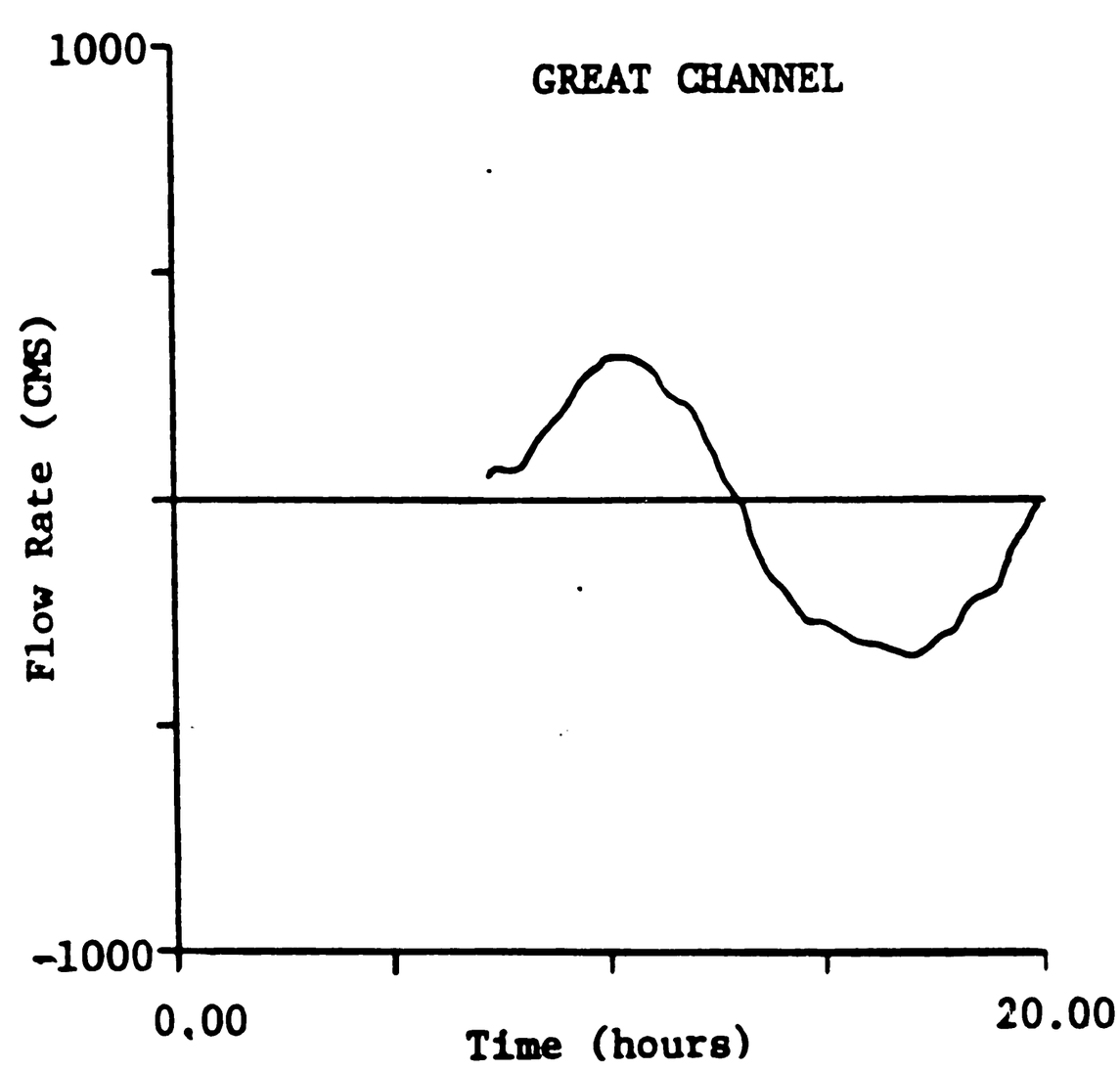


**Figure 2-6:** Flow Rate vs. Time in Ingram Thorofare and Great Channel, Neap Tide, after Schuepfer 1985

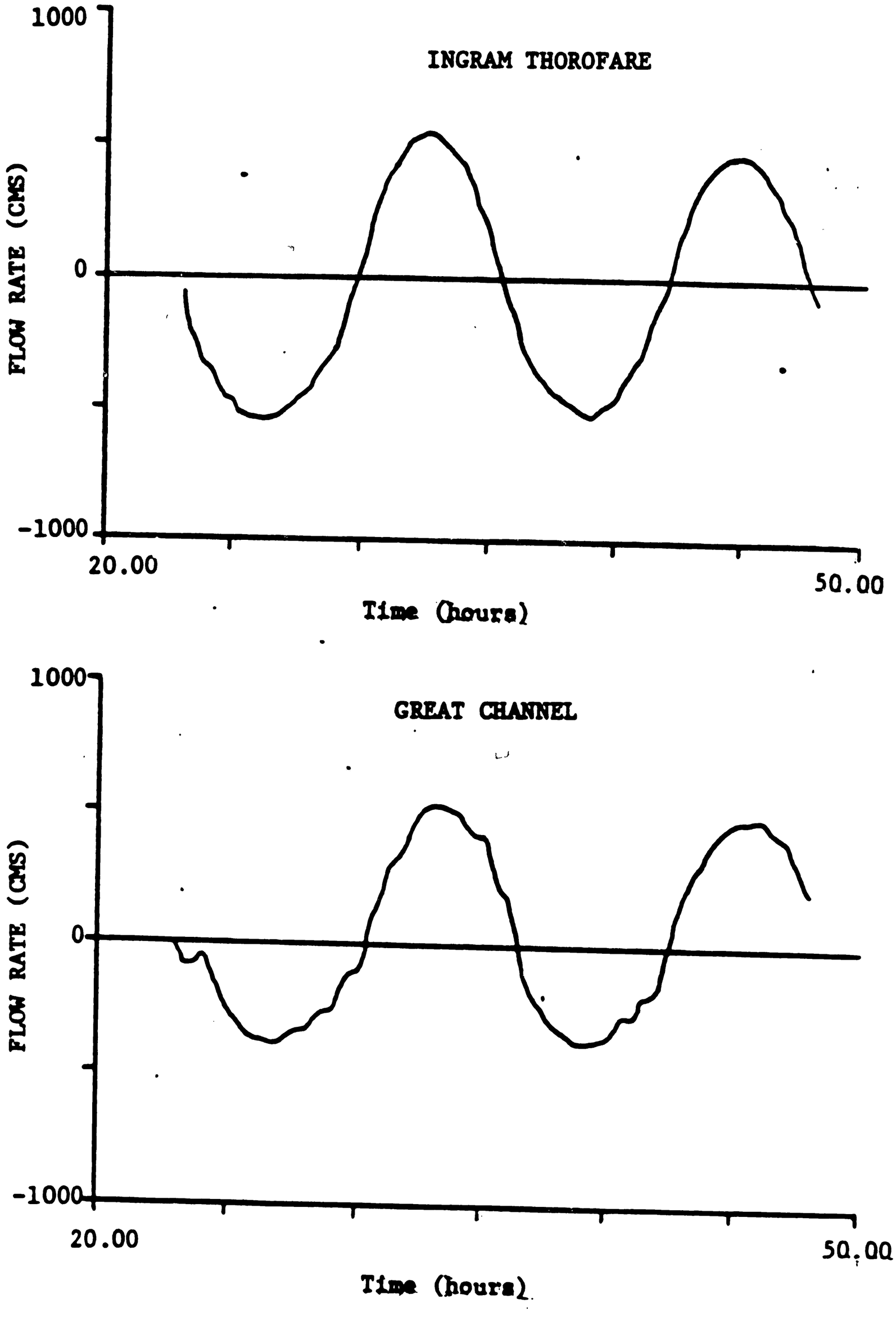


**Figure 2-7:** Flow Rate vs. Time in Ingram Thorofare and Great Channel, Mean Tide, after Schuepfer 1985

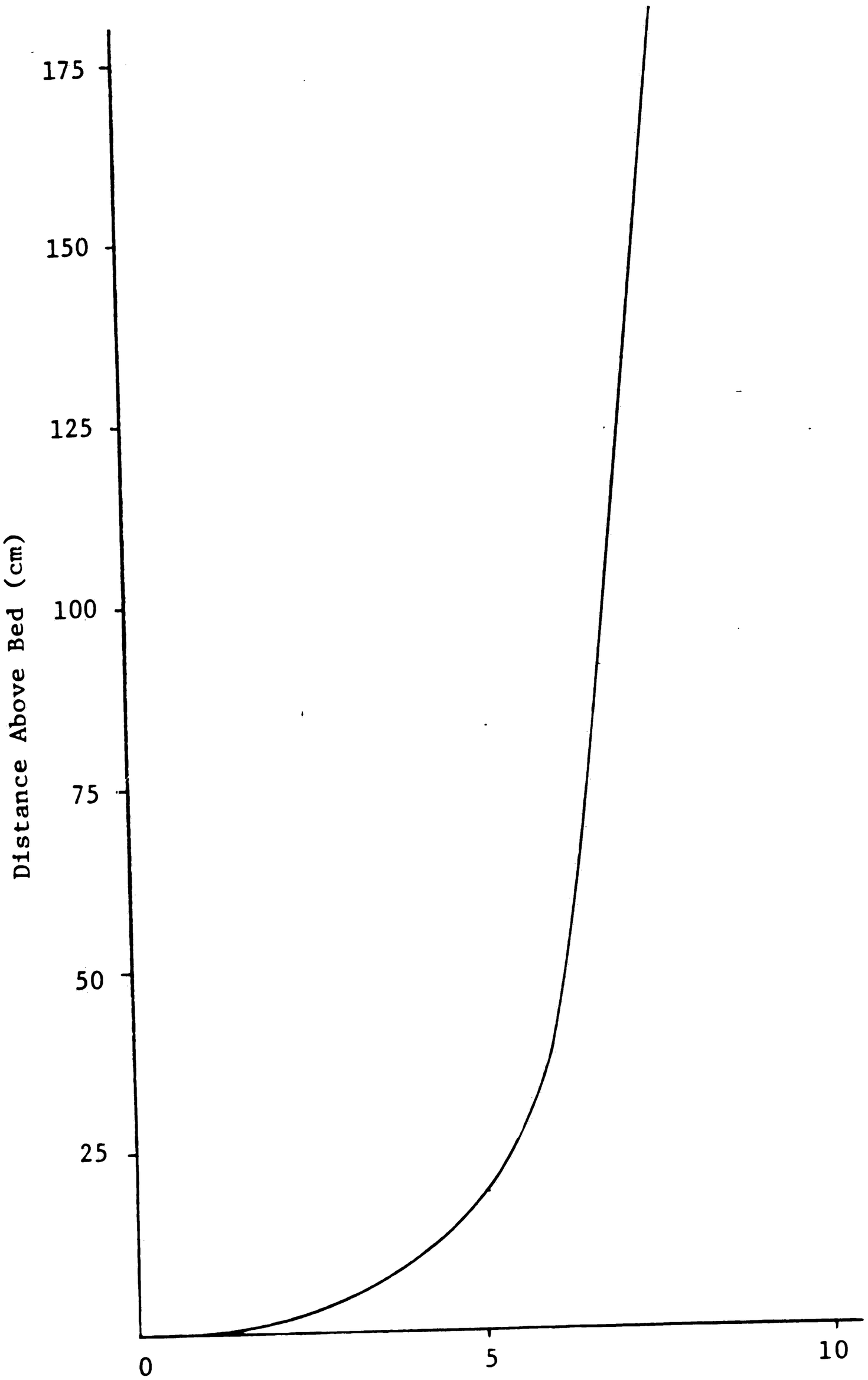


**Figure 2-8:** Velocity Profile in Great Sound for GS 3, Spring Tide, as shown in Table 2-1, after Grizzle, 1985

| | NEAP TIDE | | SPRING TIDE | |
|---|---|---|---|---|
| STATION | $u_*$(cm/s) | $\bar{u}$(cm/s) | $u_*$(cm/s) | $\bar{u}$(cm/s) |
| GST 1 | 1.29 | 7.5 | 0.55 | 7.4 |
| | 0.87 | ≈7.5 | 1.47 | 12.4 |
| GST 2 | 0.59 | 7.1 | 1.47 | 10.6 |
| | 0.81 | 5.9 | - | - |
| GS 2 | 2.32 | 14.0 | 1.24 | 11.9 |
| | 1.09 | 6.8 | 1.54 | 11.9 |
| GS 3 | 0.55 | 3.9 | 0.60 | 5.9 |
| | 0.69 | 6.3 | 0.75 | 7.1 |
| GS 6 | 1.57 | 15.2 | 1.14 | 20.3 |
| | 2.23 | 30.8 | 1.63 | 30.0 |
| GS 7A | 0.44 | 14.3 | 3.11 | 42.1 |
| | 1.63 | 24.0 | 3.05 | 41.1 |
| GS 9 | - | - | 0.97 | 5.4 |
| GS 13A | - | - | 1.26 | 8.3 |
| GS 13D | 0.32 | 3.6 | 1.83 | 9.6 |
| GS 15 | - | - | 0.57 | 5.8 |
| GS 17 | 0.53 | 7.9 | 0.56 | 7.4 |
| | 0.51 | 7.1 | 0.94 | 11.8 |
| GS 19 | 0.22 | 5.1 | 0.63 | 5.5 |
| | - | - | 1.35 | 9.5 |
| GS 22 | 1.77 | 19.1 | 1.23 | 30.3 |
| | 1.58 | 25.7 | 1.05 | 39.5 |

**Table 2-1:** Flow and Shear Velocities in Great Sound, after Grizzle, 1985; dash indicates data not available

| FRACTION # | EQUIVALENT DIAMETER* (microns) | SETTLING VELOCITY (mm/s) | AVERAGE PARTICLE DENSITY ($kg/m^3$) |
|---|---|---|---|
| 1 | <2.0 | 0.002 | 1.67 |
| 2 | 2.0–2.8 | 0.004 | 2.42 |
| 3 | 2.8–4.6 | 0.008 | 2.45 |
| 4 | 4.6–7.8 | 0.022 | 2.76 |
| 5 | 7.8–13.2 | 0.0565 | 2.75 |
| 6 | 13.2–22.1 | 0.166 | 2.57 |
| 7 | 22.1–37.0 | 0.460 | — |
| 8 | 37.0–62.5 | 1.26 | — |
| 9 | >62.5 | 3.43 | — |



* Quartz Sphere, $\rho = 2.65$ $kg/m^3$

Dash indicates data not available

**Table 2-2:** Particle Sizes, Settling Velocities and Average Densities, after Carney, 1982

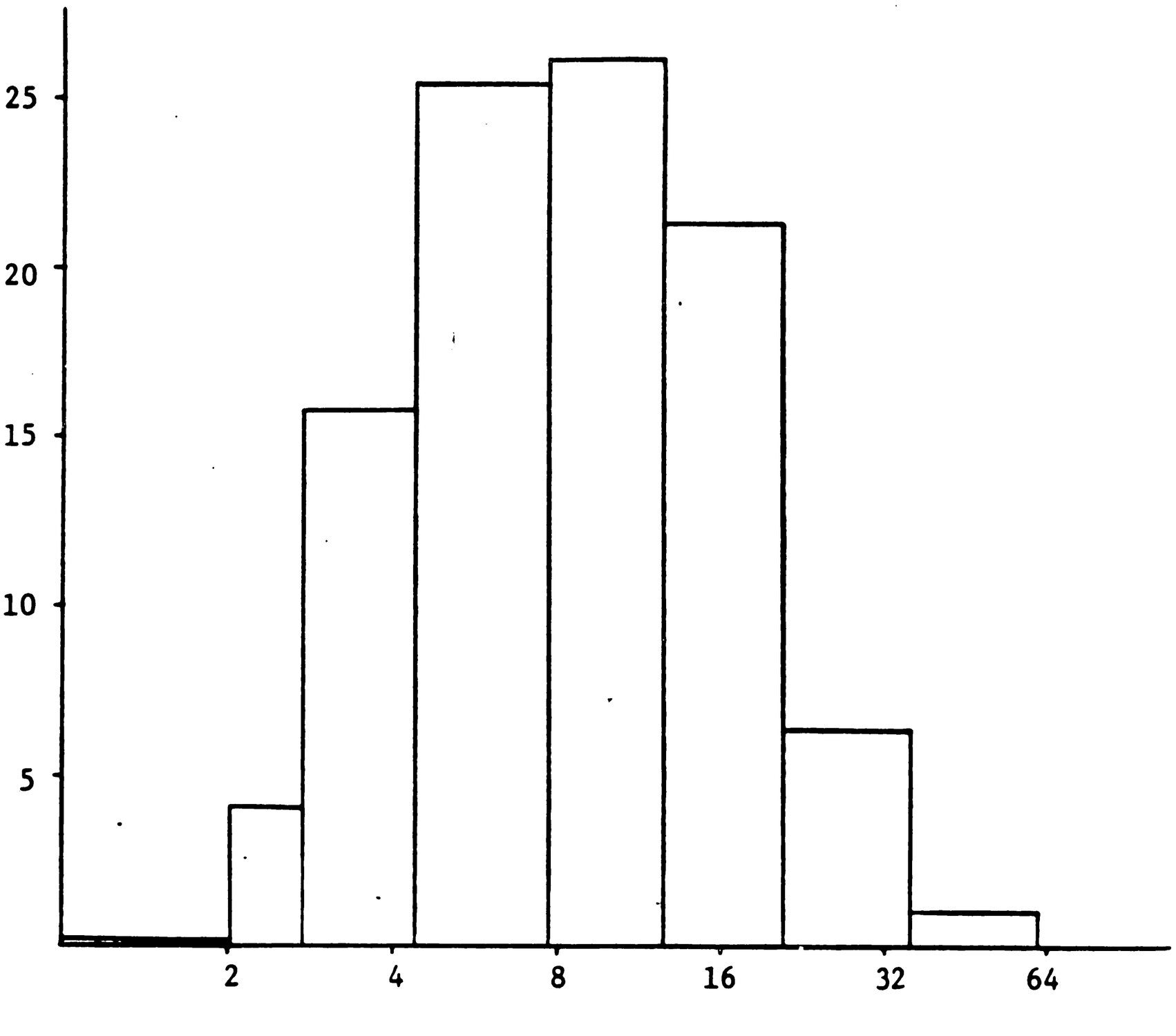


**Figure 2-9:** Volumetric Distribution of Sediment, after Carney, 1982

## 2.3 Sediment Characteristics

Suspended sediment is transported through Ingram Thorofare and Great Channel into Great Sound with each flood tide. To characterize the sediment transported through the channels, Carney (1982) took sediment samples in Great Channel at the location indicated in Figure 2-1. Instead of taking samples periodically through a single tidal cycle, Carney took one sample at the same time of day for 15 consecutive days. Since the tide shifts by approximately an hour each day, Carney was able to simulate a complete tidal cycle using this method. As a result, however, his concentration hydrograph represents a range of tidal and weather conditions.

The sediment is made up of two types of aggregate particles, fecal pellets and flocculates, also known as organic-mineral aggregates or agglomerates. These are classified as cohesive particles. Only the inorganic fraction is considered in this study because organic matter is volatilized and does not contribute to the sediment accumulation. The inorganic portion of the flocculates consists of fine sand- to clay-size grains. Most flocculates observed by Carney were less than 60 microns in size.

Carney defined the sediment size classification in terms of quartz grain equivalent diameters. The particle equivalent size range is from 2 to 64 microns. Table 2-2 shows the equivalent particle sizes and settling velocities determined for each of the nine settling velocity fractions established in the analysis, along with the average densities for the first six fractions as presented by Carney. Note that the settling velocities vary by three orders of magnitude. The volumetric distribution of sediment for the nine size fractions is shown in Figure 2-9. Faas (1984) determined the bulk density of bottom sediments in

Great Sound to be 1.5 g/cc.

Sediment concentrations in the Sound have been recorded by Carney (1982) and Griffith (1986) at locations shown in Figure 2-1. In fair weather, the average concentration over a tidal cycle is typically 10 mg/l. Figures 2-10 and 2-11 show fair weather concentration hydrographs recorded by Carney and Griffith, respectively. As mentioned previously, Carney's data was recorded over 15 days, one reading at a different time in the tidal cycle each day, while Griffith's data was taken periodically through a single tidal cycle. As the figures show, the maximum concentrations are closely related to the maximum flood and ebb flows.

The concentration also varies as a function of existing meteorological conditions. In storm conditions the concentration may vary by up to two orders of magnitude. Suspended sediment concentrations in the Chesapeake Bay were recorded during Hurricane Agnes which exceeded 100 times the fair weather concentrations (Schubel, 1975). No attempt has been made to record concentration data in Great Sound during such a storm event. Griffith (1986) measured the concentration profile in the Intracoastal Waterway the day after Hurricane Gloria passed through the region (September 28, 1985), as shown in Figure 2-12. The prevailing meteorological conditions that day would be classified as "fair weather". However, as Figure 2-12 shows, post-storm concentrations are an order of magnitude above normal fair weather concentrations.

No frequency of occurrence curves are available for concentration data in the Sound. A concentration versus frequency diagram which may parallel concentration frequencies in the Sound is shown in Figure 2-13. The diagram

was established by Maa et al. (1985) based on 265 days of data recorded at a marina on Florida's east coast.

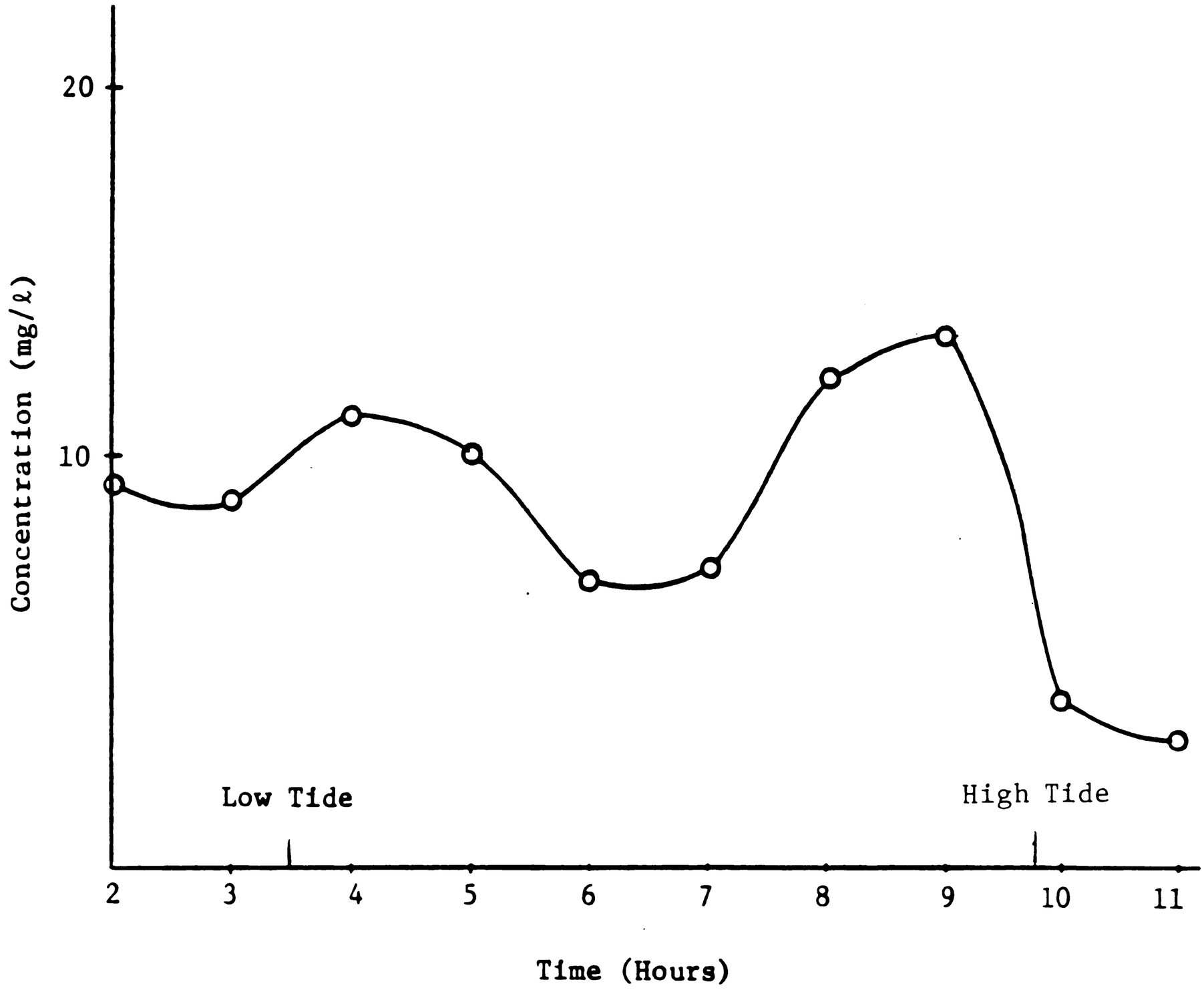


**Figure 2-10:** Fair Weather Near Bottom Inorganic Sediment Concentration Hydrograph in the Intracoastal Waterway, after Carney, 1982

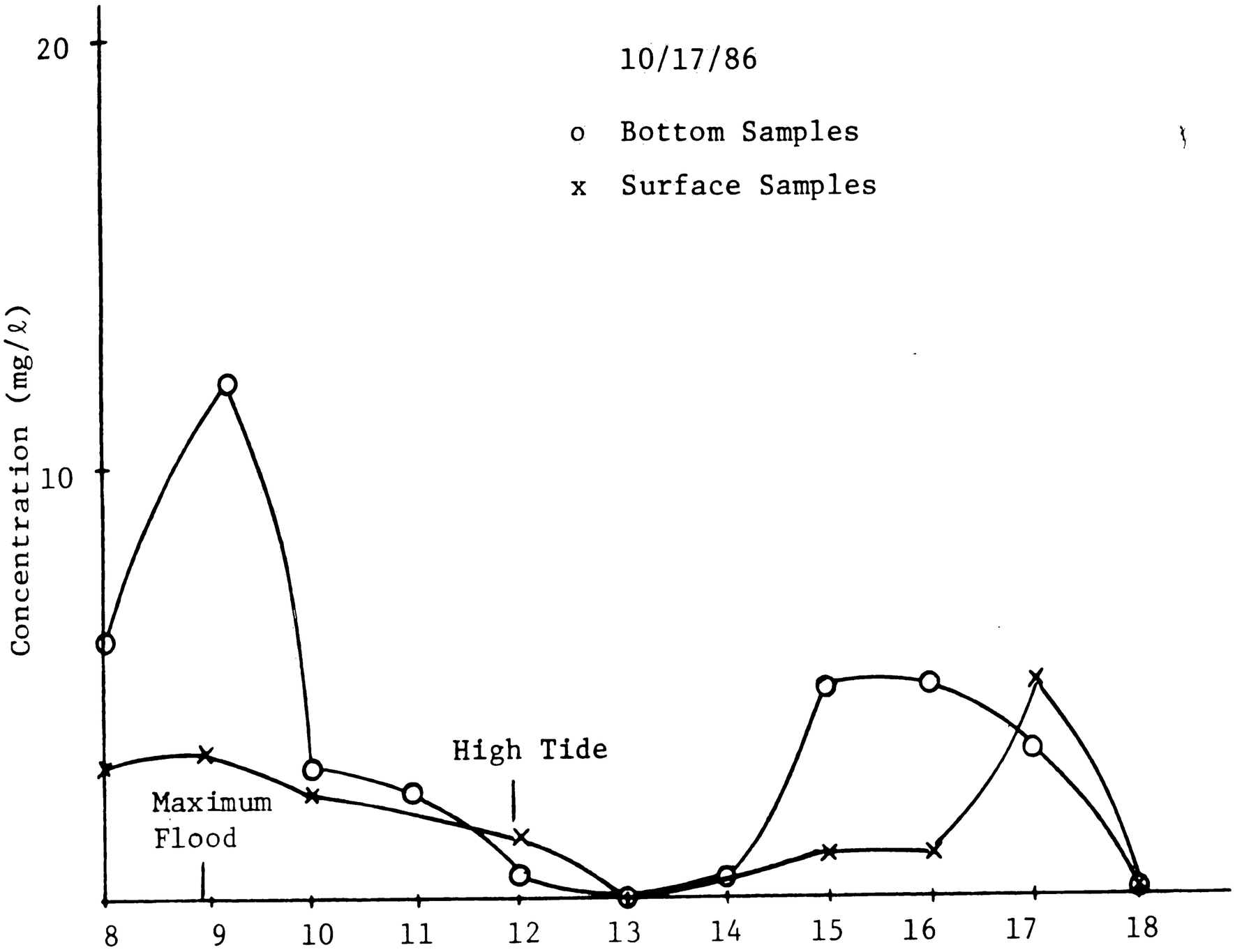


**Figure 2-11:** Fair Weather Inorganic Sediment Concentration Hydrograph in the Intracoastal Waterway, after Griffiths, 1986

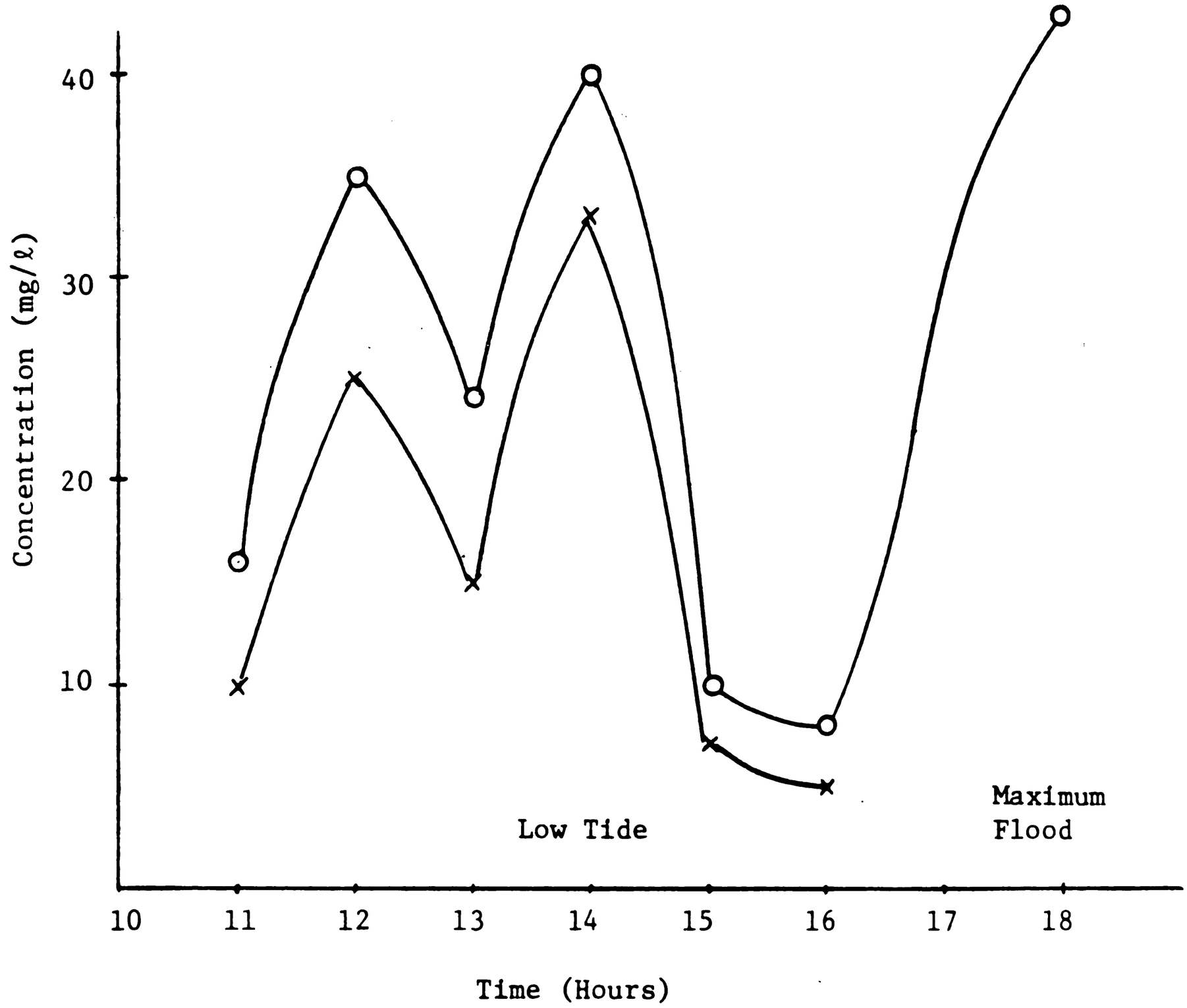


**Figure 2-12:** Inorganic Sediment Concentration Hydrograph, Post Hurricane Gloria, after Griffiths, 1986

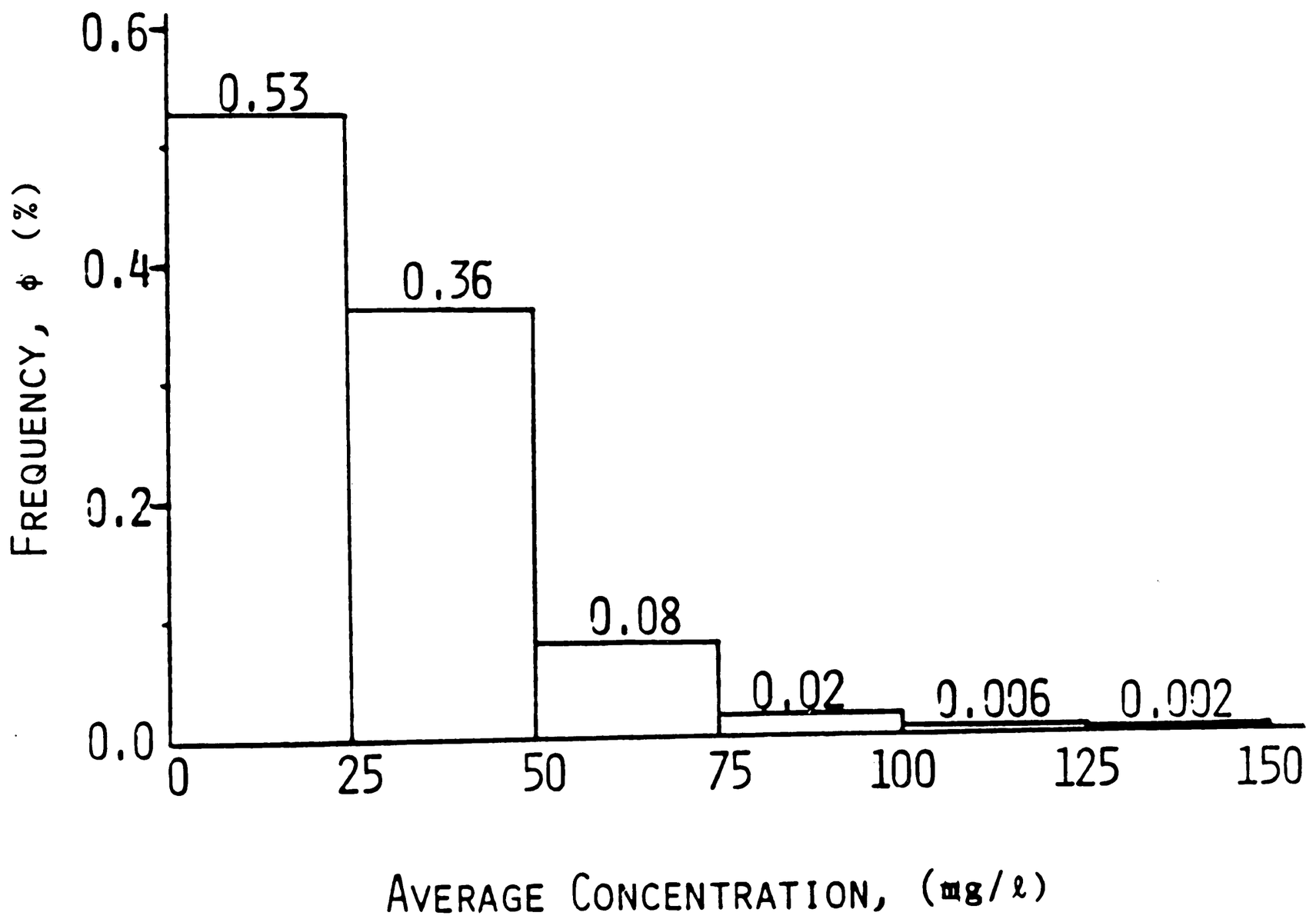


**Figure 2-13:** Concentration vs. Frequency in a Florida Marina, after Maa et al., 1985

# Chapter 3
# Development of the Model

## 3.1 The Basic Settling Tank Concept

The physical characteristics of Great Sound, including its small areal extent, protected location, uniform topography and low east-west flow velocities, are the basic characteristics found in a sediment deposition basin. These characteristics, along with the shallow depth and limited data mentioned in Section 1.4, encourage the use of a settling tank model to analyze sediment deposition in Great Sound, while evaluating the adaptability of such a model to the coastal environment.

Thomas Camp (1946), in his paper on the design of settling tanks, defines an "ideal basin" as a hypothetical settling tank in which settling takes place in exactly the same manner as in a quiescent settling container of the same depth. In extending his analysis to regions of continuous flow, Camp defines the following characteristics for an "ideal continuous flow basin":

1. The direction of flow is horizontal and the velocity constant in all parts of the settling zone.

2. The concentration of suspended particles of each size is the same at all points in the vertical cross section at the inlet end of the settling zone.

3. A particle is removed from suspension when it reaches the bottom of the settling zone.

Four basic types of particle settling can occur in such a settling basin (Barfield et al., 1981).

1. Discrete Particle - settling in low concentration solutions where particles tend to fall independent of one another.

2. Flocculant - settling in which dilute solutions of particles coalesce to form particles of larger mass and higher settling velocity.

3. Hindered - particles are so concentrated that forces between particles hinder the settling of neighboring particles.

4. Compression settling - particles are concentrated to the point of forming a structure requiring compression for further settling to take place.

Tapp et al. (1981) have shown that all four types of settling can occur simultaneously in a settling tank. In the Sound, cohesive sediment particles exist in very low concentrations, and thus, settle as discrete particles. Many of these particles are flocculated, as previously described, but the flocculation process occurs prior to the entrance to the Sound, not in the Sound itself. Because of the very low concentrations existing in the Sound, hindered particle settling does not occur. Compression settling may occur at the bottom of the Sound, but its effects are incorporated in the bulk density.

Figure 3-1 shows an ideal settling tank. The tank is comprised of four zones according to function. (1) An inlet zone where the suspensate is uniformly dispersed over the cross section of the tank. (2) The settling zone in which all the settling takes place. (3) An outlet zone in which the clarified liquid is collected uniformly over the cross section of the tank. (4) A deposition zone where the sediment collects at the bottom.

In the settling zone, the trajectory of settling particles is defined by the vector sum of the particle settling velocity ($V_s$) and the horizontal fluid velocity ($U_x$) in which the particle is transported. In the ideal basin, the paths of all discretely settling particles will be straight lines, with all particles of the same settling velocity moving in parallel paths. A particle starting at the surface of the inlet zone which settles precisely at the outfall defines the critical settling

velocity of the given basin, $V_{s_{cr}}$. In equation form,

$$\frac{V_{s_{cr}}}{U_x} = \frac{H}{L} \tag{3.1}$$

The path of $V_{s_{cr}}$ is shown in Figure 3-1. All particles of settling velocity $V_s > V_{s_{cr}}$ will be deposited. Particles of $V_s < V_{s_{cr}}$ will deposit at a rate equal to the ratio of $V_s/V_{s_{cr}}$. That is, if the path of $V_s$ is traced back from the bottom of the outlet, its resulting depth at the inlet will determine the percentage of particles $V_s$ which are deposited. Thus, if at the inlet, $V_s$ is at fifty percent of the depth of the tank, then fifty percent of the particles $V_s$ will deposit, and the ratio $V_s/V_{s_{cr}} = 0.5$, as shown in Figure 3-1.

To determine the efficiency of a settling tank for retaining sediment, the most common parameter is the trapping efficiency E, where

$$E = \frac{M_{in} - M_{out}}{M_{in}} \times 100 \tag{3.2}$$

Here, E is the percent of mass that is trapped, and $M_{in}$ and $M_{out}$ are the masses of sediment flowing in and out of the tank, respectively. Equation (3.2) is actually a modification of the mass balance equation which states that the mass in minus the mass out must equal the rate of change of mass in the system, which, in this case, is the trapped sediment.

## 3.2 Extending the Settling Tank Concept to Unsteady Flow

For unsteady flow conditions, Barfield et al. (1981) list the following factors which control sediment motion through a basin:

1. Physical characteristics of the sediment
2. Hydraulic characteristics of the basin
3. The sediment concentration hydrograph

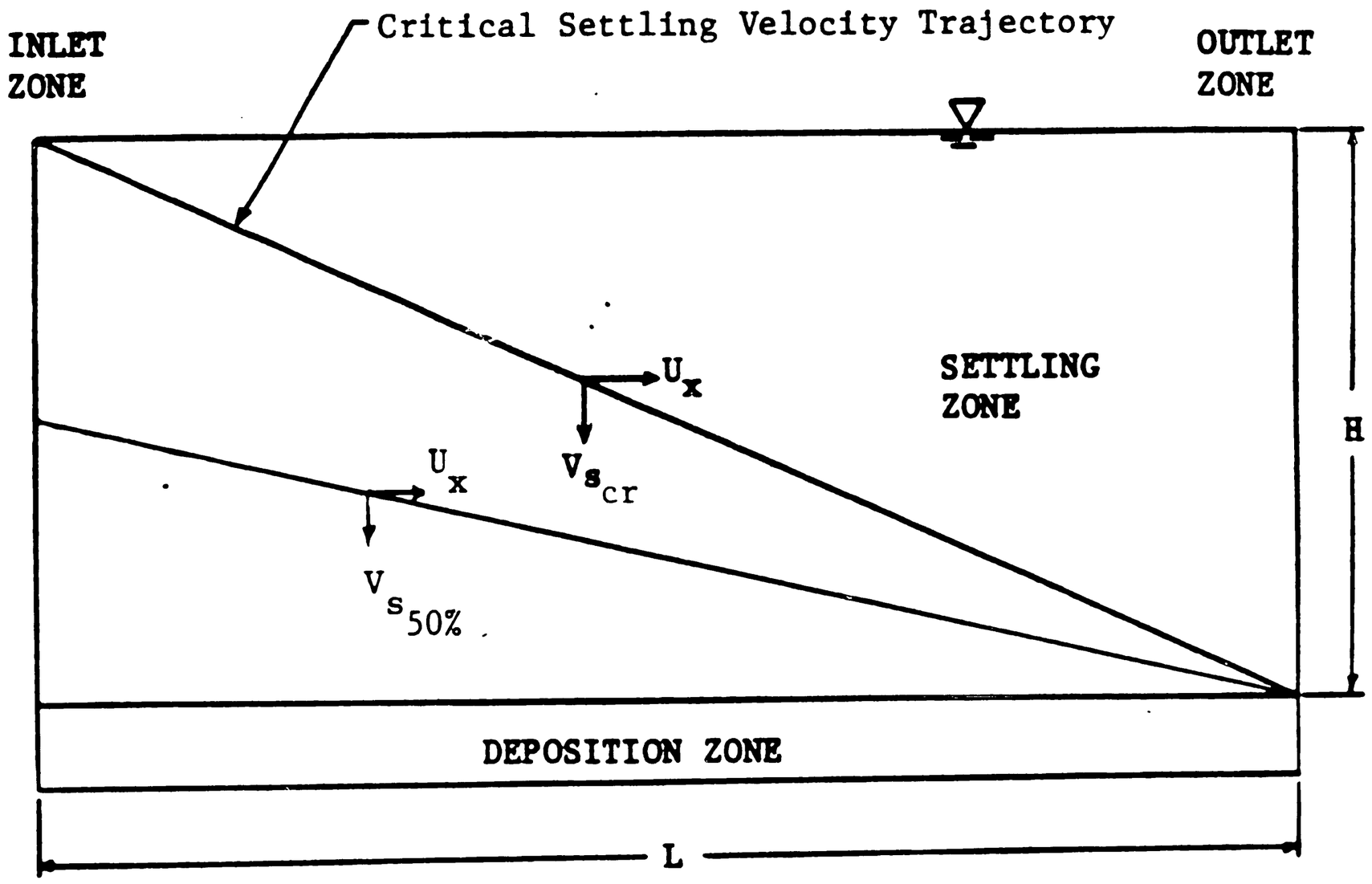


**Figure 3-1:** An Ideal Settling Tank Showing the Critical Settling Trajectory and the 50% Settling Trajectory

4. The inflow hydrograph

5. The basin geometry

6. The chemistry of the water and the sediment

These parameters form the basis from which numerical models have been developed to analyze sediment deposition in settling basins where unsteady flow conditions exist. Two of these models are mentioned here.

Ward, Haan and Barfield (1977) developed a conceptual model called DEPOSITS (Deposition Performance Of Sediments in Trap Structures) to simulate the performance of ponds in trapping sediment particles. The DEPOSITS model uses plug flow to route storm water and sediment through a settling basin. In plug flow, volumes (plugs) of fluid move through a settling basin without mixing with one another. Thus, flow is on a first in, first out basis. Stokes' Law is used to model the settling of sediment particles in the water column. Each plug is divided into four distinct horizontal layers. Because theoretical plug flow rarely occurs in real detention basins, factors are incorporated to approximate non-plug flow conditions. One factor is used to allow some of the dead storage in a pond to be excluded from the calculations. Another is used to simulate basin short circuiting by putting more sediment into each plug. Also, since Stokes' Law only applies to quiescent settling conditions, a factor is included to account for the effect of turbulence on reducing the particle settling velocity. Each of these factors are at best approximations and their use in the DEPOSITS model is cautioned by the model developers.

Another model, developed by the EPA (1976), is used mostly in the analysis of surface mined sediment ponds. In the EPA model, the particle size

distribution is divided into fractions, with a settling velocity determined for each fraction. The critical settling velocity $V_{s_{cr}}$ is determined along with the trapping efficiency, E. An outflow particle size distribution is calculated based on the fraction of particles removed.

## 3.3 Adaptation of Camp's Settling Tank Concept to Great Sound

### 3.3.1 Characteristics of Tidal Basins

Two unique characteristics of tidal basins must be considered to modify Camp's (1946) settling tank model to the Sound. These characteristics are: 1) a single inlet/outlet for the flow and 2) an oscillating flow field due to the astronomical tide.

Figure 3-2 profiles the settling tank model for Great Sound shown in plan view in Figure 2-1. For such a single inlet/outlet system, instead of flow occurring as first in, first out (as for a sediment detention basin), it occurs as first in, last out. As flow passes through Great Channel and Ingram Thorofare, it approaches the nodal point in the Intracoastal Waterway previously described in Section 2-2. Flow then proceeds across the Sound from the Intracoastal Waterway. Thus, the Intracoastal Waterway is defined as the inlet and outlet of the settling tank model.

The unsteady flow field imposed on Great Sound by the astronomical tide was analyzed by Schuepfer (1985) using the finite difference model HYDTID developed by Masch et al. (1977). The depth, velocity and direction of flow are variable in time and space and simulated as such in the HYDTID model. The flow rates at the Sound boundary determined previously in Section 2.2 are

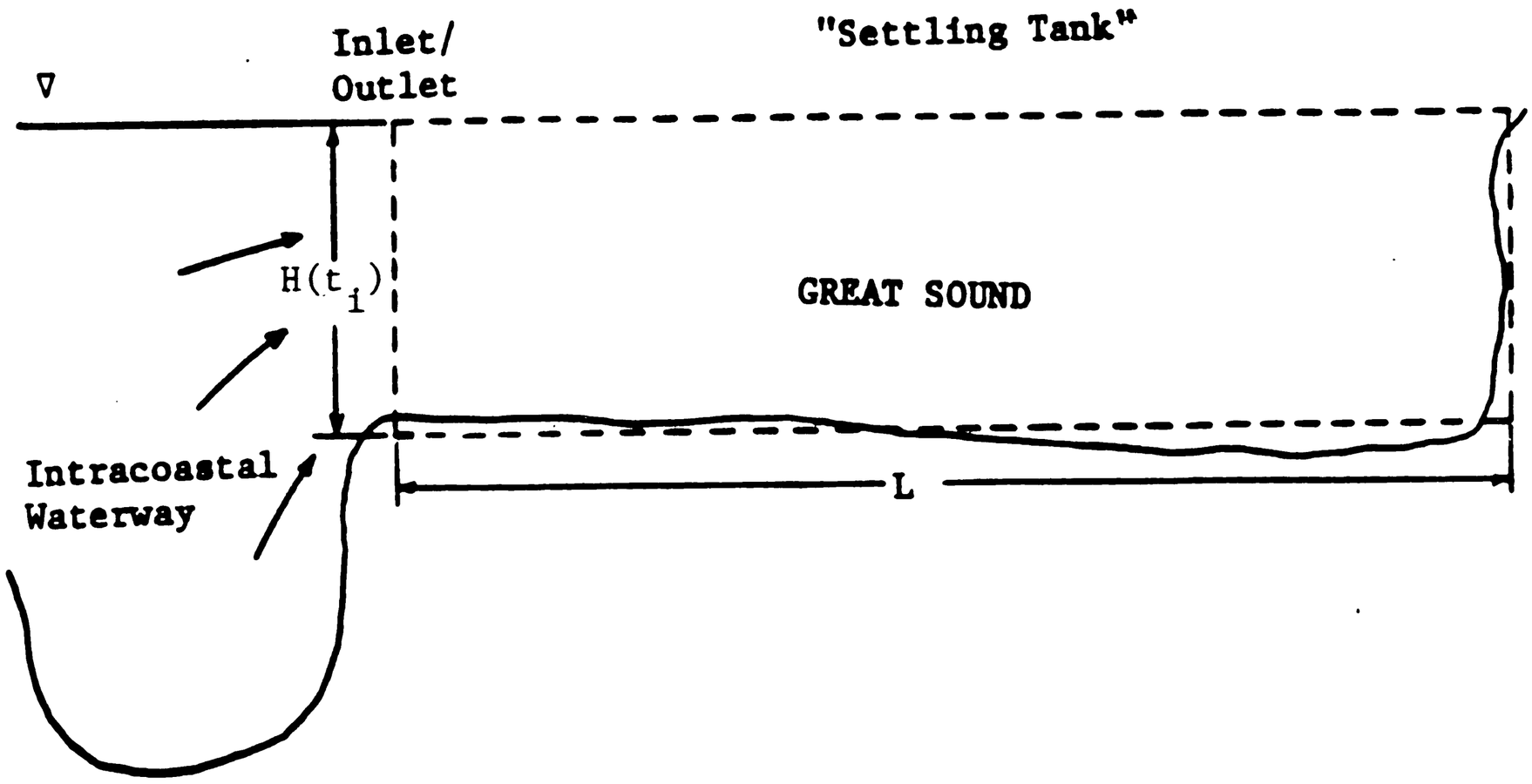


**Figure 3-2:** Settling Tank Model for Great Sound

entered as input data to the settling tank model, which simulates the tidal hydrodynamics with the "plug flow" approach used in the DEPOSITS model (Ward et al. 1977). To justify the use of a plug flow model, an analysis of mixing by dispersion and diffusion processes preceeds the analysis of tidal hydrodynamics.

### 3.3.2 Diffusion and Dispersion Processes

To validate the use of a plug flow model in which no diffusion or dispersion takes place, it must be shown that the role of diffusion and dispersion processes in the Sound is negligible. This is accomplished in the following paragraphs by showing that the dispersion terms in the one-dimensional convective-diffusion equation are small enough to neglect.

In the literature, diffusion is frequently used interchangeably with the term dispersion, causing an occasional difficulty with terminology. Holley (1969) suggests the following definition for diffusion:

> Diffusion - transport in a given direction at a point in the flow due to the difference between the true convection in that direction and the time average of convection in that direction.

Fischer (1979) defines two kinds of diffusion, molecular diffusion and turbulent diffusion. Molecular diffusion occurs by random molecular motion. Turbulent diffusion describes the random motion of lumps of fluid, which is analogous to molecular diffusion, but with "eddy" diffusion coefficients.

For dispersion, Holley (1969) suggests:

> Dispersion - transport in a given direction due to the difference between the true convection in that direction and the spatial average of the convection in that direction.

Thus, convection here refers to transport by the temporally and spatially

averaged flow. It will be shown that, for the Sound, convection dominates.

Fischer (1979) has shown that the effects of dispersion in the longitudinal direction are up to forty times the magnitude of turbulent mixing (diffusion). Thus, the effects of diffusion can be incorporated into the dispersion analysis. The basic dispersion equation for a quiescent fluid is described by the continuity equation which incorporates Fick's Law,

$$\frac{\partial C}{\partial t} = D \frac{\partial^2 C}{\partial x^2} \tag{3.3}$$

Here, C is the mass concentration of diffusing solute and D is the coefficient of proportionality, or the dispersion coefficient. D has the dimensions of length squared per time.

In any body of water, the total rate of mass transport is the sum of the convective plus diffusive flux. The result is the two-dimensional convection-dispersion equation which includes a sink term representing deposition.

$$\frac{\partial C}{\partial t} + U \frac{\partial C}{\partial x} + V \frac{\partial C}{\partial y} = D_x \frac{\partial^2 C}{\partial x^2} + D_y \frac{\partial^2 C}{\partial y^2} + R_d \tag{3.4}$$

Here, U and V are the depth-averaged flow velocities in the x and y directions, $D_x$ is the longitudinal dispersion coefficient, $D_y$ is the lateral dispersion coefficient and $R_d$ is the rate of deposition.

The relative effects of lateral and longitudinal dispersion are important considerations in the analysis. Because the Sound can be assumed to be a very wide channel with the inlet along the Intracoastal Waterway (Figure 2-1), the velocity is assumed uniform across the width. Thus, the transverse (y-directional) flow is negligible, $\partial C/\partial y$ is zero for an assumed line source across the flow and the effects of lateral dispersion are inconsequential. Based on this result, the one-dimensional convection-dispersion equation can be applied:

$$\frac{\partial C}{\partial t} + U \frac{\partial C}{\partial x} = D \frac{\partial^2 C}{\partial x^2} + R_d \qquad (3.5)$$

where D is now the longitudinal dispersion coefficient which may be scale and time dependent.

For unidirectional flow, Fischer (1967) shows that the longitudinal dispersion coefficient is time dependent during an initial period, where the one-dimensional equation is still not applicable. In tidal regions, however, the initial period occurs in the feeder channels and flow is well mixed as it reaches the Sound. Thus, the one-dimensional equation is applicable for conditions in the Sound. Also, in laboratory experiments on dispersion in an oscillating flow (e.g. tidal flows), Holley and Harleman (1965) have shown that the time dependence of the longitudinal dispersion coefficient may be neglected. Therefore, in an oscillating flow, the longitudinal dispersion coefficient, D, is assumed to depend only on x.

The dispersion coefficient, D, was derived by Elder (1959) for flow in an infinitely wide channel as

$$D = 5.9\, d\, U_* \qquad (3.6)$$

where d is the flow depth, and $U_*$ is the shear velocity. However, experiments by Godfrey and Frederick (1970), and Fischer (1968,1975) show clearly that Elder's result does not apply to real streams. The range of values of $D/dU_*$ for wide channels varies from 8.6 to 7500, but is predominately in the range of 150 to 500 (Fischer et al., 1979). Harleman et al. (1968) presents an equation for the dispersion coefficient in estuaries, where D depends primarily on the magnitude of the tidal velocity, as

$$D = 7.15\, n\, U_{x,t}\, R_h^{5/6} \qquad (3.7)$$

where n is the Manning roughness coefficient, $R_h$ is the hydraulic radius (m), $U_{x,t}$ is the tidal velocity (m/s), and D has the units of $m^2/s$.

By non-dimensionalizing the one-dimensional convective-dispersion equation (3.5), the relative effect of the dispersion term can be evaluated. The following terms in the equation are non-dimensionalized:

$C' = C/C_o$ where $C_o$ = mean concentration
$t' = t/T$ where $T$ = one diurnal cycle (12 hours, 25 minutes)
$u' = u/U_{max}$ where $U_{max}$ = peak velocity
$x' = x/L$ where $L$ = length of the sound

Inserting these expressions into Equation (3.5) yields:

$$\frac{C_o(\partial C')}{T(\partial t')} + u' U_{max} \frac{C_o(\partial C')}{L(\partial x')} = D \frac{C_o(\partial^2 C')}{L^2(\partial x'^2)} \tag{3.8}$$

Multiplying by $T/C_o$ yields:

$$\frac{\partial C'}{\partial t'} + A' u' \frac{\partial C'}{\partial x'} = D' \frac{\partial^2 C'}{\partial x'^2} + R_d \frac{T}{C_o} \tag{3.9}$$

where $D' = DT/L^2$ and $A' = U_{max} T/L$. Thus, using Equation (3.7) for $D$, the resulting dimensionless dispersion coefficient, $D'$, is

$$D' = 7.15\, n\, U_{x,t}\, R_h^{5/6}\, T/L^2 \tag{3.10}$$

The maximum value of the dimensionless dispersion coefficient, $D'_{max}$, occurs when $U = U_{max}$, or

$$D'_{max} = 7.15\, n\, U_{max}\, R_h^{5/6}\, T/L^2 \tag{3.11}$$

The dimensionless coefficients, $D'$ and $A'$ are calculated for the mean tidal range in the Sound of $R_h = 1.25\ m$. From the data presented in section 2.2, $U_{max} = 0.35\ m/s$; $T = 43200\ 3s$; $L = 2200\ m$, and Manning's n is assumed to

have a maximum value of 0.03. Then,

$$D'_{max} = 8.07 \times 10^{-4} \tag{3.12}$$

and

$$A' = 6.87 \tag{3.13}$$

The maximum dispersion coefficient is four orders of magnitude less than the coefficients of the other terms. Note that $u'$ ranges from 0 to 1. At slack low or high tide, when $u' = 0$, the equation reduces to

$$\frac{\partial C'}{\partial t'} = C_1 R_d \tag{3.14}$$

which is the equation defining quiescent settling where the concentration change with time equals the sediment deposition.

When $u' = 1$, flow velocity is maximum and Equation (3.9) becomes:

$$\frac{\partial C'}{\partial t'} + 6.87 \frac{\partial C'}{\partial x'} = 6.7 \times 10^{-4} \frac{\partial^2 C'}{\partial x'^2} + C_1 R_d \tag{3.15}$$

If the relative concentration gradient with distance, $\partial C'/\partial x'$, is small as expected, it can be stated that $\partial C'/\partial x' > \partial^2 C'/\partial x'^2$. The validity of this assumption can be checked by working backward from the results generated by the model. Thus, based on the coefficents, the first term on the right hand side of Equation (3.15) is considered negligible compared to the other terms.

The dimensional analysis shows, therefore, that for Great Sound the dispersion term in the one-dimensional equation is orders of magnitude smaller than all other terms including the convection term. This result supports the use of the plug flow modeling technique, which mathematically approximates the remaining equation

$$\frac{\partial C'}{\partial t'} + A' u' \frac{\partial C'}{\partial x'} = C_1 R_d \tag{3.16}$$

In their calculations of sediment accumulation in a small Florida marina, Maa et al. (1985) also eliminated the dispersion term.

### 3.3.3 Tidal Hydrodynamics as Implemented in the Model

#### Plug Flow Modeling

With the exception of storm wind conditions, the predominant force impacting hydrodynamics in the Sound is the astronomical tide. A sinusoidal forcing function is used to model this flow into and out of the Sound over each tidal cycle. The plug flow concept is applied to the sinusoidal inflow as follows. Plugs of fluid, which are considered to be discrete or non-mixing, are traced across the Sound during the flood, and back out during the ebb, at equal time intervals. Figure 3-3 is a sinusoidal flow versus time curve broken up into a histogram using equal time intervals of twenty minutes for flow entering and leaving the Sound. Each block of the histogram is the volume of a plug and, as the figure shows, the volume of fluid in the plugs is variable as a fuction of time.

A finite volume of fluid exists in the Sound at slack ebb (MLW). This volume of fluid is considered to always be present in the Sound. As the tide rises, plugs of flow begin entering the Sound from the Intracoastal Waterway, pushing the original volume further into the Sound. Figure 3-4 shows the first plug of fluid entering the Sound over the first twenty minute interval as the flood tide begins. Figure 3-5 shows the change of position and geometry of plug 1 as a function of time. The increase and then decrease in velocity as peak flood approaches and wanes is seen in the increasing and then decreasing horizontal distance between plug positions over the flood. Because the volume of plug 1 remains constant as the depth increases, the width must decrease with

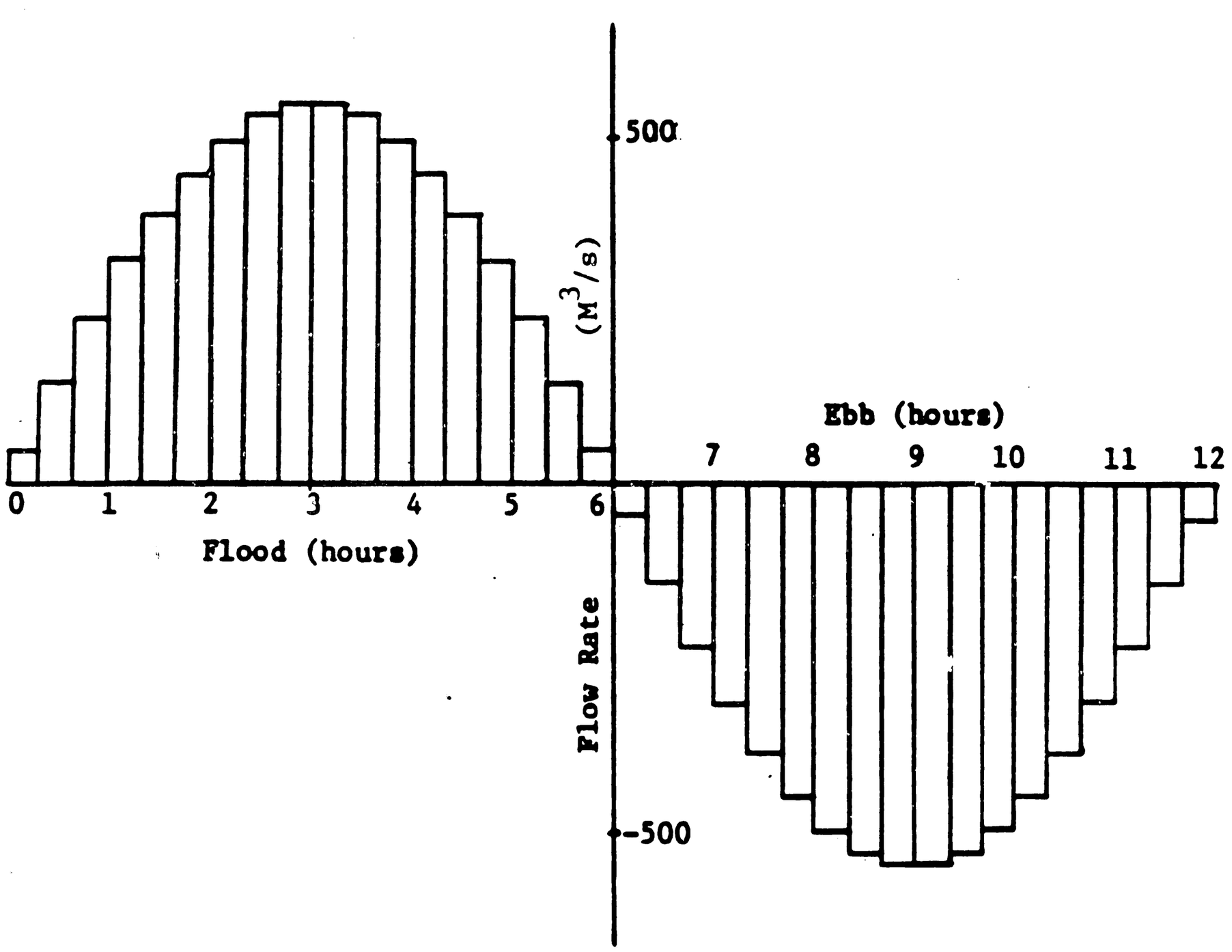


**Figure 3-3:** Plug Flow Approximation of a Nearly Sinusoidal Inflow to Great Sound

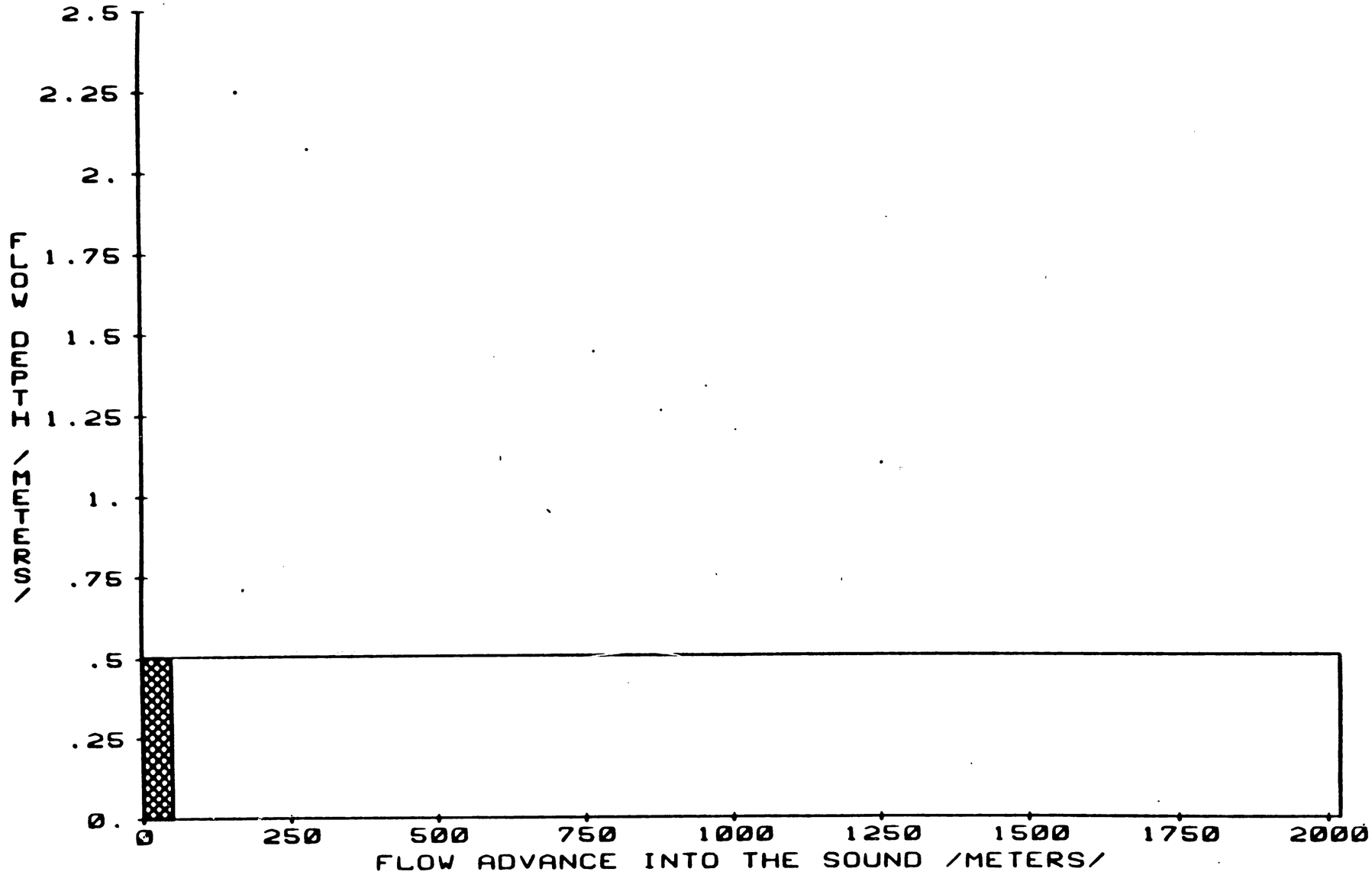


**Figure 3-4:** **Plug 1 Entering the Sound**

$t_i$ = Time Step i

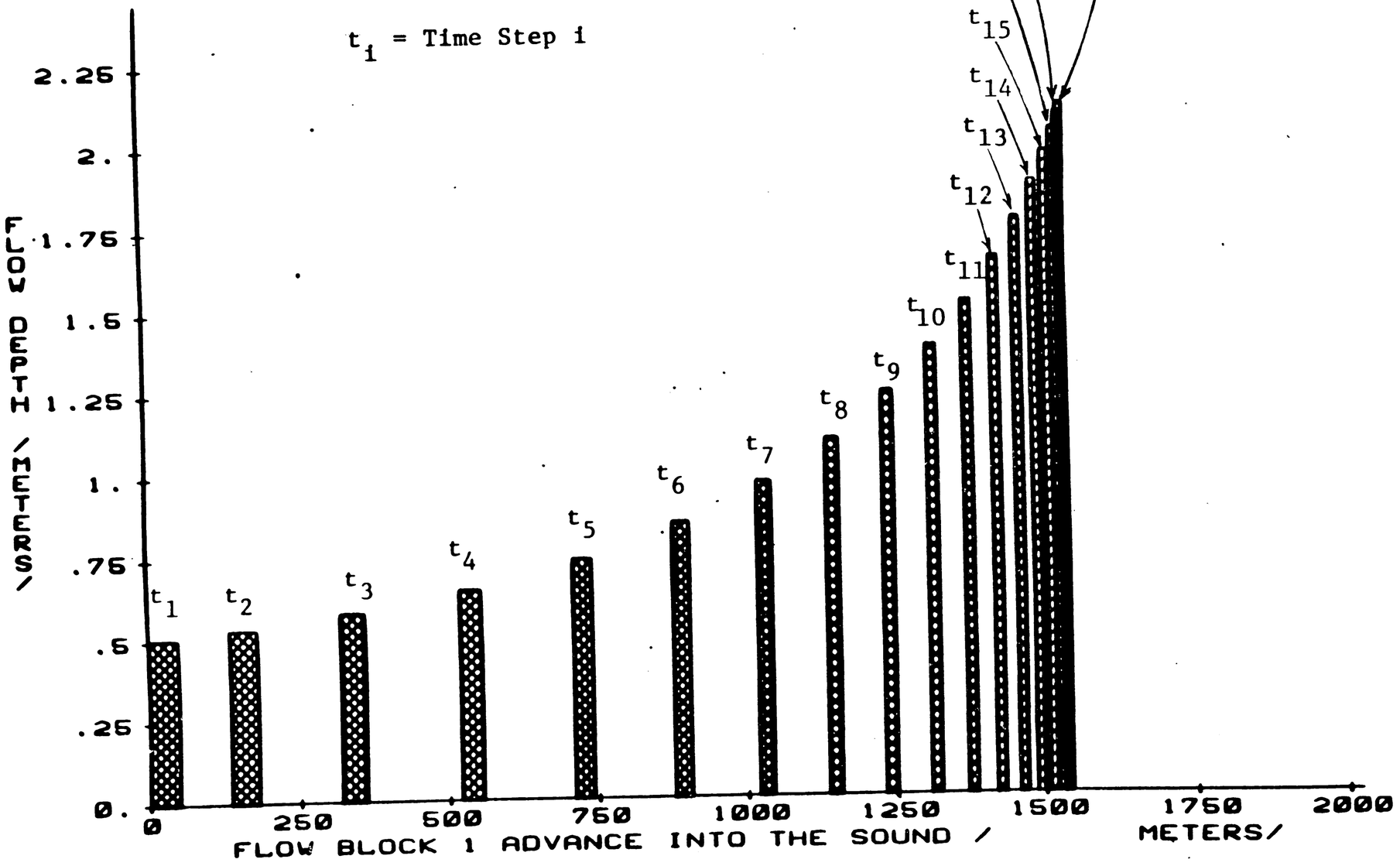


Figure 3-5: Flow Dynamics of Plug 1 Over the Flood

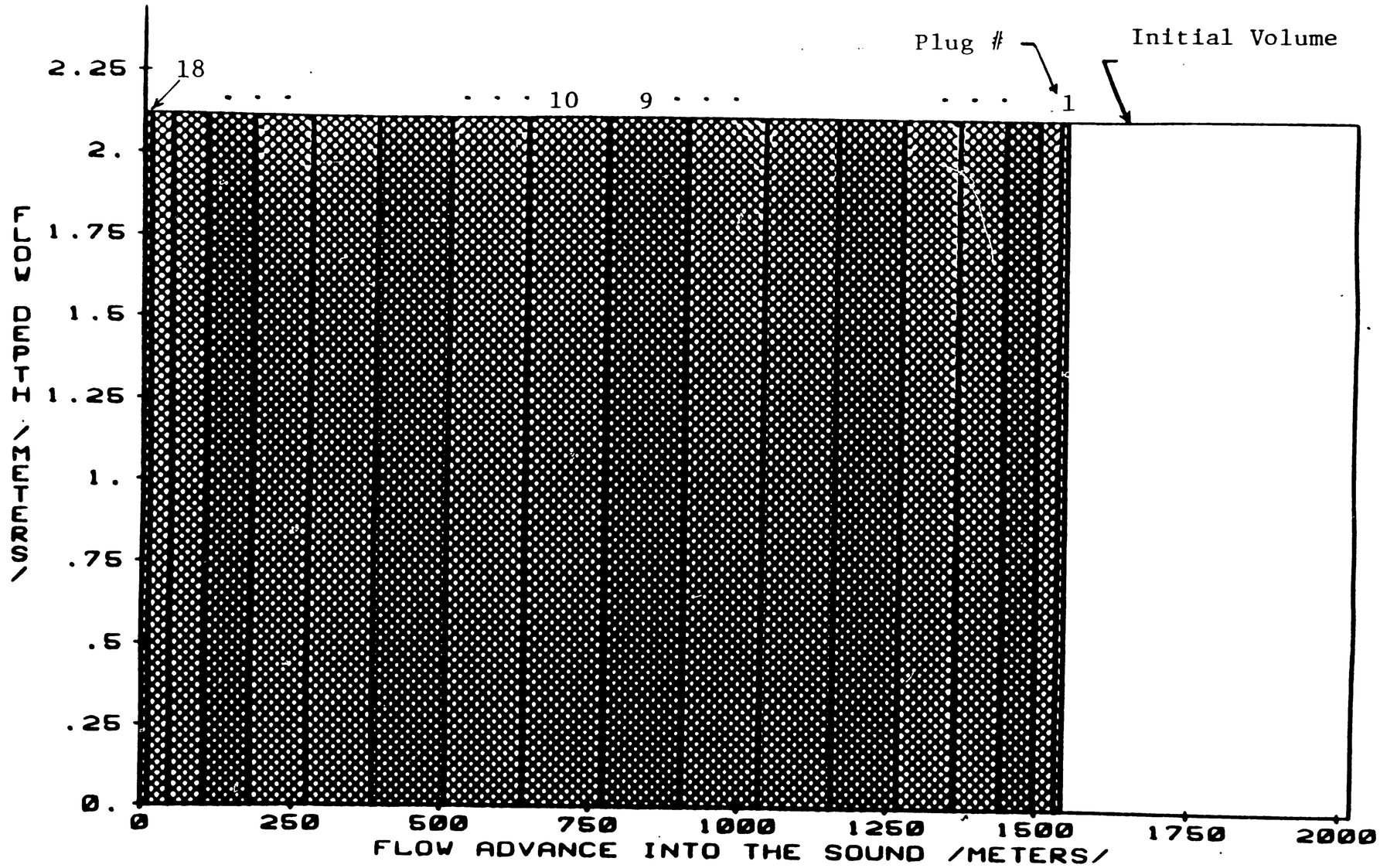


**Figure 3-6:** The Sound at High Tide - All Plugs Entered

time over the first half of the tidal cycle.

Figure 3-6 shows the Sound at maximum high tide, when all the plugs of fluid have entered. The initial volume of fluid in the Sound at MLW (unhatched region) has been pushed to the back of the Sound by the plugs of fluid entering during the flood. Plug 1 is the small crosshatched region in contact with the initial volume. The plug volumes increase up to peak flow (plugs 9 and 10) and then decrease again until slack high tide is reached (plug 18). During the ebb, the process reverses with the last plug to enter being the first to exit and so on.

The number of plugs entering the Sound correspond to the number of time steps used over the flood. During the ebb, these same plugs leave the Sound. Thus, if N plugs enter the Sound, the total time in the Sound for plug 1 is 2N time steps. Plug 2 remains in the Sound for a total of 2N-2 time steps, etc. Finally, some part of the $N^{th}$ plug remains in the Sound for up to two time steps, which, in Figure 3-6, is the $18^{th}$ plug.

### 3.3.4 Hydrodynamics Within Each Plug

During an expanding or contracting flow (flood or ebb), surface water particles rise or fall with time by a finite height (dH), while bottom water particles remain on the bottom. A linear variation of this expansion or contraction is assumed between the free surface and the bottom. Figure 3-7 shows the expansion in a plug over one time interval. Note that a water particle at mid-depth is always at mid-depth. To accurately monitor the relative vertical motion of sediment and water in this expanding flow, the plugs are divided into M layers.

Dividing each plug into a finite number of horizontal layers results in a

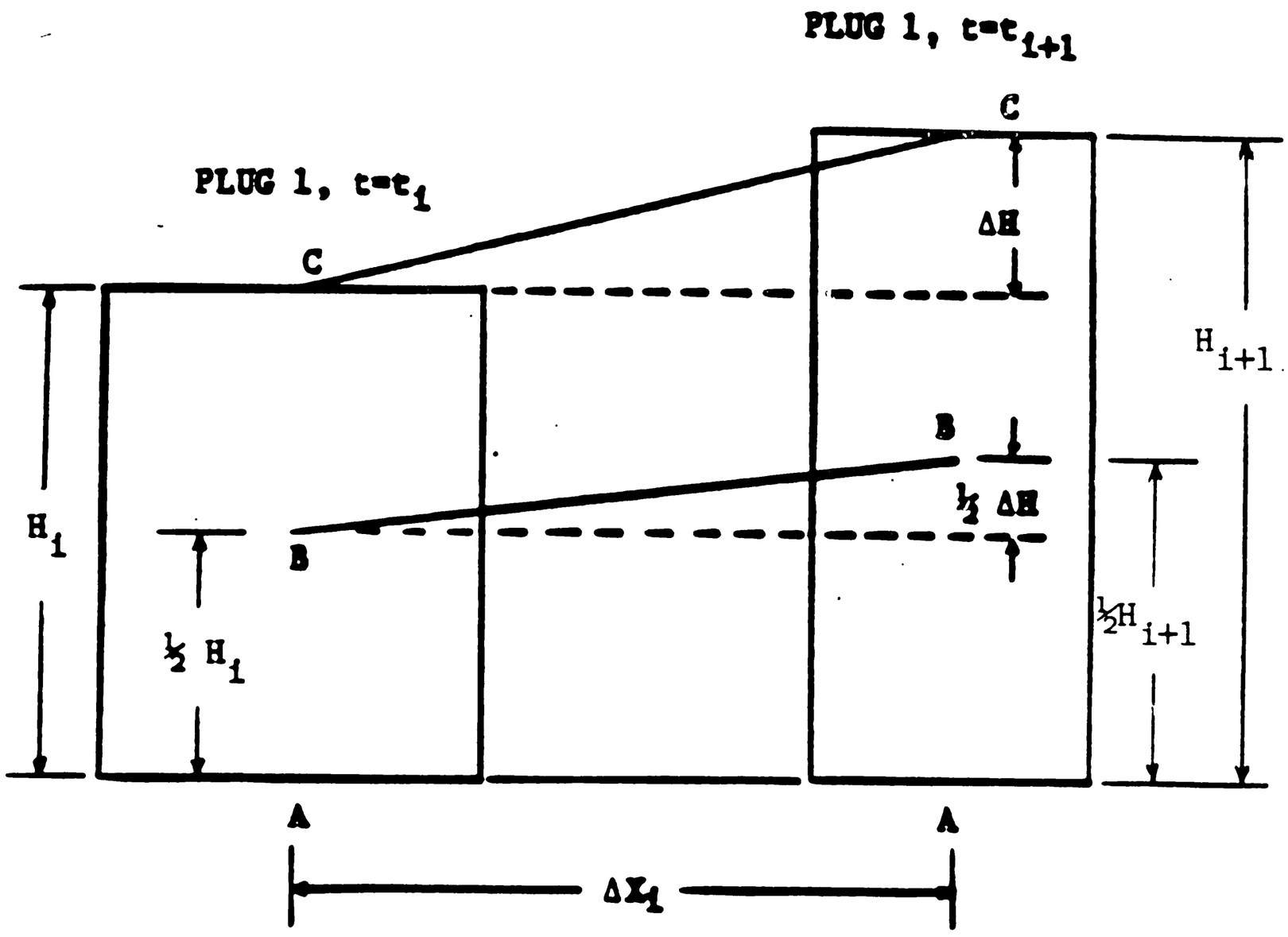


**Figure 3-7:** Vertical Flow Expansion of Water Particles During Flood in a Typical Plug

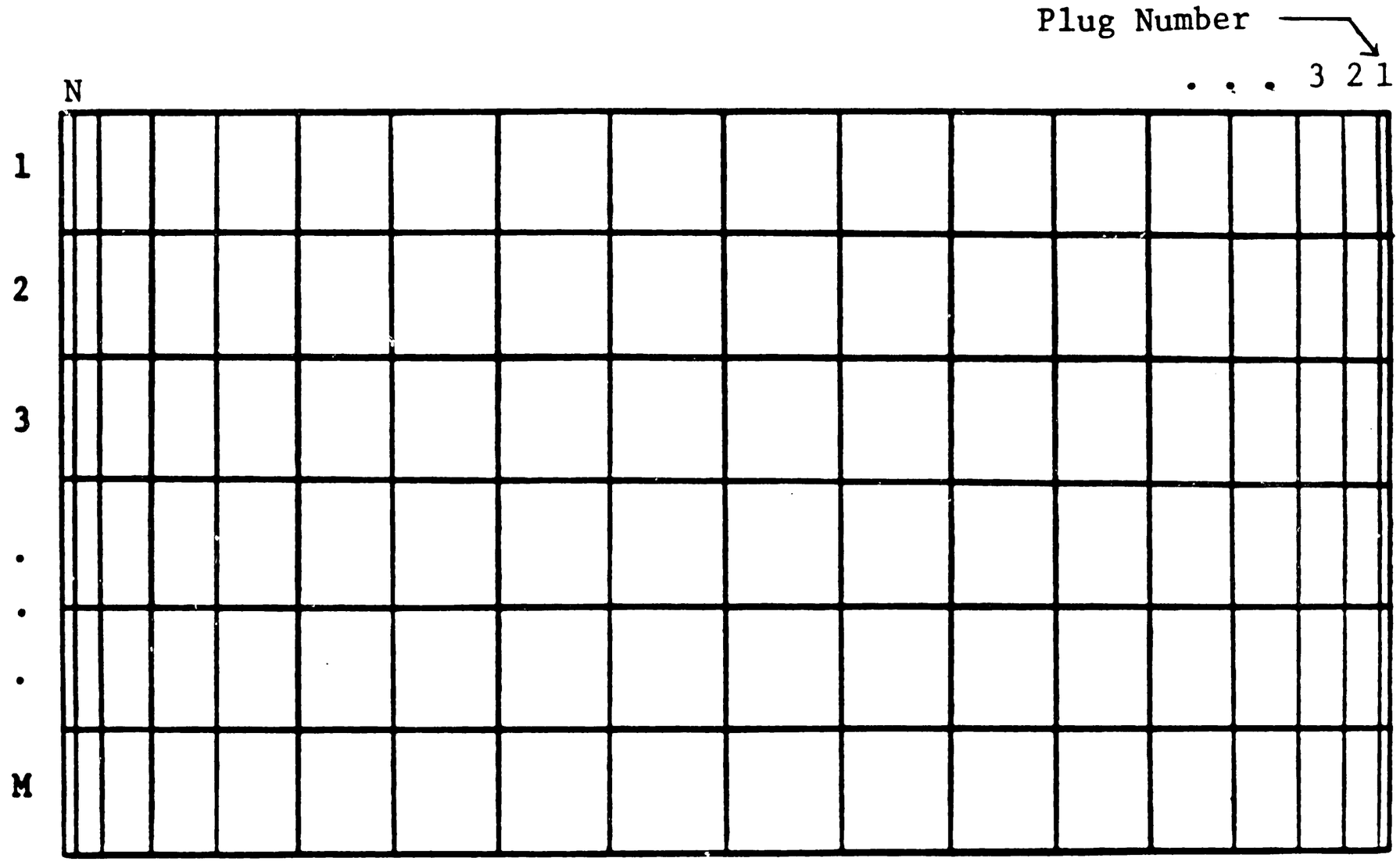


N = Number of Plugs

M = Number of Layers

**Figure 3-8:** Cell Representation of the Settling Tank Model at any Time, $t_i$

model of M by N finite cells within the settling tank representing the Sound. The cell representation is shown in Figure 3-8, where N is the number of plugs and M is the number of layers into which the plugs are divided. Each cell represents a finite "settling tank" of depth $H_i/M$, where $H_i$ is the depth in the sound at the given time interval, i.

The flow conditions in a plug over the $i^{th}$ time interval are shown schematically in Figure 3-9, including the change of width, depth, and velocity with time. The variables used for defining fluid particle motion within each plug are introduced as follows:

$H_i$ = plug depth at time $t_i$
$dH_i$ = increase in plug depth from time $t_i$ to $t_{i+1}$
$dx_i$ = plug width at time $t_i$
$V_i$ = velocity at time $t_i$

The changing vertical position of the layers within each plug is shown in Figure 3-10. The figure describes the change in vertical position of the surface of the j (th) layer, $P_{j,i}$, and actual fluid particle rise in each layer, $r_{j,i+1}$, as a function of depth.

The following equations can be written at each time interval to define the fluid particle motion based on Figures 3-9 and 3-10:

1) The horizontal distance a fluid particle travels over the interval $t_i$ - $t_{i+1}$ is defined using the average velocity,

$$\Delta x_i = \frac{(V_i+V_{i+1})dt}{2} \qquad (3.17)$$

2) The initial vertical position of the surface of the $j^{th}$ layer relative to datum (the floor of the Sound), $P_{j,i}$, at time $t_i$ is

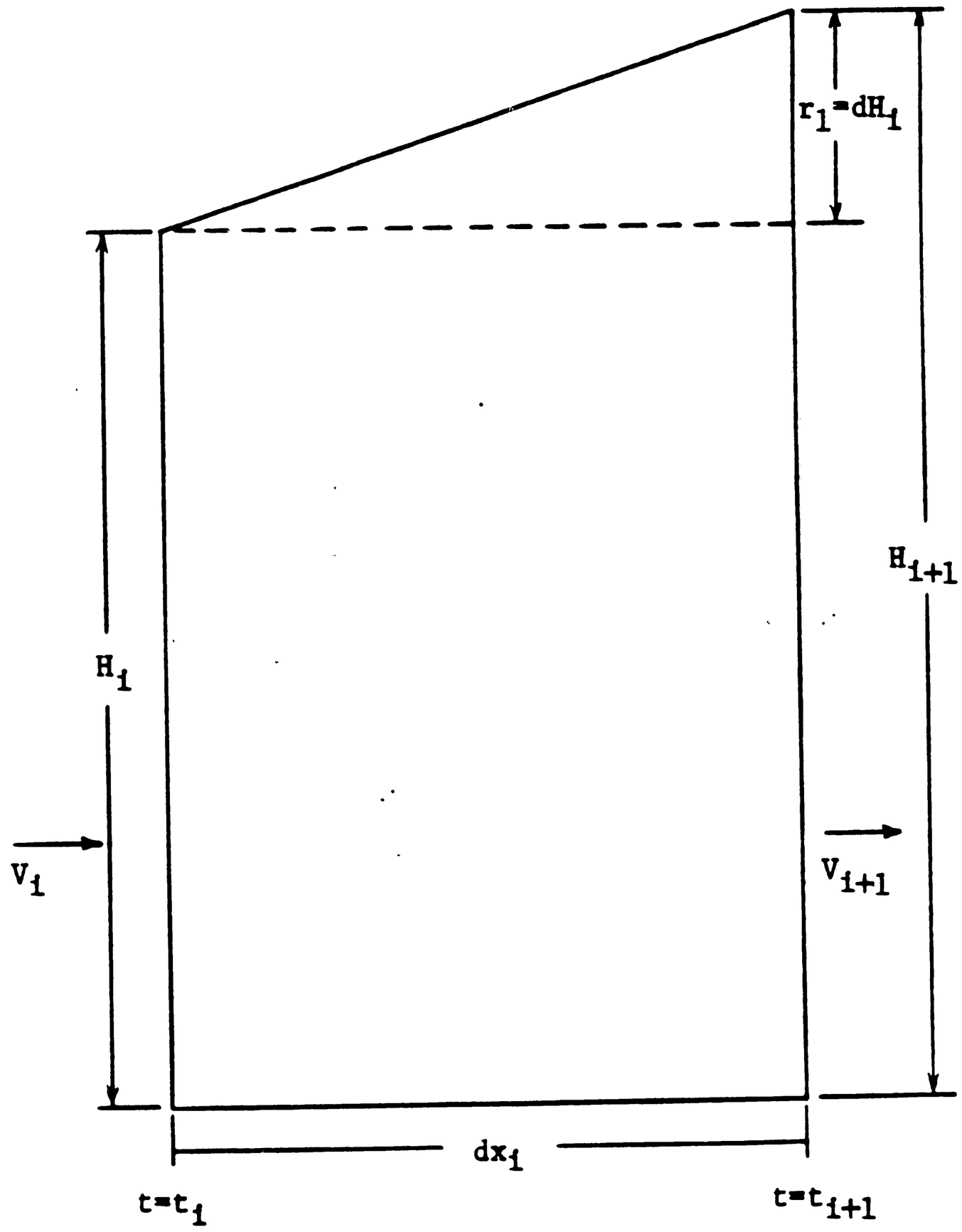


**Figure 3-9:** Definition Sketch of Flow Conditions in a Plug from Time $t_i$ to $t_{i+1}$

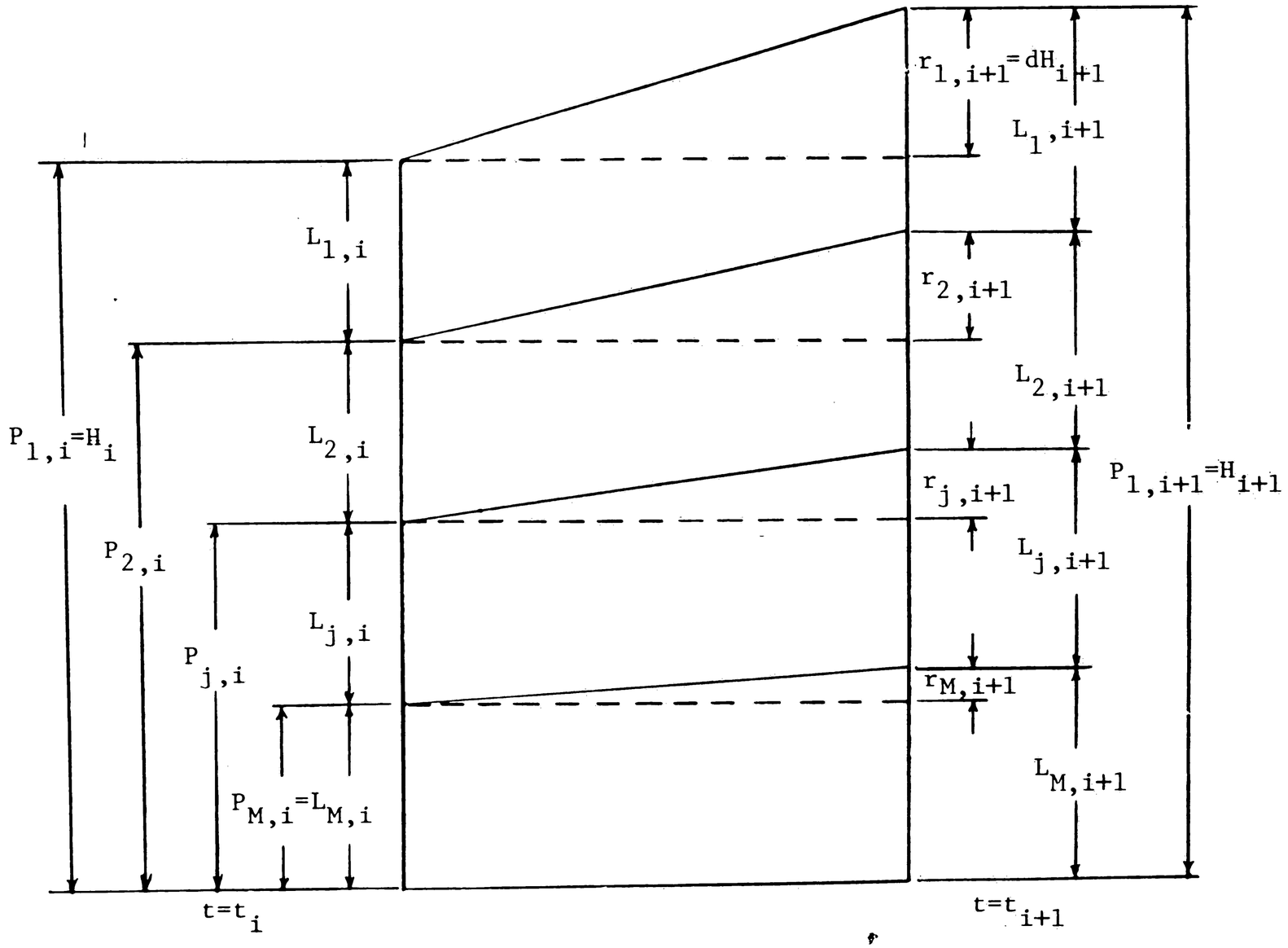


**Figure 3-10:** Layer Rise Over the $i^{th}$ Time Interval

$$P_{j,i} = \frac{H_i \times (M - j + 1)}{M} \tag{3.18}$$

where j=1,M layers, j=1 being the top of the uppermost layer (the free surface of Figure 3-10). Thus, for the top layer, $P_{1,i} = H_i$ and for the bottom layer, $P_{M,i} = L_{M,i}$.

3) The vertical rise, $r_{j,i+1}$, of each layer surface relative to its initial vertical position ($P_{j,i}$), for j=1,M layers, is

$$r_{j,i+1} = \frac{(M-j+1)\times dH_{i+1}}{M} \tag{3.19}$$

4) The vertical position of a layer surface with respect to the bottom of the Sound at time $t_{i+1}$ is the sum of Equations (3.18) and (3.19)

$$P_{j,i+1} = P_{j,i} + r_{j,i+1} \tag{3.20}$$

From Equations (3.17) through (3.20) it is obvious that the magnitude of the rise of a layer surface, $r_{j,i+1}$, is dependent on the vertical position of the layer in the flow field. As Figure 3-10 shows, over each time interval the rise in a layer surface varies linearly with depth such that the surface rise of the top layer ($r_{1,i+1}$) is the actual tidal rise, $dH_{i+1}$, while the surface rise of the bottom layer, $r_{M,i+1}$, is only 1/M times the rise of the top layer, or $dH_{i+1}/M$. Figure 3-10 also shows that, because $H_i$ is changing with each time step, the layer height $H_i/M$ is also changing. However, relative to one another, the layers are of equal height at any instant, such that $L_{1,i} = L_{2,i} = L_{3,i} = L_{M,i} = H_i/M$ and $L_{1,i+1} = L_{2,i+1} = L_{3,i+1} = L_{M,i+1} = H_{i+1}/M$. Therefore, the layer height $L_{j,i+1}$, can be written as $L_{i+1}$ since it is independent of the layer number, j.

### 3.3.5 Sediment Motion and Deposition

#### Individual Sediment Particle Motion in a Steady Flow

Consider a single plug of fluid entering an ideal settling tank in which flow is steady. Since the sediment at the inlet is assumed well mixed, each plug is assumed to contain uniformly distributed particles. Because of the Channel-Sound geometry (see Figure 3-2) this assumption is much better in Great Sound than in many settling tank problems where the depth at the inlet is not as low. If, for the present, we only consider one size of particle with settling velocity $V_s$, then the trajectory of all sediment particles will be parallel. The sediment particle residing at the surface of the plug is traced through the tank. This surface particle will be the last to settle out of the plug. Because all particles of the same size have a parallel settling path, the percentage of the total vertical distance the surface particle has settled will define the percentage of particles of settling velocity $V_s$ which have been deposited. For example, if the surface particle has settled through fifty percent of the plug vertically, then fifty percent of the particles of equal settling velocity will have been deposited.

#### Sediment Deposition for Unsteady Flow

Based on the calculation of hydrodynamic variables within each cell, the motion of individual sediment particles can be calculated for the "model Sound". It is assumed that there is no slippage of sediment particles in the flow and, therefore, the sediment particle horizontal velocity component is equal to the horizontal velocity component of the fluid. The vertical velocity component of sediment particles relative to the floor of the Sound is equal to the particle settling velocity, $V_s$, minus the vertical velocity component of the fluid caused by the rising or falling tide.

As shown previously, all layer heights $L_i$ are equal, but change in time, increasing over the flood. As a result, the sediment deposition analysis is greatly simplified by considering individual layers as follows. Figure 3-11 shows that, relative to the final vertical position of the layer surface, $P_{j,i+1}$, particles have settled an equal distance in every layer over the given time interval. The constant relative distance settled from each layer surface, $S_{L_{j,i+1}}$, from $t_i$ to $t_{i+1}$, is

$$S_{L_{j,i+1}} = V_s \times dt \tag{3.21}$$

For each time interval then, the fraction of particles deposited from each layer is calculated in the same manner described previously for plugs in steady flow. The fraction of particles leaving each layer, $N_{d_{j,i+1}}$, is given by:

$$N_{d_{j,i+1}} = \frac{S_{L_{j,i+1}}}{L_{i+1}} \tag{3.22}$$

where $S_{L_{j,i+1}}$ is the relative distance settled by the particle at the layer surface at time i, and $L_{i+1}$ is the layer height. Thus, since the layer heights are all equal and particles settle an equal distance in each layer, the same percentage of sediment leaves each layer at each time step. Therefore, the fraction of particles leaving each layer, $N_{d_{j,i+1}}$, can be written as $N_{d_{i+1}}$ since it is not layer dependent. For some larger sediment particles, $S_{L_{j,i+1}}$ may be greater than $L_{i+1}$. That is, a particle may settle through more than one layer in a given time interval, and as a result, $N_{d_{i+1}} > 1$.

Descending down a plug vertically, the percent leaving layer 1 falls into layer 2, the percent leaving layer 2 falls into layer 3, etc. Note that actual deposition into the Sound from each plug is only occurring in the bottom ($M^{th}$) layer. Therefore, if $N_{d_{i+1}}$ percent by volume deposits from each of a total of M

layers, then the total percent by volume deposited from the entire plug during time $t_i$ to $t_{i+1}$, (that which deposits through the $M^{th}$ layer) is

$$T_{d_{i+1}} = \frac{N_{d_{i+1}}}{M} \tag{3.23}$$

Thus, the percent deposited from the plug is 1/M times the percent passing through each individual layer during a given time increment.

**Determination of the Total Deposition**

In the previous sections, sediment deposition has been determined for a single settling velocity fraction in a single plug of flow over a single time interval. This deposition is calculated as percent of total volume of sediment in the plug, Equation (3.23). To determine the total deposition of sediment over the entire tidal cycle, the deposition must be summed for each particle size fraction, for each time increment and for each plug of fluid which enters the Sound.

1) The total deposition from a plug over one time step $t_i$ to $t_{i+1}$ (the sum over all size fractions, $k_1 = 1,n$) is

$$F_{tot} = \sum_{k_1=1}^{n} T_{d_{i+1,k_1}} \tag{3.24}$$

where n is the number of size fractions.

2) The total deposition from a plug which has entered and exited the Sound (the sum over the number of time intervals the given plug remained in the Sound, $k_2 = 1,t$) is

$$P_{tot} = \sum_{k_2=1}^{t} F_{tot_{k_2}} \tag{3.25}$$

where t is the number of time intervals the given plug remains in the Sound.

3) The total deposition from the entire system over a tidal cycle (the sum

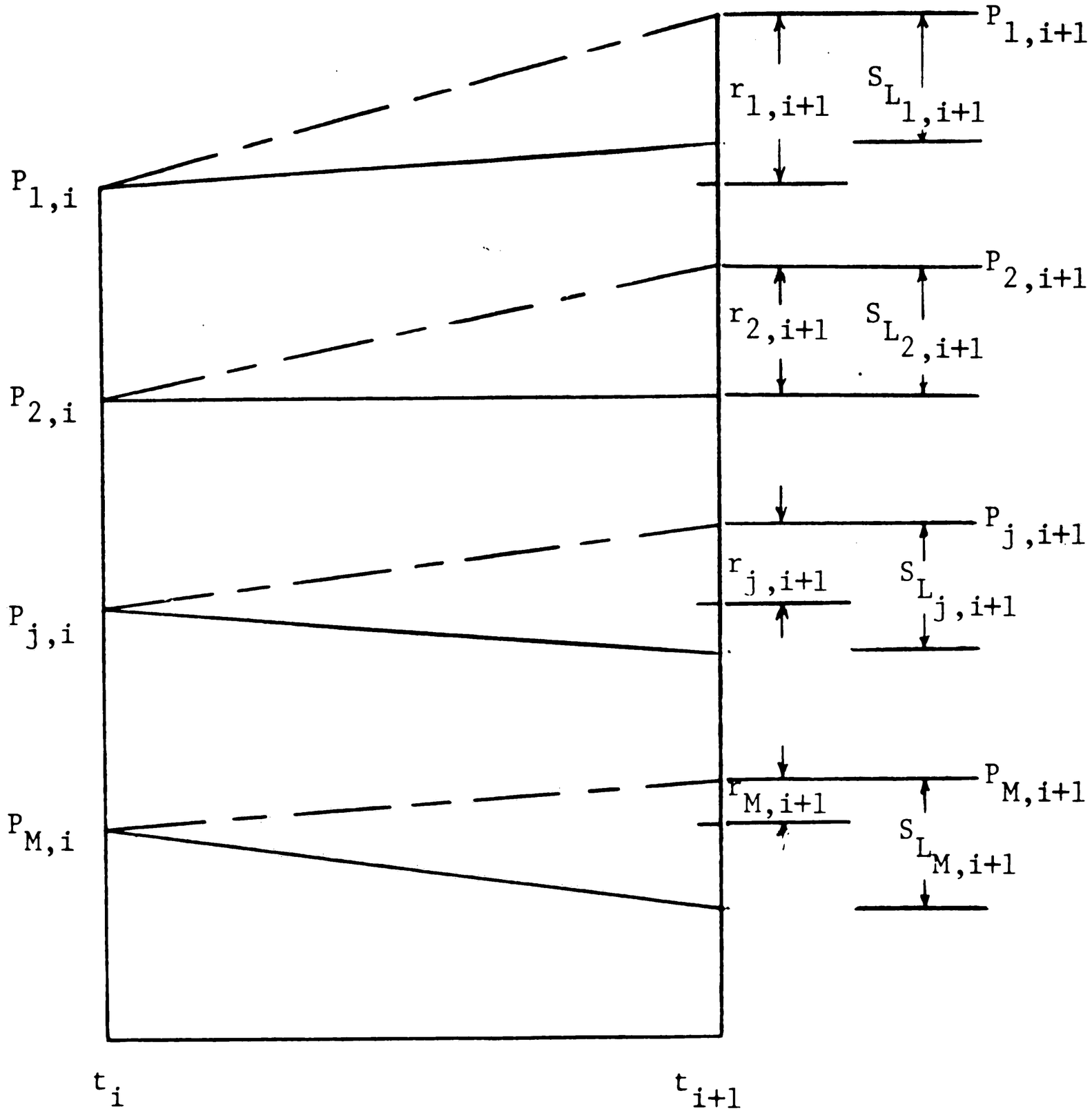


**Figure 3-11:** Sediment Trajectories Within Each Layer

of the deposition from each plug entering the system, $k_3 = 1,N$) is then

$$V_p = \sum_{k_3=1}^{N} P_{tot_{k_3}} \tag{3.26}$$

where $V_p$ is the cumulative volume by percent deposited from the system and N is the number of plugs which enter the Sound over the tidal cycle.

Dividing the actual mass of sediment entering the Sound, $M_{sed}$, by the bulk density of deposited sediment, $D_b$ yields the total volume of deposited sediment, $V_{sed}$, should all the sediment deposit.

$$V_{sed} = \frac{M_{sed}}{D_b} \tag{3.27}$$

Multiplying the percent volume deposited, $V_p$, by the total volume of available sediment yields the actual volume deposited, $V_d$.

$$V_d = V_p \times V_{sed} \tag{3.28}$$

The average depth of accumulation is then

$$d_{ave} = \frac{V_d}{A_S} \tag{3.29}$$

where $A_S$ is the area of the Sound.

**Sediment Distribution**

The distribution of sediment as a function of time and position can also be calculated by the model. Although an average depth of total accumulation is calculated using Equation (3.29), the actual distribution of sediment across the Sound is not uniform. Also, the volumetric distribution of the various size fractions changes with position.

The sediment distribution is determined by dividing the Sound into finite intervals perpendicular to the flow direction, and then recording the deposition within each interval. By tracing the sediment deposited across an interval by

each plug and summing for all plugs which cross the interval, a distribution by position is determined. Figure 3-12 shows an example of three plugs passing across an interval in one time step. If, over the time step, the starting point and ending point of the plug surround the interval, then the average deposition from the plug is recorded for that interval. For the case shown in Figure 3-12, the average depostion from plug B is recorded for the interval. The average deposition from A is recorded in the next interval, while the average deposition from C is recorded for the previous interval. Thus, the deposition by position can be determined to any desired accuracy based on the width of the interval chosen.

Since the concentration at x=0 is a time variable, the rate of deposition as a function of time is also variable for a given interval. The deposition versus time curve for a given interval is determined in the same manner as for the positional distribution. Instead of distributing over intervals of length, the distribution is defined over intervals of time.

## 3.4 Summary of the Model

The basic settling tank concept provides the foundation for determining sediment deposition in Great Sound. Modification of the settling tank concept to unsteady flow is accomplished using a plug flow approach. By dividing the plugs into layers, the settling tank is viewed as a matrix of cells. Sediment deposition is then determined within each cell. The resulting deposition from each cell is accumulated to determine deposition by plug, and subsequently the total deposition from all plugs over the tidal cycle.

The basic simplifications and assumptions concerning the Sound, which are made to accomodate the use of a plug flow settling tank model, are summarized

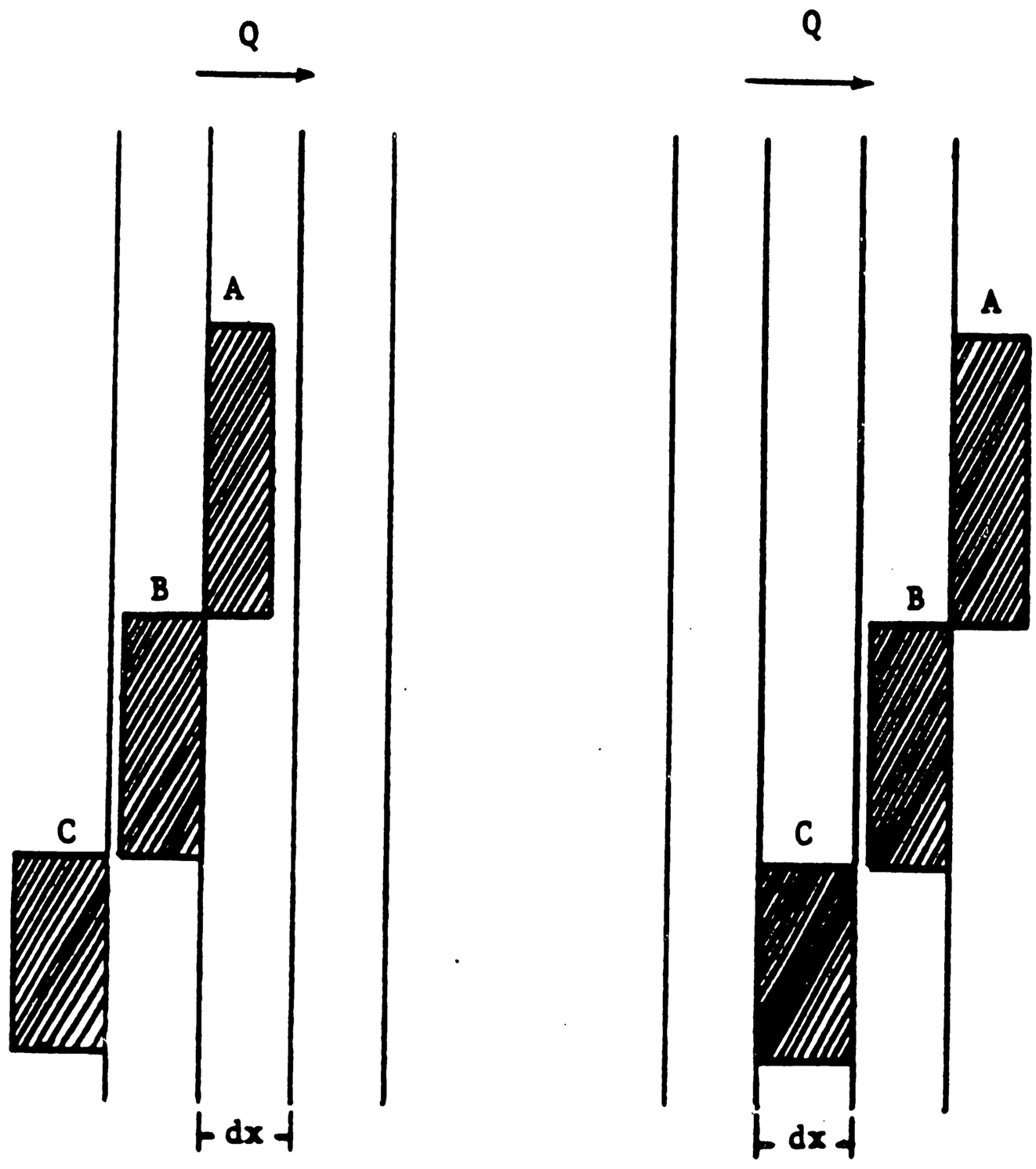


**Figure 3-12:** Plugs Passing Across an Interval

here. The settling tank model assumes a uniform bathymetry across the Sound, and a simplified geometry (a rectangular tank of plan area equal to the Sound). Also, the incoming flood tide is modeled as a one-dimensional flow moving into the Sound from the Intracoastal Waterway. The sediment deposition analysis considers only an average horizontal velocity. Throughout the vertical section at the inlet, the sediment is assumed to be uniformly distributed. This assumption is based on the high level of mixing which occurs in the channels and at the edge of the Sound where the flow spills from the Intracoastal Waterway out into the Sound.

Plug flow hydrodynamics assumes that no mixing occurs between plugs of fluid. This assumption is justified in an analysis of diffusion and dispersion processes which shows that the dispersion term in the one-dimensional convective-diffusion equation is negligible. Factors present in the DEPOSITS model mentioned previously which account for non-plug flow conditions are not applicable to Great Sound. The factors accounting for dead storage and basin short circuiting apply to cases where a finite width inlet feeds a wide basin. In the Sound, the inlet width equals the width of the basin. Also, the nature of turbulence in the Sound is such that the probability of hindering or enhancing particle settling is equally likely (Graf, 1971), and thus no factor considering turbulent effects is necessary.

Another implication of the use of plug flow modeling concerns the initial volume of water existing in the Sound at slack low tide. As the flood occurs, this initial volume is assumed to move to the back of the Sound as plugs continually enter and "push" the preceeding flow further along. On this basis it is assumed the entering plugs never reach the back of the Sound because the

initial volume occupies that space. Thus, the model records no deposition in the back of the Sound. In reality, of course, sediment does reach the back of the Sound in small amounts not taken into account by the model.

Finally, the model strictly considers deposition and does not account for the resuspension of deposited sediment by wind driven currents or waves.

The model was run on a CDC Cyber 850 mainframe computer. The source code is available in Young et al. (1986).

# Chapter 4
# Application To Great Sound

## 4.1 Model Inputs Required

The model calculates the sediment deposition in Great Sound based on specific planimetric, hydrodynamic and sediment input data previously obtained for the Sound. The model inputs are divided into two groups; those entered as constants and those which are time variable throughout the tidal cycle. Inputs which are constant throughout the tidal cycle include the number of sediment size fractions, the settling velocity of each fraction, the volumetric distribution of sediment within each fraction and the bulk density of the sediment. Other constant input data entered include the length and width of the Sound and the time increment used over a tidal cycle. Inputs which are time variable include the flow rate hydrograph, the sediment concentration hydrograph and the frequency of occurrence of the given concentration hydrograph over a year.

The data used in the model testing have been presented previously in Chapter 2. The inputs which are constant include Carney's (1982) particle size fractions and settling velocities, Table 2-2, and the volumetric distribution of sediment, Figure 2-9. Also, the bulk density of the sediment, 1.5 g/cc, is used as determined by Faas (1984). Finally, the length and width parameters used for modeling the Sound are 2200×2200 meters.

The time variable inputs used include the spring, neap and mean tide flow rate hydrographs and three concentration hydrographs. The flow rate hydrographs used are those developed by Schuepfer (1985) shown in Figures 2-5, 2-6 and 2-7. They are input from slack low to slack low tide. The three

concentration hydrographs include those for fair weather conditions, pre/post storm conditions and storm conditions. These are explained in the following paragraphs.

A fair weather concentration hydrograph was developed for the six hour flood portion of the tidal cycle from slack low to slack high tide. Using Griffiths' fair weather concentration hydrograph, Figure 2-11, recorded in the Intracoastal Waterway at the location shown in Figure 2-1, two-thirds of the necessary input data can be determined. The usable portion of Griffiths' data is taken from hour 8 through hour 12. The input concentration hydrograph was developed from Griffiths' data, as shown in Figure 4-1. Conditions from hour 6 through hour 8 were extrapolated from the existing slope of Griffiths' concentration hydrograph at hour 8. The resulting concentration hydrograph, Figure 4-1, has the same general shape as Griffiths' concentration hydrograph, with concentrations in the range of those obtained by Carney (Figure 2-10). Based on available data, Figure 4-1 is representative of a typical concentration hydrograph of the inorganic fraction entering Great Sound.

A modification of the pre/post storm hydrograph determined by Griffiths (Figure 2-12) and a hypothetical storm hydrograph are also used in model simulations. The modified pre/post storm concentration hydrograph employs a curve similar in shape to the fair weather hydrograph, but for the pre/post storm concentration range. This concentration hydrograph represents all conditions which cause an increase in concentration above fair weather including high winds and precipitation events of lesser intensity than severe storms. The hypothetical storm concentration hydrograph results from increasing the modified pre/post storm hydrograph by one order of magnitude. This increase is based

on the concentration measurements taken in Chesapeake Bay during hurricane Agnes which exceeded 100 times the fair weather concentration range (Schubel, 1975). The modified pre/post storm concentration hydrograph and hypothetical storm concentration hydrograph for the six hour input period (slack low to slack high tide) are shown in Figure 4-2.

Because no concentration-frequency data in or near Great Sound is known to exist, the frequency of occurrence curve developed by Maa et al. (1985), shown in Figure 2-13, was adapted for use in the Sound. Instead of six concentration increments, three were developed as shown in Figure 4-3, corresponding to the three concentration hydrographs. The data were modified by applying the slope of Maa et al.'s original graph to the concentration range for the Sound and dividing it into three increments. By multiplying the frequency of occurrence times the number of tidal cycles occurring annually, the number of tidal cycles for each concentration hydrograph is determined. A greater amount of data exists for low concentration days (fair weather days) than for high concentration days (storm days). Therefore, the actual frequency of occurrence is assumed to be more reliable for fair weather conditions than for storm conditions.

From the input data, the model determines the sediment deposition over a single tidal cycle. The model also calculates other variables for each time step and each plug. The flow depth, flow velocity, fluid volume and initial sediment volume are each calculated for all plugs along with the initial width of each plug as it enters the Sound. The cumulative flow volume in the Sound and the advance of each plug across the Sound are logged at each time interval throughout the tidal cycle. The concentration hydrograph is also determined on

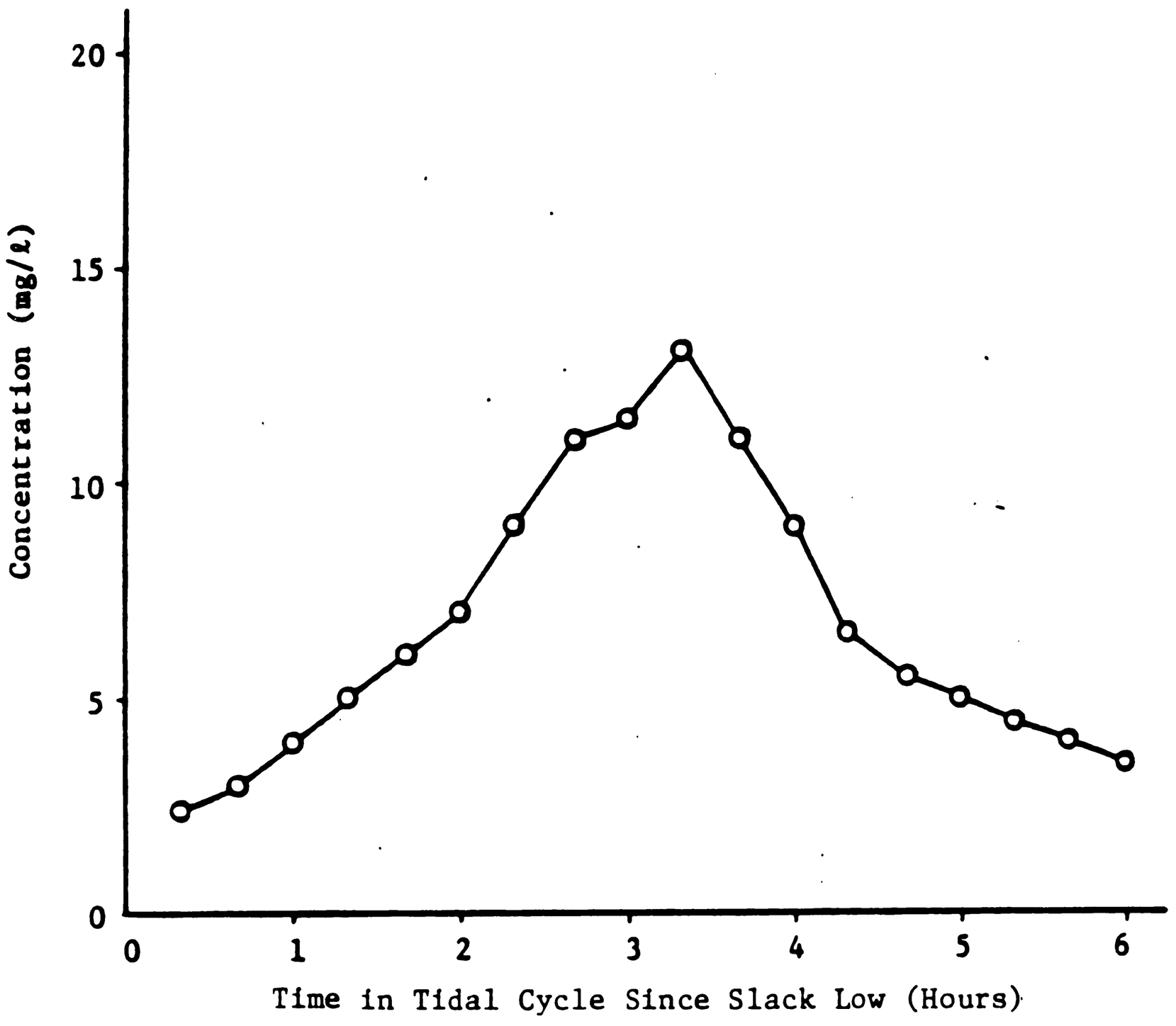


**Figure 4-1:** Model Input Fair Weather Concentration Hydrograph Modified from Griffiths' Data

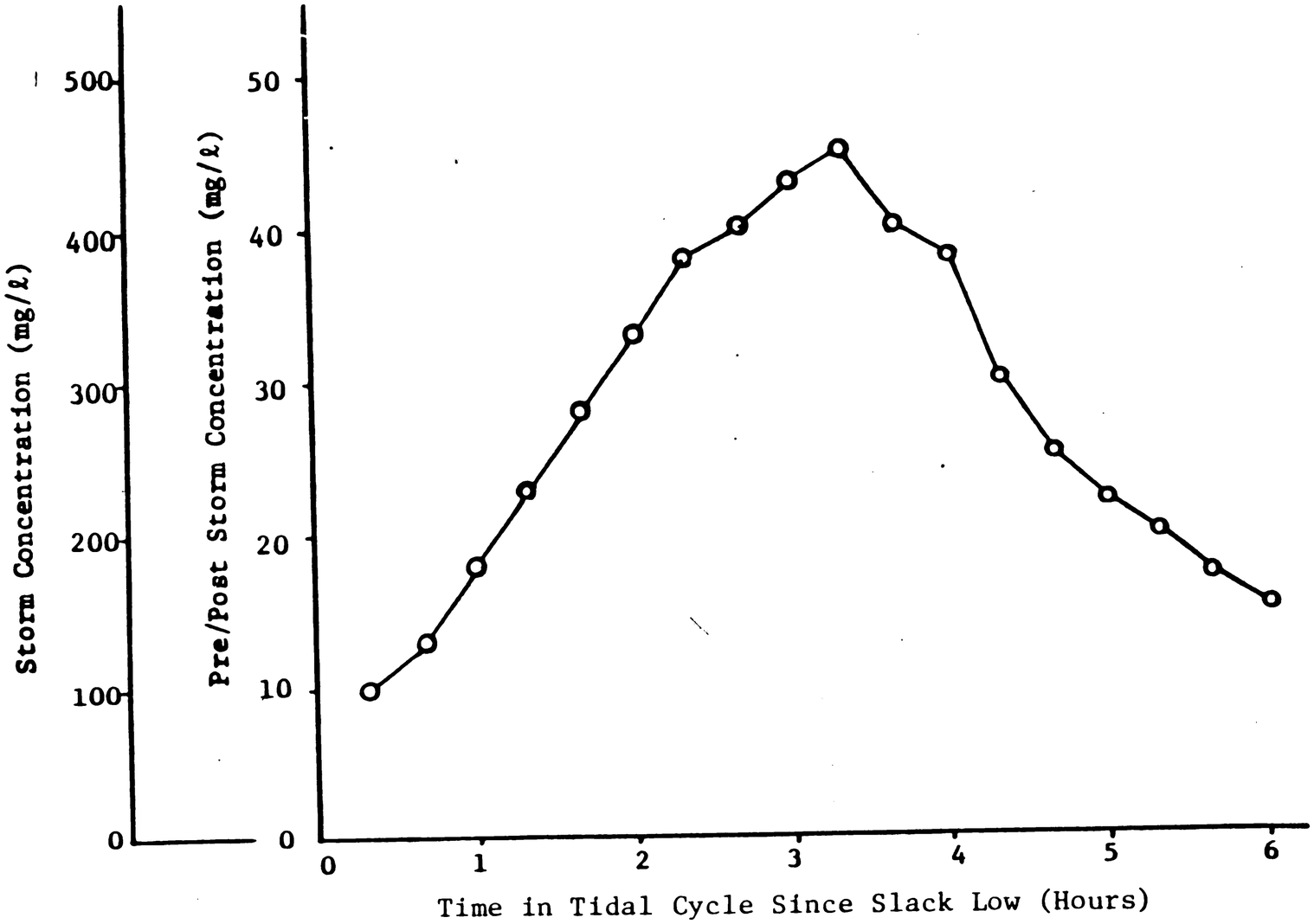


**Figure 4-2:** Model Input Concentration Hydrographs: Pre/Post Storm Modified from Griffiths' and Hypothetical Storm

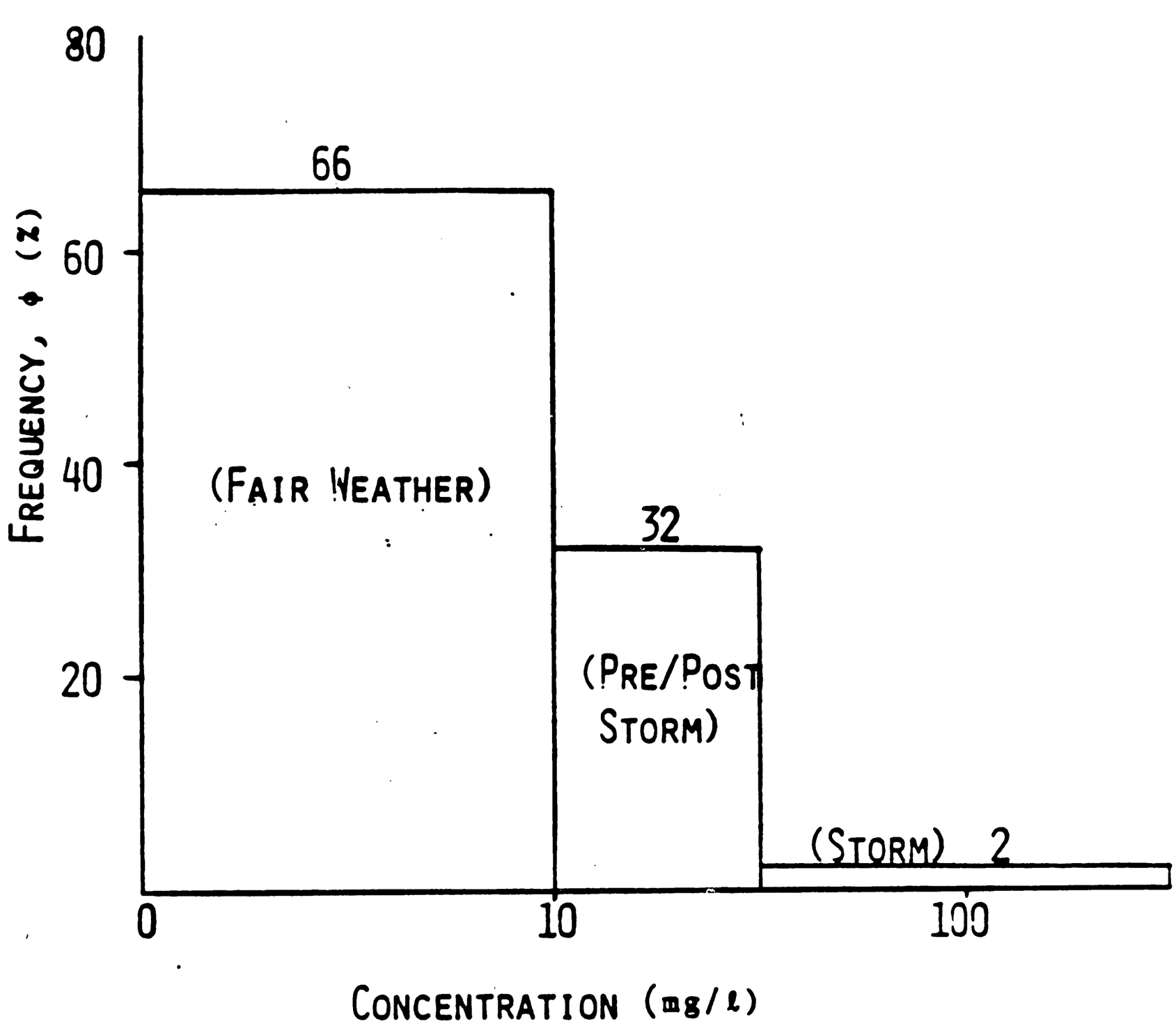


**Figure 4-3:** Frequency of Occurrence Curve for Great Sound Modified from Data Presented by Maa et al. (1985 )

the ebb, which can be compared to field data.

## 4.2 Model Testing and Test Results

Three main tests were conducted involving various aspects of the sediment deposition in Great Sound. In the first test the fair weather deposition occurring during spring, neap and mean tidal conditions was compared, and ebb flow concentration hydrographs were then generated for a mean tide under each of the three meteorological conditions defined. The fair weather ebb flow concentration hydrograph was compared to available field data. The second test determined the annual accumulation rate for Great Sound. The final test defined the impact of storms on the annual accumulation relative to the predominant fair weather conditions.

**Test I**

In the first part of this test, a comparison was run between spring, neap and mean tidal influence on deposition in the Sound. Using the fair weather concentration profile over a hypothetical "fair weather year" the deposition caused by a spring, neap and mean tide was determined. For modeling purposes, a "year" consisted of 705 tidal cycles. The fair weather concentration hydrograph was used for each tidal condition because peak velocities are similar for each. The differences between tidal conditions are due mainly to the varying volumes of water. The second part of the test determined the ebb flow concentrations for each meteorological condition.

The results of the first part, expressed as the accumulation that would occur over 705 fair weather tidal cycles, are as follows. For spring tide, the resulting average annual fair weather deposition rate was 3.7 mm/yr, while for neap tide the result was 2.3 mm/yr. Thus, a spring tide deposits over 50

percent more sediment than is deposited during a neap tidal cycle. This result shows the controlling influence of the spring tide on sediment deposition in the Sound. The implications of such a variation between spring and neap tides is significant when considering storms. A storm that coincides with a spring tide is likely to have a much greater impact on the deposition than one which coincides with a neap tide.

The resulting average annual fair weather deposition for mean tide was 3.1 mm/yr. The average deposition from the spring and neap tides is 3.0 mm/yr. The mean tide is less than 5% higher than the spring and neap tide average and, for subsequent tests, the mean tide is used.

The deposition profile for spring and neap tides for the hypothetical fair weather year are shown in Figure 4-4. Based on the plug flow modeling technique, the spring tide advances further into the Sound because of the increased tidal prism. Thus, the deposition curve extends further into the Sound for the spring tide than the neap tide. As Figure 4-4 shows, the deposition curves follow a consistent path across the Sound relative to one another.

Subtracting the percentage of total sediment depositing from each plug from the input sediment volume for each plug yields the ebb flow concentration hydrograph for the given tidal and meteorological condition. The ebb flow concentration hydrographs for fair weather, pre/post storm, and storm conditions are shown in Figures 4-5, 4-6, and 4-7, respectively. Because of the close agreement between spring, neap and mean tide ebb flow concentrations, only the mean tide concentrations are plotted on the ebb. The resulting fair weather ebb flow concentration hydrograph lies favorably within the range of the ebb

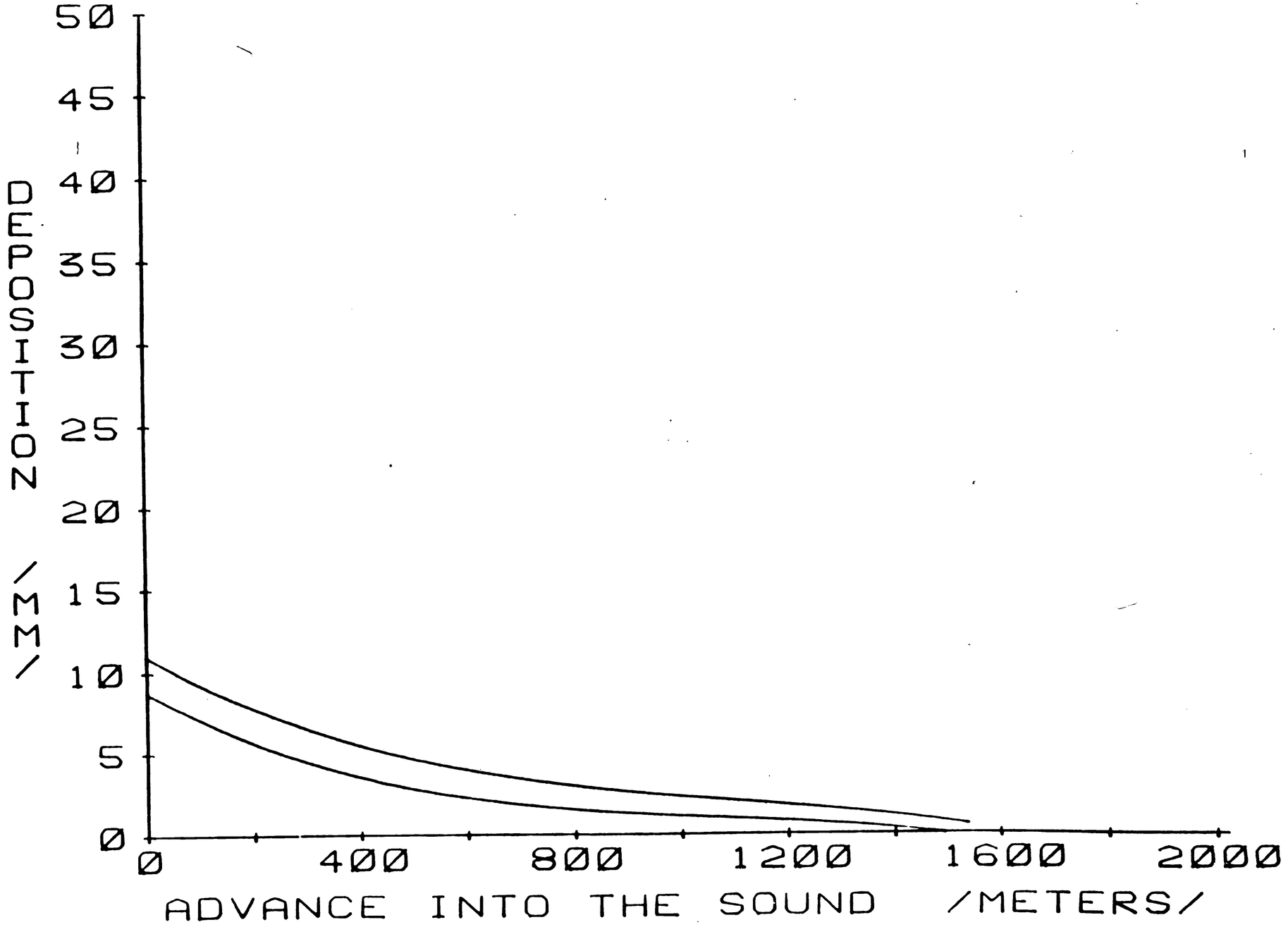


**Figure 4-4:** Spring vs. Neap Tide Yearly Deposition Profiles

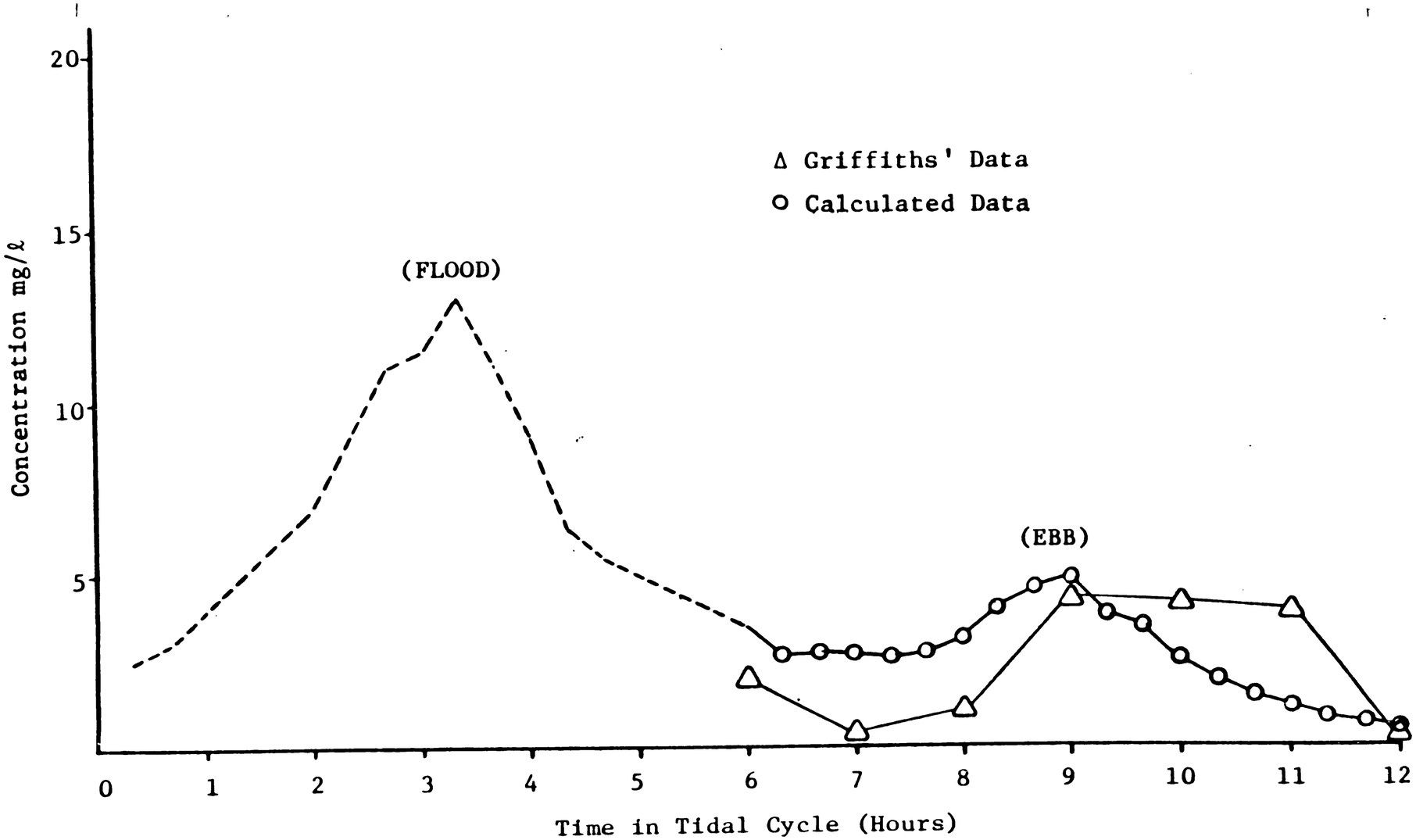


**Figure 4-5:** Fair Weather Sediment Concentration Hydrograph

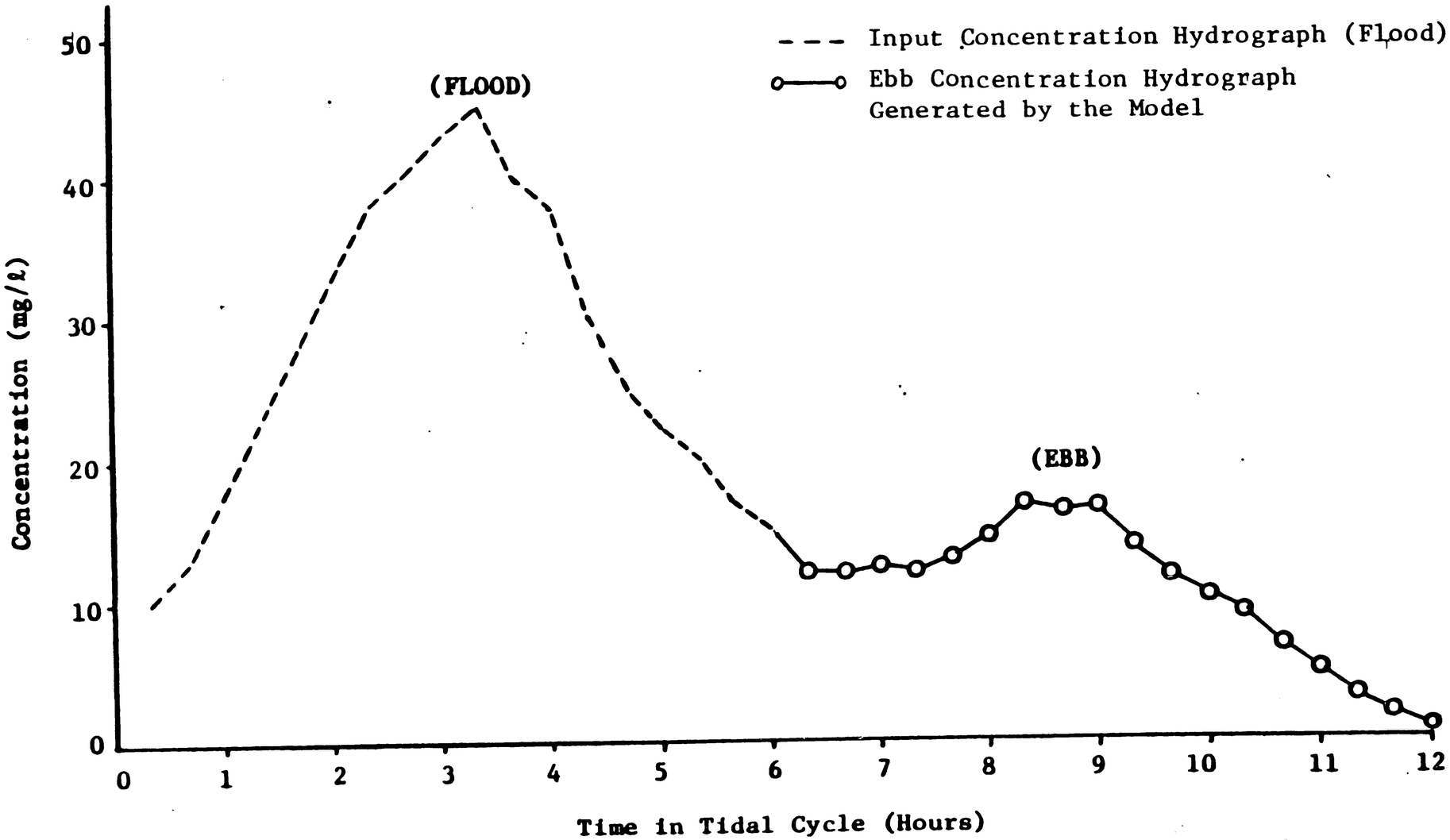


**Figure 4-6:** Pre/Post Storm Sediment Concentration Hydrograph

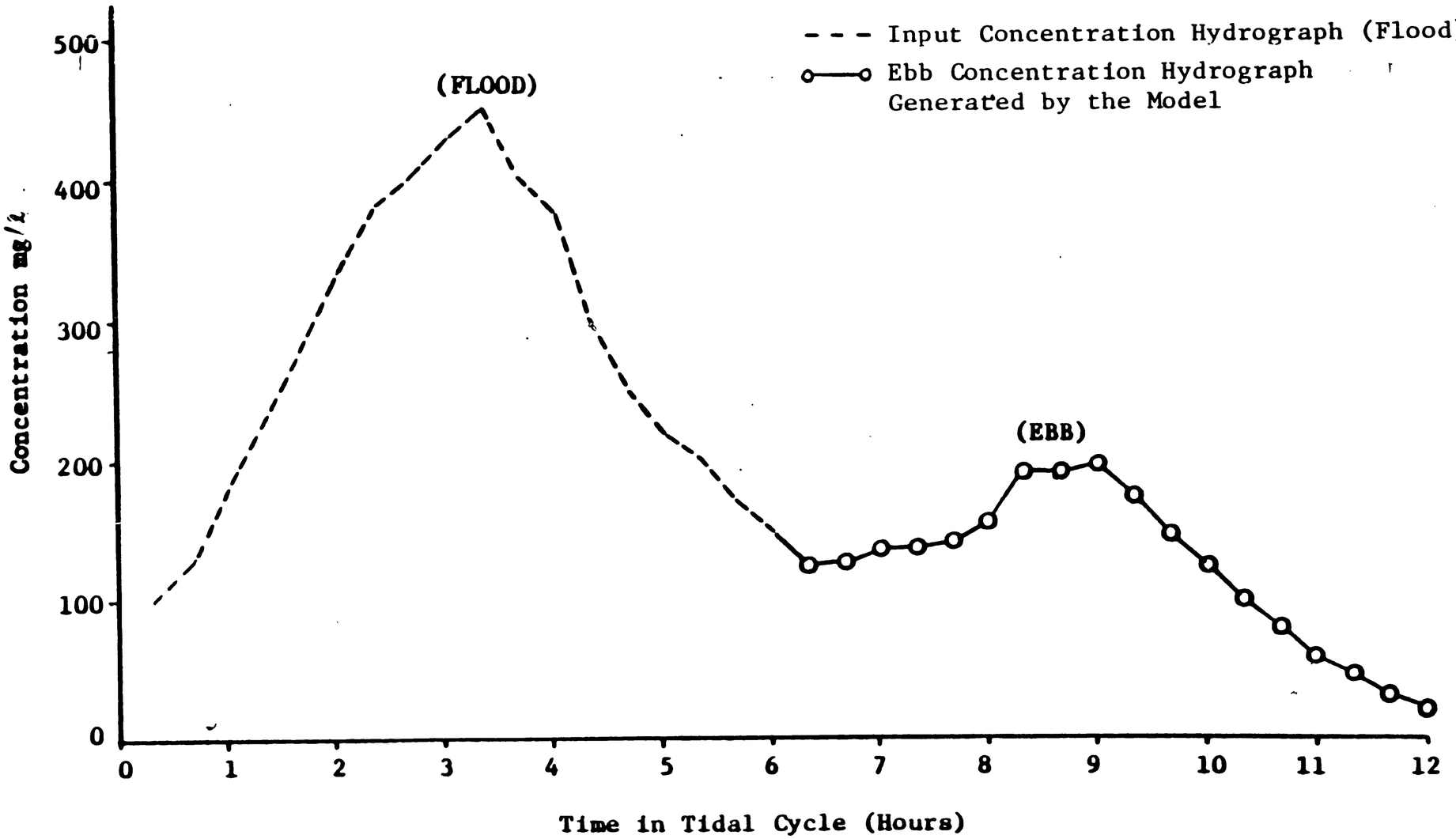


**Figure 4-7:** Storm Condition Sediment Concentration Hydrograph

flow portion of Griffiths' fair weather hydrograph (hours 12 through 18) as shown in Figure 2-11. No field data exists for a comparison with the model results generated for the pre/post storm and storm ebb hydrographs, but Griffiths may yet obtain these data.

**Test II**

A primary objective of the research was to determine an annual average sediment deposition rate in the Sound. To accomplish this, the second test was divided into three parts. Recalling the close agreement between the mean tide deposition and the spring and neap tide average deposition demonstrated in Test I, the mean tidal flow hydrograph was used in Test II for fair weather and pre/post storm conditions. To simulate storm conditions (storm surge), the spring tide flow hydrograph was used along with an initial depth in the Sound of 0.7 m as opposed to 0.5 m for the mean tide. Each concentration hydrograph was run for a single tidal cycle, defining the three parts of the test.

After running each concentration hydrograph, the resulting accumulation per tidal cycle was multiplied by the frequency of occurrence (number of tidal cycles per year) of the given concentration hydrograph to yield the total annual accumulation from each condition. The total annual accumulation was calculated by summing the results for these three conditions.

In Test II the yearly sediment deposition rate for Great Sound is calculated as shown in Table 4-1. Column 2 shows the the concentration hydrograph used in each part of the test. In column 3, the sediment accumulation from each of the three profiles is shown for a single tidal cycle. Multiplying this accumulation by the frequency of occurrence, column 4, yields the yearly deposition from each concentration hydrograph as shown in column 5.

The resulting total yearly accumulation for Great Sound as calculated by the model is, therefore, 8.9 mm/yr.

The resulting accumulation rate is a probable maximum annual rate because of the high concentrations of the storm days incorporated in the calculation. One test of the model's validity is to compare the results with a simple mass balance equation to determine the total sediment influx into the Sound.

The mass balance for the Sound is shown in Table 4-2. Column 2 shows the average concentrations for the concentration hydrographs listed in column 1. Integrating these hydrographs over the tidal cycle (mean tide for fair and pre/post storm, spring tide for storm) yields the mass of sediment entering per tidal cycle from each hydrograph as shown in column 3. Dividing by the bulk density (1.5 g/cc), the resulting volume of sediment is determined for a single tidal cycle as shown in column 4. Using the frequency of occurrence (column 5), the resulting volume from each concentration hydrograph over a year is calculated in column 6. The total volume accumulated is then 75830 $m^3$. Dividing by the area of the Sound yields an accumulation of 15.7 mm/yr. This result means that enough sediment enters the Sound each year to cause an accumulation of 15.7 mm if it all deposited. Thus, based on the result of the mass balance, the model simulates 57% of the entering sediment depositing in the Sound. This result does not consider particle resuspension and transport out of the Sound as previously stated, and, therefore, represents a probable maximum deposition for Great Sound.

The sediment deposition distribution across the Sound was calculated as described previously in Section 3.3.5. Figure 4-8 shows the deposition profile of

| TEST SECTION | CONCENTRATION HYDROGRAPH | ACCUMULATION PER TIDAL CYCLE (mm) | % FREQUENCY # CYCLES/YR | ACCUMULATION PER YEAR (mm) |
|---|---|---|---|---|
| PART I | Fair | 0.00446 | 66 (462) | 2.1 |
| PART II | Pre/Post Storm | 0.01799 | 32 (224) | 4.0 |
| PART III | Storm | 0.17991 | 2 (14) | 2.8 |

**TOTAL ACCUMULATION = 8.9 mm/yr**

**Table 4-1:** Yearly Sediment Deposition Rate for Great Sound

| (1) | (2) | (3) | (4) | (5) | (6) |
|---|---|---|---|---|---|
| CONCENTRATION HYDROGRAPH | AVERAGE CONCENTRATION (mg/ℓ) | SEDIMENT MASS (g/cycle) | SEDIMENT VOLUME ($m^3$/cycle) | FREQUENCY OF OCCURRENCE (%) | ANNUAL VOLUME ($m^3$) |
| Fair | 10 | $6.78 \times 10^7$ | 45.2 | 66 | 20880 |
| Pre/Post Storm | 35 | $20.7 \times 10^7$ | 138.0 | 32 | 30910 |
| Storm | 350 | $257.5 \times 10^7$ | 1717 | 2 | 24040 |

**Total** = 75830 $m^3$

$$\frac{75830\ m^3}{4840000\ m^2} = 15.7\ mm/yr$$

**Table 4-2:** Sediment Mass Balance for Great Sound

Test II as displayed in Table 4-1. from the Intracoastal Waterway to the back of the Sound. The distribution is skewed significantly toward the Intracoastal Waterway. The reason for such a distribution is shown more clearly in Figure 4-9, where the breakdown of distribution by size fraction is shown. In general, larger particles dominate near the Intracoastal Waterway, while smaller particles dominate near the back of the Sound. In Figure 4-9, the area under the bottom curve defines the location and volume of deposition of the largest size fraction, F1. The area between the bottom curve and the curve above it defines the location and volume of deposition for the second largest size fraction, F2, and so on. The top curve, therefore, defines the location and volume of the smallest fraction, F9, when considering the area between it and the next curve below it, while also defining the cumulative location and volume of sediment settled in the Sound from all of the fractions. The figure shows that the sediment from the three largest fractions has all deposited within the first 600 meters of the Sound. It is also obvious that the largest four fractions settle in less than half the tidal cycle. As a result, there is more sediment accumulation near the Intracoastal Waterway. The deposition from the smaller fractions, in contrast, is fairly uniform across the Sound, because these fractions do not deposit all of their sediment before the tidal cycle is complete.

**Test III**

The final test was run to determine the relative influence of infrequent major storm events on the yearly deposition. To determine this, the fair weather concentration profile was run for a "fair weather year" at the mean tide condition as in Test I. The storm concentration hydrograph was then run until it had produced the equivalent accumulation. Thus, the number of storm

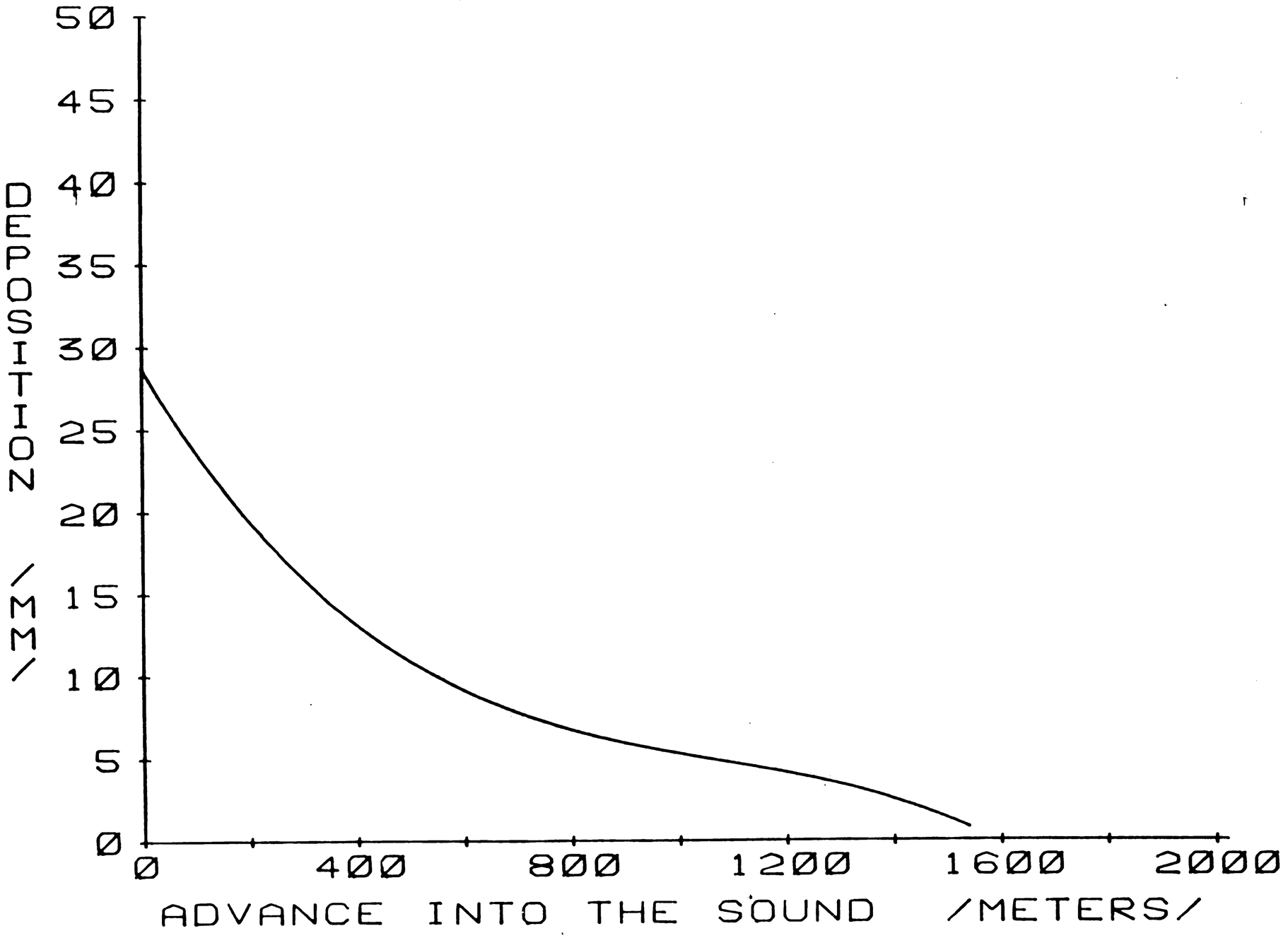


**Figure 4-8:** Yearly Sediment Deposition Profile for Great Sound

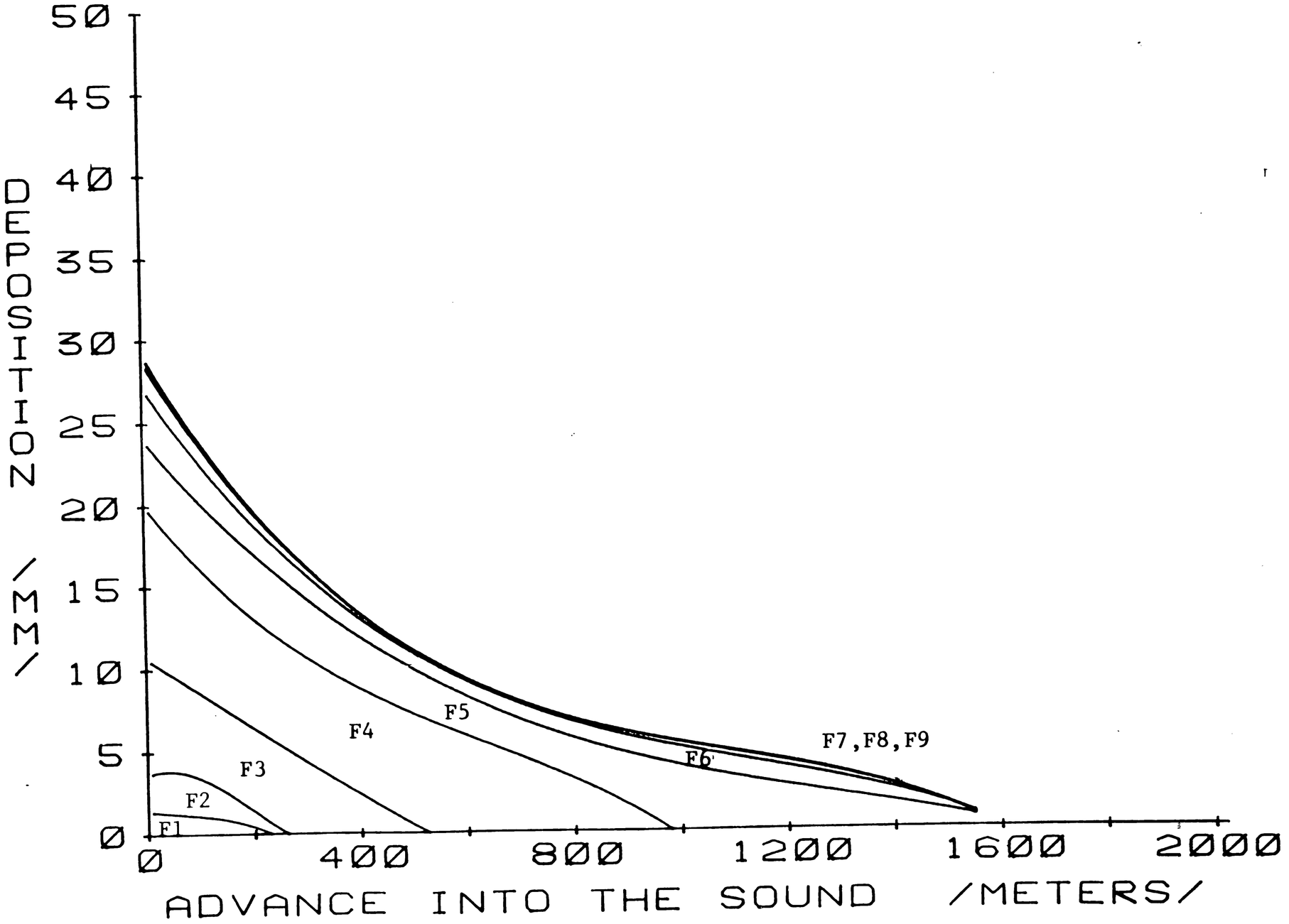


**Figure 4-9:** Layered Distribution of Sediment by Size Fraction; Largest Fraction, F1, Through the Smallest Fraction, F9

condition tidal cycles required to produce an accumulation equivalent to a year of fair weather was determined.

As calculated previously, the resulting deposition for a mean tide fair weather year was 3.1 mm/yr. The storm concentration profile was then run at storm conditions until an equivalent amount of sediment was deposited. The number of tidal cycles required was 16. Thus, with approximately 8 days of peak storm conditions, the fair weather deposition over an entire year is matched. This result shows that deposition from major storm events can weigh equally with predominant fair weather conditions in controlling sediment deposition in the Sound. However, the actual frequency of storm events producing concentrations above 100 mg/l in southern New Jersey is still unknown.

## 4.3 Discussion of Accumulation Rates

Kelley (1975) estimated accumulation rates in Great Sound to range from 5 to 10 mm/yr based on profiles of stable Pb in the bottom sediment of the Sound. A more detailed evaluation of sediment accumulation rates by Thornbjarnarson et al. (1984) determined a rate of long term average accumulation of between 1 and 5 mm/yr in the western half of the Sound using a lead isotope Pb-210 geochronology. The results obtained using the stable Pb profiles (Kelley) and Pb-210 profiles (Thornbjarnarson) are in the same range. Levy (1978), using a sediment trap, recorded sediment depths ranging from 5 to 300 mm/yr in sediment trap structures located in neighboring Jenkins Sound. The sediment trap structures yield deceptively higher results because they trap re-suspended sediment and moving bedload along with the suspended sediment.

The resulting average accumulation rate of 8.9 mm/yr generated by the

model, is in strong agreement with results of the Pb profiles from Kelley. Also, when considering the distribution shown in Figure 4-8, the average accumulation rate in the western half of the Sound agrees strongly with the results of Thornbjarnarson et al (1984). Recalling the sediment mass balance equation which calculated the maximum available sediment accumulation to be 15.7 mm/yr, it is clear that the upper bound of the sediment trap structure results are out of range.

The recent sea level trend at Sandy Hook, New Jersey has been determined by Hicks et al. (1983) based on tidal data collected continuously since 1933. Sandy Hook is located within 100 miles of Great Sound and, therefore, the trends presented are assumed representative of those occurring at Great Sound. The recent historic sea level rise is approximately 45 cm per century, or 4.5 mm/yr. This result is a combination of both global and local effects. The average global effects account for 1.2 mm/yr, thus local effects contribute the remaining 3.3 mm/yr. Currently then, the calculated rate of annual accumulation, 8.9 mm/yr, is higher than the current sea level rise trend of 4.5 mm/yr. Even with the rate of annual deposition perhaps increasing, it appears that the influence of sea level rise will have a greater impact on Great Sound than sediment deposition based on projections of increased rates of sea level rise in the future (see Hoffman et al., 1983).

# Chapter 5
# Summary, Conclusions and Recommendations

## 5.1 Summary

A sediment deposition model was developed to determine the sediment deposition characteristics of Great Sound. The settling tank concept is applied in the analysis of sediment motion and deposition in the Sound. Incorporated into the settling tank scheme is a plug flow approach to the tidal hydrodynamics. The assumptions inherent in a plug flow settling tank model include no mixing of plugs and a uniform velocity profile. The necessary model inputs, including sediment concentration hydrographs, sediment size distributions and volumetric distributions, were based on field data obtained for Great Sound by other researchers. The concentration frequency of occurrence was based on research by Maa et al. (1985) in a Florida marina. Hydrodynamic inputs were based on results from the HYDTID model (Schuepfer, 1985).The model predicts the average annual sediment accumulation rate in the Sound. Also, the model defines the relative influence on sediment deposition caused by fair weather versus pre/post storm and storm conditions, and spring tide versus neap tide tidal ranges. Ebb flow concentration hydrographs are defined for each of the meteorological conditions considered.

The model successfully predicts annual sediment accumulation rates in Great Sound as verified by its agreement with predictions based on Pb profiles. The resulting annual accumulation rate predicted by the model is 8.9 mm/yr compared to 5-10 mm/yr as estimated by Kelley (1975) and 1-5 mm/yr in the

western half of the Sound as estimated by Thornbjarnarson et al. (1984).

The model also allows comparison of the relative influence on sediment deposition caused by (a) fair weather, pre/post storm and storm conditions, and (b) spring tide versus neap tide tidal ranges. A comparision between the mean tide fair weather accumulation rate and accumulation under storm conditions determined the relative influence of storms on the annual accumulation rate. Only 16 storm condition tidal cycles (about 8 major storm days) are required to produce an accumulation equivalent to a year of fair weather deposition. A comparision between spring and mean tide accumulation rates determined the influence of the tidal condition on deposition. Deposition from a spring tide was found to be 1.5 times the deposition from a neap tide. Also, ebb flow concentration hydrographs were determined by the model which compared favorably with available data obtained by Griffiths (1985).

## 5.2 Conclusions

Based on the results calculated by the model, the following can be concluded:

1. The sediment deposition model developed for Great Sound accurately predicts the annual sediment accumulation rate based on combined fair weather, pre/post storm and storm conditions.

2. The model reasonably predicts the ebb flow concentration hydrograph for a fair weather condition, but no data are available for comparing the pre/post storm and storm ebb flow concentration hydrographs generated by the model.

3. The model can be used to define the depth distribution of the annual accumulation across Great Sound and assess that distribution by sediment size fraction.

4. The effects of storm conditions on the annual accumulation rate can be assessed by the model, as well as the relative impact of spring,

neap and mean tidal conditions.

5. Results based on average conditions over a single tidal cycle can be effectively applied to the prediction of longer term (annual) accumulation rates.

## 5.3 Recommendations for Future Work

Further investigations should be performed to verify the results of this study. This modeling effort is part of an ongoing interdisciplinary work benefiting geologists, biologists, ecologists and others concerned with back bay coastal processes.

Additional sediment concentration data are necessary at the edge of the Intracoastal Waterway where the incoming flow spills over into Great Sound. This includes the need for sediment concentration hydrographs over a single tidal cycle during various meteorological conditions including major storms, and concentration frequency data from a location more localized to the study area. Concentration data from within Great Sound would provide a helpful check on model results as well.

Finally, the model should be expanded to utilize the detailed hydrodynamic information available from the HYDTID model. Also, consideration of the effects of resuspension would improve the accuracy of the simulation of sediment deposition over a tidal cycle.

# References


Barfield, B.J., Warner, R.C., and Haan, C.T.
Applied Hydrology and Sedimentology for Disturbed Areas
Oklahoma Technical Press, 1981.

Camp, T.R.
Sedimentation and the Design of Setting Tanks
ASCE Transactions, paper no. 2285, 1946.

Carney, K.F.
The Nature and Importance of Fine-Grained Sediment Aggregation Processes in the Coastal Lagoon Complex at Store Harbor, N. J.
M.S. Thesis Lehigh University, Bethlehem, PA, 1982.

Chen, C.N.
Design of Sediment Retention Basins
National Symposium on Urban Hydrology and Sediment Control, University of Kentucky, Lexington, 1975.

Chu, W. and Gardner, S.
A Two-Dimensional Particle Tracking Estuarine Transport Model
Water Resources Bulletin, v22. no. 2, April 1986.

Cole, P. and G.V. Miles
Two-Dimensional Model of Mud Transport
ASCE Journal of Hydraulic Engineering, v109, Jan. 1983.

Daily, J.W. and Harleman, D.R.F.
Fluid Dynamics
Addison-Wesley, 1966.

Dobbins, W.E.
Effect of Turbulence on Sedimentation
ASCE Transactions, paper no. 2218, 1944.

Elder, J.W.
The Dispersion of Marked Fluid in Turbulent Shear Flow
Journal of Fluid Mechanics, v5, 1959.

Evans, G. and Collins, M.B.
Transportation and Depostion of Suspended Sediment over the Intertidal Flats of the Wash
Nearshore Sediment Dynamics and Sedimentation,

Hails, J. and Carr, A. Ed., Wiley Publishing Co., 1975.

Faas
Department of Civil Engineering, Lafayette College, Easton, PA.
personal communication, 1984.

Ferrara, R.A. and Harleman, D.R.F.
Hydraulic Modeling for Waste Stabilization Ponds
Proceeding Journal of Environmental Engineering, ASCE
v107, Aug. 1981.

Fischer, H.B.
The Mechanics of Dispersion in Natural Streams
Proceedings, Journal of Hydraulics Division, ASCE
v93, no. 6, Nov. 1967.

Fischer, H.B.
Dispersion Predictions in Natural Streams
Proceedings, Journal of Sanitary Engineering, ASCE
v94, 1968.

Fischer, H.B.
Discussion of "Simple Method for Predicting Dispersion in Streams"
by R.S. McQuivey and T.N. Keefer, Proc. Journal of Environmental
Engineering, ASCE, v101, 1975.

Fischer, H.B. Ed.
Transport Models for Inland and Coastal Waters
Proceeding of a Symposium Predictive Ability,
Academic Press, 1977.

Fischer, H.B., List E.J., Koh, R.C.Y., Imberger, J. and Brooks, N.H.
Mixing in Inland and Coastal Waters
Academic Press, 1979.

Godfrey, R.G. and Frederick, B.J.
Dispersion in Natural Streams
US Geological Survey Professional Paper 433-K, 1970.

Graf, W.H.
Hydraulics of Sediment Transport
McGraw Hill, Inc., 1971.

Greenwood, B. and Davis, R.A.Jr., Ed.
Hydrodynamics and Sedimentation in Wave-Domintated Coastal
Environments.
Elsevier Science Publishing Co., 1984.

Griffiths, W.
Lehigh University Department of Geological Sciences,
Bethlehem, PA.
Personal Communication on Research in Progress, 1986.

Grizzle, R.
Rutgers University Center for Coastal and Environmental Studies,
New Brunswick, NJ
Personal Communication on Research in Progress, 1985.

Harleman, D.R.F., Lee C.H., and Hall, L.C.
Numerical Studies of Unsteady Dispersion in Estuaries
Proceeding Journal of Sanitary Engineering A.S.C.E.
October, 1968.

Hicks, S.D., Debaugh, H.A., and Hickman, L.E.
Sea Level Variations for the United States 1855-1980
Rockville, Maryland: National Ocean Service, Jan. 1983.

Hoffman, J.S., Keyes, D., and Titus, J.G.
Projecting Future Sea Level Rise: Methodology, Estimates
to the Year 2100, and Research Needs
Washington, D.C.: U.S. Environmental Protection Agency,
Office of Policy and Resource Management, October, 1983.

Holley, E.R.
Unified View of Diffusion and Dispersion
Proceeding Journal of Hydraulics Division, A.S.C.E.,
v95, no.2, March 1969.

Ippen, A.T., Ed.
Estuary and Coastline Hydrodynamics
New York, McGraw-Hill Book Co., 1966.

Kelley, J.T.
Sediment and Heavy Metal Distribution in a Coastal Lagoon
Complex, Stone Harbor, N.J.
Bethlehem, PA, Lehigh University, Wetlands Reprint Service,
no. 3, 1975.

Levy, J.
Comparision of Texture, Minerology and Organic Content of
Suspended Accumulating and Bottom Sediments Within a Coastal
Lagoon, Stone Harbor, N.J.
M.S. Thesis, Bethlehem, PA, Lehigh University, 1978.

Maa, P.Y., Srivastaua, M., and Mehta, A.J.

Prediction of Fine Sedimentation in Small Marinas
Hydraulics and Hydrology, (Florida Sea Grant), 1985.

MacDonald, G.J. and Weisman, R.N.
Oxygen-Sag in a Tidal River
ASCE Journal of Environmental Engineering, June,1977.

Masch, E.D., Brandes, R.J., amd Reagan, J.D.
Numerical Simulations of Hydrodynamics, v1, App.2
Technical Report, U.S. Army Corps of Engineers, Coastal Engineering Research Center, and U.S. Army Engineer Waterways Experiment Station, 1977.

McAnally, W.H.Jr., Letter, J.V.Jr., Stewart, J.P., Thomas, W.A. and Brogdon, N.J.Jr.
Columbia River Hybrid Modeling System
Journal of Hydraulic Engineering, v110, no. 5, May, 1984.

Schubel, B.
Effects of Hurricane Agnes on Suspended Sediments in Chesapeake Bay and Contiguous Shelf Waters
from The Effects of Tropical Storm Agnes on the Chesapeake Bay Estuarine System, Chesapeake Research Consortium, J. Davis, Ed., US Army Engineer District, Corps of Engineers, 1975.

Schuepfer, F.E.
Hydrodynamic Model of an Inlet Sound System in Southern N.J.
M.S. Thesis, Lehigh University, Bethlehem, PA, 1985.

Tapp, J.S.
A Guide to the Use of Deposits on the HP3000 Mini Computer IMMR/059
Institute for Mining and Minerals Research, University of Kentucky, Lexington, KY, 40512

Tapp, J.S., Barfield, B.J., and Griffin, M.L.
Predicting Suspended Solids Removal in Pilot Scale Sediment Ponds Utilizing Chemical Flocculation
Techinal Report of Institute for Mining and Mineral Research, University of Kentucky, Lexington, KY, 1981.

Taylor, G.R.
The Dispersion of Matter in Turbulent Flow Through a Pipe
Proceeding Royal Society of London, Series A, v223, no. 1155, May 1954.

Thorbjarnarson, K.W., Nittrouer, C.A., DeMaster, D.J., and McKinney, R.B.
Sediment Accummulation in a Back-Barrier Lagoon, Great Sound,

New Jersey
Journal of Sedimentary Petrology, v55, no. 6, Nov. 1985.

U.S. Environmental Protection Agency
Erosion and Sediment Control-Surface Mining in the Eastern U.S.
Volumes I and II, E.P.A. -615/2-76-006
U.S. Environmental Protection Agency, Washington, D.C., 1976.

Van Rijn, L.C.
Mathematical Modeling of Suspended Sediment in Nonuniform Flows
Proceeding Journal of Hydraulics Division, A.S.C.E., v112,
no. 6, June 1986.

Wang, F.C.
The Atchafalaya River Delta Report 7: Analytical Analysis of the
Development of the Atchafalaya Rive Delta
Technical Report HL-82-15 U.S. Army Corps of Engineers,
Hydraulics Lab., Sept. 1985.

Ward, A.J., Haan, C.T. and Barfield, B.J.
Simulation of the Sedimentology of Sediment Detention Basins
Kentucky Water Resources Research Institute, Lexington, KY
June 1977.

Ward, A.J., Haan, C.T. and Barfield, B.J.
Simulation of the Sedimentology of Sediment Detention Basins
Research Report No. 103, University of Kentucky, Water
Resources Research Institutes, Lexington, KY.

Young, C.L., Weisman, R.N. and Lennon, G.P.
Sediment Deposition Modeling in Great Sound, New Jersey
Imbt Hydraulics Lab Report #IHL-111-86, 1986.

# Appendix I

## Notation

| | |
|---|---|
| $A_s$ | Area of the Sound |
| $A'$ | Dimensionless Coefficient for the Convection Term |
| C | Mass Concentration |
| $C_o$ | Mean Concentration |
| $C'$ | Dimensionless Concentration |
| d | Flow Depth |
| $d_{ave}$ | Average Depth of Accumulation |
| $dH_i$ | Increase in Fluid Depth Over Time $dt_i$ |
| $d_t$ | Time Interval |
| $dx_i$ | Distance Plug Travels Over $dt_i$, width of plug |
| D | Dispersion Coefficient |
| $D_b$ | Bulk Density |
| $D_x$ | Longitudinal Coefficient |
| $D_y$ | Lateral Dispersion Coefficient |
| $D'$ | Dimensionless Dispersion Coefficient |
| $D'_{max}$ | Maximum Value of Dispersion Coefficient |
| E | Efficiency of a Settling Tank |
| $F_{tot}$ | Total Volume Deposited from the Entire Plug by all Fractions over I time step |
| H | Depth of Water in the Sound |
| $H_i$ | Depth at Time i |
| j | Layer Number |
| L | Length of the Sound |
| $L_i$ | Layer Height at Time $t_i$ |
| $L_{lx}$ | Horizontal Flow Velocity |
| M | Number of Layers |
| $M_{in}$ | Mass of Sediment Inflow |
| $M_{ont}$ | Mass of Sediment Outflow |
| $M_{sed}$ | Actual Mass of Sediment Entering Great Sound |
| n | Manning Roughness |
| N | Number of Plugs |
| $N_d$ | Fraction of Particles Leaving Each Layer |
| $P_{j,i}$ | Initial Vertical Position of a Layer Surface |
| $P_{tot}$ | Total Volume Deposited From the Entire Plug by all Fractions over the Tidal Cycle |
| Q | Flow Rate |
| $r_j$ | Vertical Rise of Each Layer Surface |

| | |
|---|---|
| $R_d$ | Rate of Deposition |
| $R_h$ | Hydraulic Radius |
| $S_{net_i}$ | Net Distance a Particle Settles |
| $S_{L_{j,i+1}}$ | Relative Distance Settled from each Layer Surface |
| $t'$ | Dimensionless Time |
| $T$ | One Diurnal Cycle |
| $T_{d_i}$ | Total Volume Deposited from the Entire Plug of 1 Size Fraction over 1 Time Step |
| $u$ | Velocity |
| $u'$ | demensionless velocity |
| $U$ | Depth Averaged Flow Velocity |
| $U_{max}$ | Peak Flow Velocity |
| $U_{x,t}$ | Tidal Velocity |
| $U_*$ | Shear Velocity |
| $V$ | Depth Averaged Flow Velocity |
| $v_d$ | Actual Sediment Volume Deposited |
| $V_i$ | Velocity at Time $t_i$ |
| $V_p$ | Cumulative Volume Deposited From the System |
| $V_s$ | Particle Settling Velocity |
| $V_{sed}$ | Total Available Sediment Volume (Settled) |
| $V_{s_{cr}}$ | Critical Settling Velocity of a Particle |

# Vita

The author was born on August 4, 1963, to George B. and Marie J. Young in Baltimore, Maryland. After completing high school, he attended Lehigh University and studied toward a Bachelor of Science Degree in Civil Engineering, graduating in 1985. While at Lehigh, the author performed research in groundwater contamination recovery and water resource optimization planning. He was elected to Chi Epsilon, the National Civil Engineering Honor Society, and also received his E.I.T. in the State of Pennsylvania.

After graduation in June of 1985. the author served as a short term missionary in West Africa designing and constructing an addition to the local mission hospital.

The author then continued his academic career at Lehigh University in September, 1985. He worked for a year as a research assistant mathematically modeling sediment deposition and then for a semester as a teaching assistant in fluid mechanics. He expects to be granted a Master of Science degree in Civil Engineering in January, 1987, and then begin work in hydraulic modeling before eventually returning to the mission field.